# APPENDIX N:    Water Quality Modeling Report

# BLACK BUTTE COPPER PROJECT, MONTANA

## FINAL WATER QUALITY MODEL REPORT
Revised Mine Operating Permit Application

Prepared for

**Tintina Montana, Inc.**
**White Sulphur Springs, MT**

Prepared by

1807 W. Dickerson St., Suite D
PO Box 1685 (59771)
Bozeman, Montana 59715

6 September 2016

# Executive Summary

Tintina Montana, Inc. is applying for a Mine operating permit application for its Black Butte Copper Project, located approximately 17 miles north of the town of White Sulphur Springs, Montana.  Using hydrogeochemical monitoring, hydrogeological modeling and geochemical testing data, Tintina has designed its underground (UG) workings, temporary waste rock storage pad (WRS), cemented tailings facility (CTF), process water pond (PWP), contact water pond (CWP), and water treatment plant (WTP) to minimize impacts to water quality.  Here, Enviromin presents water quality predictions for Tintina's proposed facilities, during operations and at closure.

### Objectives

Enviromin has predicted water quality for the proposed i) UG workings (i.e., access, declines, and stopes), ii) WRS, iii) CTF, and iv) PWP.  In the UG, we estimate water quality at year 6 of mining operations and at post-closure conditions, when the top of the water table has recovered to near premining conditions.  For the WRS facility, we estimate water quality only at the end of year 2, when it will begin to be dismantled to provide material for the tailing impoundment interior liner and rock drain.  For the CTF, we estimate water quality at year 6 of production and at the start of closure, prior to placement of the cover which is expected to eliminate all subsequent seepage.  Apart from groundwater in the underground workings at closure, water from all of the modeled facilities during construction and operations will ultimately report to the water treatment facility, where it will be treated to meet non-degradation standards and discharged to groundwater.

### Methods and Assumptions

- The UG model estimates contributions from fractured walls based on a calculated reactive mass ($R_m$) within an equivalent porous media (EPM) model.  The measured $R_m$ and flow rate in humidity cell tests (HCT) are scaled to estimated field conditions to calculate mass loads (e.g., metals and acidity) from each unit.
- For the paste backfill and the cemented tailings, the model uses the surface area and flow rate to scale mass loads using diffusion test results (in the underground workings) or HCT tests (in the CTF runoff).
- The model estimates mass loads from waste rock in the CTF and WRS by scaling HCT test data to surface areas and flow rates.  Because the predicted water flow is low relative to the surface area, the reactive mass is estimated by calculating the maximum amount of waste rock that could be saturated with the estimated flow over the relevant time frame, i.e. one year for the WRS and one week for the CTF.
- Only the final, mixed solutions are allowed to precipitate minerals (Table 3.1) and exchange metals with mineral surfaces through sorption to precipitated ferrihydrite and available sulfide.  We use the *minteq.dat* thermodynamic database option in the USGS equilibrium model, PHREEQC and published sulfide sorption isotherm data to predict mineral precipitation, metal sorption, and resulting water quality.

### Results

Our predictions indicate that water in the backfilled UG will have circumneutral pH, abundant alkalinity, and moderate sulfate, with metal concentrations that meet Montana groundwater standards and non-degradation criteria post-closure.  During operations, increases in $NO_3^-$, $SO_4^{2-}$, F, Mn, Ni, As, Sb, Sr, Se, Tl, and U relative to background water quality are predicted in UG sump water that will be collected for storage in the PWP prior to treatment to meet Montana water quality standards. Of these elements, concentrations of $NO_3^-$, F, As, Ni, Sb,

Sr, Tl, and U exceed groundwater quality standards in one ore more model scenarios. Water collected on the temporary, lined WRS and the doubly lined CTF will be more acidic than the UG, with elevated metal concentrations. This water will also be routed to the PWP prior to treatment to meet water quality standards. At closure, the CTF will be covered with a final lift of 4% cemented paste, resulting in increased pH and reduced metal concentrations, followed by closure using a geosynthetic membrane to cut off infiltration and eliminate water discharge.  Specific results are summarized by facility below.

- **UG:** For the UG model, we predict water quality in year 6 of operations to be neutral, with a pH of 6.86, abundant alkalinity (183 mg/L) and a moderate increase over background concentrations in sulfate (304 mg/L) (**Table 4-4**).  We predict potential precipitation of alunite, $Ba_3(AsO_4)_2$, $Cr_2O_3$, ferrihydrite, and quartz, based on PHREEQC predictions of supersaturation in the mixed influent water in the sump. The formation of these minerals, followed by metal sorption, removes solutes from the water and allows calculation of a final of water quality. The metals Ba, Be, Zn, Cu, Pb, and As are predicted to sorb to ferrihydrite in the base case and most sensitivity scenarios, apart from the 'All HCT' scenario which does not predict ferrihydrite precipitation.

  The model includes several sensitivity analyses of the predicted underground water quality, addressing uncertainty in model inputs for i) HCT data (i.e., all data vs. weeks 1-4), ii) fracture density, iii) fracture zone thickness, iv) estimated surface area, and v) sulfide oxidation rate.  In general, the assumptions about fracture density and reactive-zone thickness have the greatest effect on predicted metal release, and the inclusion of all week HCT data has the greatest effect on the pH. Alkalinity is abundant in all sensitivity scenarios, including the analysis of several upper bound estimates of rim thickness, sulfide oxidation rate, and fracture density which together create a conservative evaluation of the reactive mass. Predicted pH ranges from 4.89 to 6.88 and sulfate ranges from 262 to 672 mg/L across the various sensitivity analyses (**Table 4-4**).  Nitrate, As, and U are predicted to exceed the Montana DEQ groundwater quality standards in the operational base case as well as in several sensitivity scenarios (**Table 4-4**).  Antimony, Sr and Tl are predicted to exceed the groundwater standard only in select sensitivity analyses which include conservative (upper bound) estimates of input parameters.  However, because all water will be collected for treatment to meet water quality standards, these operational exceedances will not affect downgradient water.

  At closure, following completion of mining, backfilling, and recovery of the water table to its original elevation, the pH (6.91) and alkalinity (151 mg/L) are predicted to be higher, with lower sulfate (115 mg/L) and metal concentrations, than predicted during operations, as sulfide oxidation will be inhibited in the flooded workings (**Table 4-5**). The predictive model is most sensitive to the estimate of reactive surface area for cemented backfill.  The lower mine workings are separated from the surface by the Volcano Valley Fault (VVF) and the base rock permeability is so low there is little to no flow through these units.  In addition, the lower workings will be separated from the upper groundwater system by construction of two hydraulic plugs where the access ramps penetrate through the VVF.  Since the lower mine working transmit little to no water, and will be separated from the upper workings and shallower hydro-stratigraphic units, they were not included in the closure model.  Enviromin predicts potential precipitation of $Ba_3(AsO_4)_2$, $Cr_2O_3$, ferrihydrite, and quartz, based on

PHREEQC predictions of supersaturation in the mixed water at closure. Metals sorb to both ferrihydrite and sulfide under closure conditions.

Mine water will be collected during dewatering operations for treatment, so the predicted chemistry at closure is the most important from an environmental perspective. The predicted changes at closure represent minor changes in water quality, relative to the background water quality (pH of 6.97, with alkalinity of 193 mg/L and sulfate 111 mg/L). The limited variation between the base case and sensitivity scenarios reflects the robust design and plan for management of the UG, which limits open stope area through concurrent backfilling with a low transmissivity material; provides for water treatment in operations and early closure; floods the lower workings with RO treated water at closure, and isolates the upper and lower workings using hydraulic plugs.

- **WRS**: Water quality predicted for the WRS base case at year 2 of mining is moderately acidic (pH 5.49) and high in sulfate (3,780 mg/L), with some elevated metals (**Table 5-1**). However, the volume of WRS seepage is small (0.9 gpm average in year two) and water will be collected on a lined pad for treatment. This prediction is thus conservative, as a result of the very small amount of water into which the mass of solutes released from the aggressively weathered HCT is scaled. We predict potential precipitation of barite, celestite, fluorite, gypsum, jarosite, MnHPO4, and quartz, with no sorption due to lack of ferrihydrite precipitation. Sensitivity analyses show that the model is sensitive to the rock:water ratio and surface area (reactive mass) assumptions do influence predicted water quality. Because the WRS will be removed in years before year 3, no closure evaluation was needed.

- **CTF:** For the CTF, water quality predicted at year 6 of mining is acidic (pH 4.13) with 765 mg/L sulfate and elevated metal concentrations (**Table 6-1**). More acidity and metals are contributed by the surface of cemented tailings than the co-deposited waste rock or access ramp/rock drain, while most sulfate comes from the wet paste and the waste rock contribution. The minerals predicted by PHREEQC to form during operations include alunite, barite, jarosite, and quartz. At closure, following placement of a 4% cement paste lift immediately prior to cover placement, a more neutral solution (pH 5.57) is predicted, with no exceedances of groundwater standards for metals predicted for the base case following precipitation of $Ba_3(AsO_4)_2$, barite, and jarosite (**Table 6-2**). Limited exceedances of groundwater standards for As and Tl were predicted for the high surface area sensitivity scenario in closure. The planned reclamation procedures (e.g., welded HDPE cover, revegetation, etc.) are not accounted for in the model, which predicts water quality prior to use of the cover to eliminate infiltration.

  Results for the CTF show that the finely ground, sulfide-rich tailings will generate higher acidity and metals, but proportionally lower sulfate due to precipitation of sulfate-rich minerals, e.g., alunite, barite and jarosite. Water quality predictions for the CTF are sensitive to the calculated surface area, implying that the surface area should be managed to limit weathering through frequent placement of fresh lifts of pasted tailings. Higher concentrations of cement (e.g., 4%) could be used to reduce disaggregation of the surface if a delay in operations will prevent frequent placement of fresh lifts.

- **PWP:** All water from the CTF sump and some water from the UG sump will report to the PWP.  These inflows mix with thickener overflow from the mill and direct precipitation.  The model predicts that the overall chemistry of the PWP is dominated by the thickener overflow, which provides 93% of the flow.  The predicted solution has a pH of 5.69, low sulfate (110 mg/L), and elevated concentrations of $NO_3$ and metals, including Cu, Ni, Pb, Sb, and Tl (**Table 7-1**).  Alkalinity is higher due to mixing with process water.  PHREEQC predicts that alunite, $Ba_3(AsO_4)_2$, barite, and ferrihydrite could form, based on supersaturation, with sorption of Cu, Pb, and As to ferrihydrite.

# TABLE OF CONTENTS

# LIST OF TABLES

# LIST OF FIGURES

# LIST OF APPENDICES

# 1   Introduction

Tintina Resources has submitted a Mine Operating Permit (MOP) application for its Black Butte Copper Project, located approximately 17 miles north of the town of White Sulphur Springs, Montana (**Figure 1-1**).  Copper in the shaley dolomite of the lower Newland Formation is associated with sulfide mineralization that is locally massive, but hosted in carbonaceous and carbonate-rich sediments with fracture-controlled transmissivity in the vicinity of the proposed underground workings.  Using hydrogeochemical monitoring, hydrogeological modeling and geochemical testing data, Tintina has designed its facilities to address the potential for sulfide mineralization to impact water quality.  Facilities where water may be influenced by geochemistry include the underground workings (UG), temporary waste rock storage pad (WRS), cemented tailings facility (CTF), process water pond (PWP), contact water pond (CWP), and the water treatment plant (WTP) (Figure 1-2).

In this report, we present water quality predictions developed for key facilities during operations and at closure.  These models integrate Tintina's proposed designs with hydrological, geochemical, and water balance data.  Models predict future water quality and related uncertainty based on sensitivity analyses at four locations:

- Groundwater quality in the UG at year 6 of mining operations and at closure;

- Seepage from temporary waste rock storage, which will be collected and transported to the CWP, in year 2 of mining;

- CTF seepage/runoff quality, which will ultimately return to the PWP and WTP for release following treatment and discharge to an underground infiltration gallery, in year 6 of tailing production and at closure; and

- Updated water quality data predictions for PWP water reporting to the WTP based on UG and CTF predictions, for year 6 of production.

The underground model applies groundwater quality (Hydrometrics 2015, Appendix B of the MOP), flow predictions (Hydrometrics 2016, Appendix M of the MOP) and geochemistry data from Enviromin (Appendix D of the MOP application, Tintina, 2016) to facility-specific conceptual models describing conditions during operations and at closure.  The analytical approach recognizes changes in the operational water balance and extent of oxidation throughout mine life, as well as solubility and sorption constraints on the quality of water in each setting.  Uncertainty has been addressed through sensitivity analyses.

## 1.1  Purpose and Scope

The purpose of Enviromin's development of the models is to predict water quality in the UG workings, the (WRS) and the CTF, as well as the overall quality of water in the PWP, which will report to the WTP.  We use the operational plans provided by Tintina, together with the groundwater quality data (MOP, Appendix B), the hydrogeological modeling (MOP, Appendix M) provided by Hydrometrics, and the geochemical test results provided by Enviromin (MOP, Appendix D) to develop a mass-load calculation of water quality for each facility under base case and sensitivity scenarios.  Each mass load solution is then evaluated for solubility and sorption controls using the USGS PHREEQC equilibrium model to calculate mineral saturation indices and metal sorption to precipitated ferrihydrite (Parkhurst and Appelo, 1999).  Sorption of metals to sulfide in saturated bedrock at closure is calculated using published isotherm data (Appendix F).

**Figure 1-1.    Project Location Map**
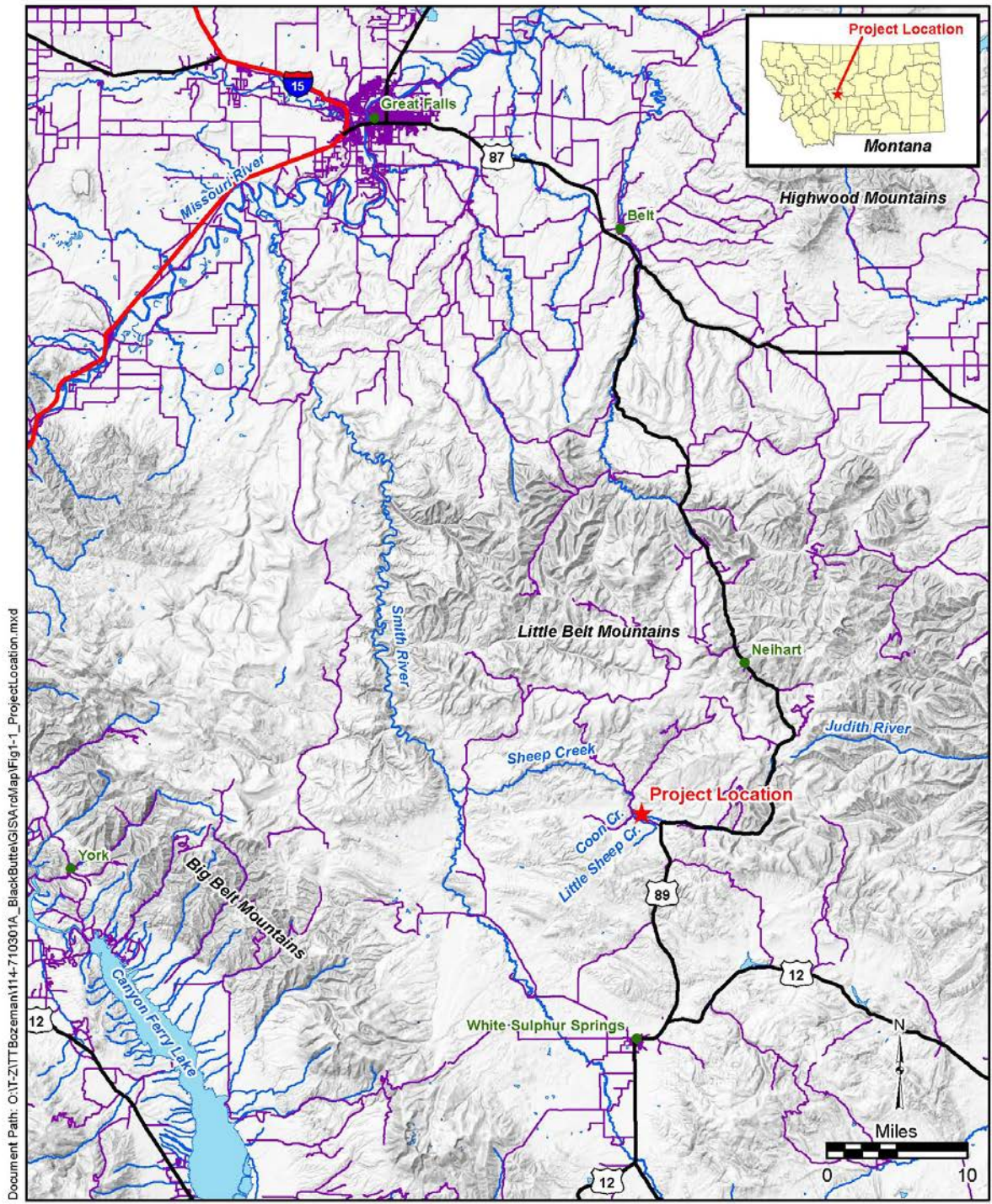
**Figure 1-2.     Black Butte Copper Project Site Facilities**



Prepared by Tetra Tech Inc. (Revised May 2016)
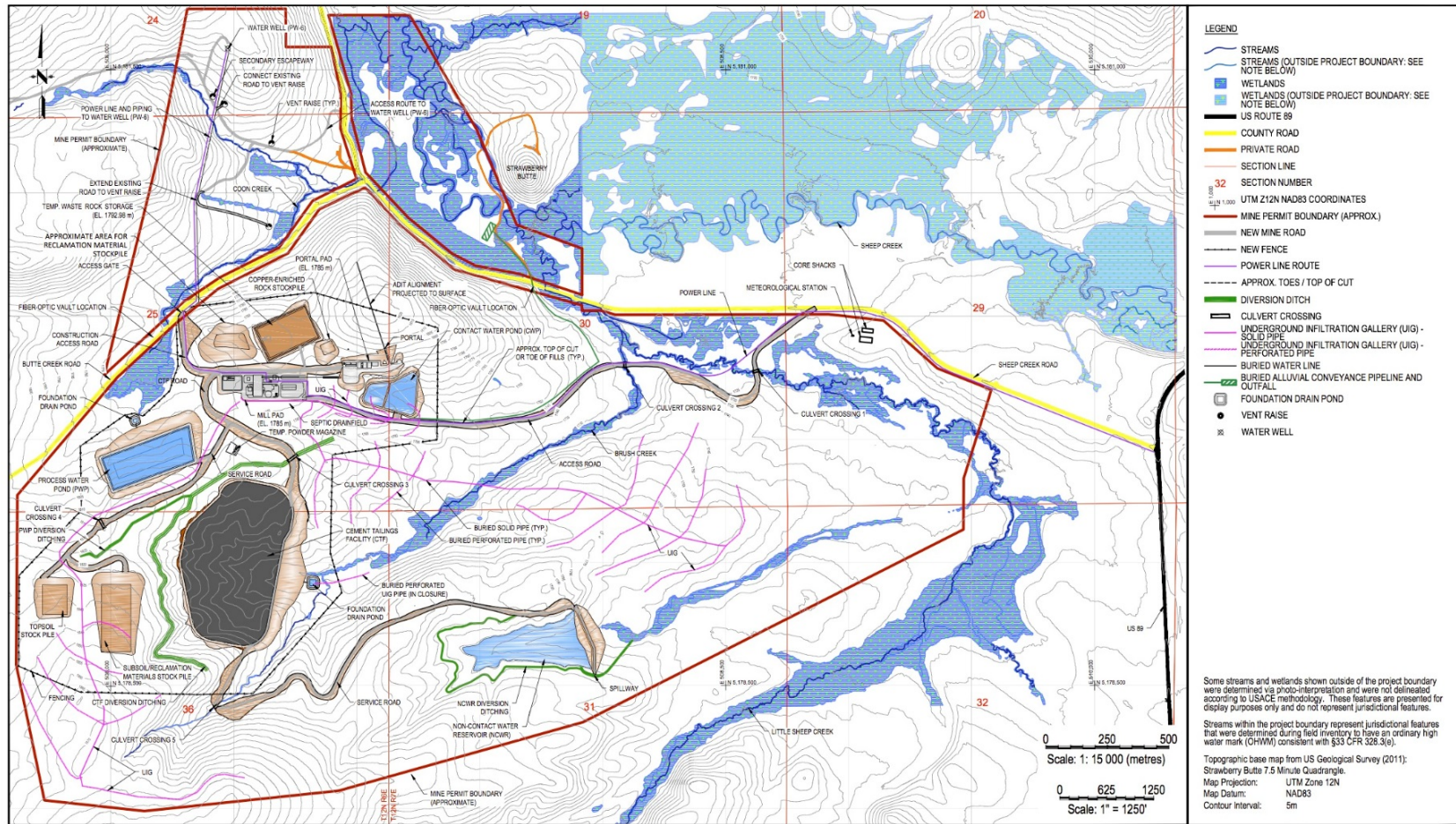
FIGURE 1−2
**Facilities Site Plan**
**Black Butte Copper Project**
**Mine Operating Permit Application**
Meagher County, Montana

**Underground Workings (UG)** – Tintina plans to advance underground operations through the proposed decline into the Upper Sulfide Zone (USZ) and deeper into the Lower Copper Zone (LCZ) (**Figure 1-3**).  Copper-enriched rock will be mined within stopes that will be open for less than 90 days at any time.  An average of 0.7% of the deposit will be open at any given time during concurrent development, extraction, and backfilling within the stopes. Tintina proposes to produce tailings via flotation and to blend them with cement to create 4% cemented paste tailings.  Using a drift and fill mining method, 45% of produced tailings will be placed as backfill into mined out underground stopes and access headings during operations.  The workings will be flooded at closure.  In addition to the Upper and Lower Copper Zones (UCZ and LCZ), the exposed lithotypes include, from largest to smallest surface area contribution; Ynl B, LZ FW, and Ynl A.  Most groundwater influx comes from the USZ/UCZ unit (50%), the Ynl B (lower decline) unit (22%) and the Ynl A (upper decline) unit (19%) (Hydrometrics, 2016).

**Waste Rock Storage (WRS)** – Rock will be stored on the WRS pad (shown in Figure **1-2**) for 2 years, and then placed in the CTF.  Waste rock will be mined primarily from (in stratigraphic order) the upper portion of the lower Newland Formation (Ynl A, 4%), the Upper Sulfide Zone (USZ, 28%), the lower portion of the lower Newland Formation (Ynl B, 32%), and the Lower Zone Foot Wall (LZ FW, 35%) as the decline is driven to access the copper-enriched rock.  This waste will be placed in lifts on the lined WRS waste rock storage pile. Little if any LZ FW will be placed on the WRS, as this formation is not anticipated to be mined before CTF construction is scheduled to be complete and the WRS pad is reclaimed.

The seepage rate through the WRS was estimated using the HELP model at an average rate of 0.9 gallon per minute (gpm) (Hydrometrics, 2016).  This water will report directly to the CWP until year 2 to 3, when waste rock will be removed from the stockpile altogether for placement in the CTF.

**Cement Tailing Facility (CTF)** – Tailings that are not backfilled (approximately 55%) will be placed as 0.5 to 2% cement-amended paste into a double lined surface tailing impoundment (the CTF, shown in **Figure 1-2**).  The CTF is designed to have little or no water stored in the facility.  Most waste rock produced during construction of the decline and other UG workings will be placed into the lowermost CTF and used to construct the ramp, where it will subsequently be covered by cemented paste tailings.  Run of mine (ROM) waste rock will also be placed around the sump to develop a positive drain within the CTF, and ROM waste rock produced later will be co-disposed with and encapsulated by paste tailings.

Tintina has proposed an innovative, cemented tailings storage design.  By incorporating cement with binders (i.e., fly ash and/or slag) into the tailings as they are placed in the lined CTF, Tintina will encapsulate sulfide minerals in a non-flowable mass of tailings and limit their exposure to oxygen and water, thereby limiting acid and metal release potential from the waste rock.  The majority of waste rock will be produced from the decline early in operations, and will therefore be placed into the lowermost part of the lined CTF.  Waste rock produced subsequently will be dumped from the ramp and encapsulated within the cemented paste backfill.  Water seeping from tailings as they consolidate and solidify will mix with runoff from direct precipitation onto the CTF; this water will be collected in a waste rock-lined sump prior to being pumped back to the PWP.

**Process Water Pond (PWP) –** Water from the UG and the CTF (Figure 1-2) will mix with process water and direct precipitation in the PWP.  Excess volume accumulating on the PWP will report to the water treatment plant (WTP).  Using the calculated predictions for the UG and the CTF, we have predicted water quality for the PWP.  This model is provided for comparison with previous predictions made by CDM (MOP, Section 3.7.3.3) using mixed

metallurgical process water and groundwater to predict water treatment needs for design purposes.

At closure, the water balance will change.  The WRS facility will no longer exist. Mining will cease and all UG stopes will be backfilled.  Dewatering will cease and groundwater will return to its original elevation, filling the decline and any gaps in backfilled stopes.  Water from the UG will no longer report to the PWP or the WTP. Contributions from the WRS will have been eliminated, reducing the solute load both to and from the CWP.  Following the placement of final tailings lifts, a geomembrane will be used to cap the CTF and a fill and soil cap will be placed over the HDPE cover, eliminating incident precipitation and greatly reducing the availability of oxygen.  Progressively less water will report to the CTF sump during closure, and solute load is expected to decline, so that the volume and chemistry of water requiring treatment will change, and ultimately be eliminated.  Water from the PWP will be treated to meet water quality standards.

**Figure 1-3.    Cross-section of proposed BBC mine workings showing stratigraphic units (Ynl A, USZ, Ynl B, and LZ FW) to be mined as waste rock and exposed in the underground workings.  Volcano Valley Fault (VVF) and Buttress Fault are shown bounding the Lower Copper Zone (LCZ).**
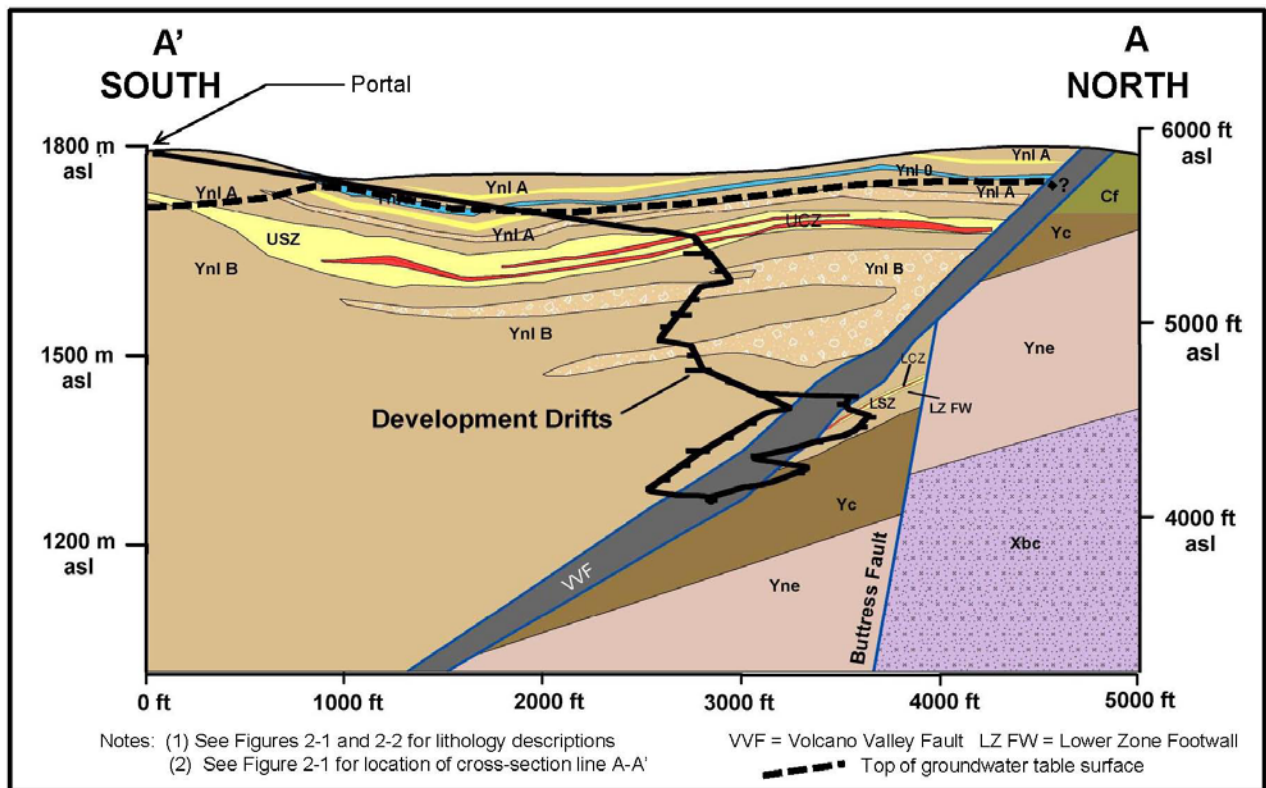
# 2  Model Source Data

The models account for data that characterize facility design, operation, closure, site geology, groundwater quality, groundwater flow, and geochemistry.  Data sources are described generally here and later examined in detail for each of the models.

## *2.1  Black Butte Copper Mine Plan*

Tintina Montana's Black Butte Copper Project will produce and ship copper concentrate mined from both the upper and lower Johnny Lee deposit zones.  The proposed operation will mine approximately 15.3 million tons (13.9 million tonnes (Mt)) of rock.  This total includes 14.5 million tons (13.2 Mt) of copper-enriched rock with an average grade of 3.1% copper, and 0.8 million tons (0.7 Mt) of waste.  Mining will occur at a rate of approximately 1.3 million tons/year (1.2 Mt/year) or 3,640 tons (3,300 tonnes) per day, over a mine life of approximately 19 years (including construction and reclamation) (Tintina MOP, 2016).

Mining will use a drift and fill method.  Approximately 45% of the mill tailings will be mixed with cement and binder to form a paste, and used to backfill all production workings during the mining of sequential drifts in the UG.  Although much of the waste rock that will be trucked to surface will be non-acid generating, as a safeguard, all waste rock will be assumed to contain sulfide minerals and will be treated as potentially acidic or metal generating.  A geomembrane lined, temporary WRS facility will be constructed between the portal and the mill.  It will receive all of the waste rock generated until construction of the CTF is completed (Figure 1-2).  The completed CTF will receive crushed waste rock for use as a protective cushion layer over the uppermost of the double high-density polyethylene (HDPE) liners.  All future waste rock will be placed into the CTF along with the mill tailings.  The temporary WRS facility will be completely reclaimed in year's two to three.  No waste rock will be left on the surface after closure.  The CTF will be dewatered (if any water is present), sealed with a cover of HDPE, and reclaimed in closure.  A separate stockpile on a smaller lined pad will be constructed off of the northwest corner of the portal pad (Figure 1-2) near the end of the construction period to contain the copper-enriched rock for mill feed.

Dewatering of UG mine workings will provide all water required for mining and milling (approximately 210 gallons per minute [gpm] or 795 Lpm).  Excess water pumped from the mine will be treated to meet non-degradation standards and released through an underground infiltration gallery to shallow bedrock.

A double HDPE-lined PWP with an underlying foundation drain and pond will store water needed for milling.  Water will be recycled between the PWP and the mill during operations.  A paste plant in the mill complex will mix fine-grained tailings from the milling process with cement for placement both UG and in the CTF.  The plant will mix approximately 45% of the tailings with approximately 4% cement and other binders to be used as paste backfill in the UG mine workings.

The remaining 55% of the tailings will be mixed with 0.5 to 2% cement and other binders to form a paste which will be pumped to the CTF.  The small amount of free water that collects in the CTF from cemented tailings seepage, precipitation and snowmelt will be pumped to the PWP.  Water not needed in the mill will be pumped directly to the reverse osmosis water treatment facility for treatment and then released to the underground infiltration galleries.

Both the CTF and the PWP will use liner systems comprised of a high-flow geonet-layer sandwiched between two layers of 100 mil HDPE geomembrane liner.  Both facilities will also incorporate foundation drains beneath the liners.  The CTF will also have an internal basin underdrain system.

The closure and reclamation plan will maintain physical and chemical stability of all facilities, to protect water quality and quantity.  No waste rock will be left on surface in closure.  Water will be removed from the tailings facility (if any is present), and from the PWP and CWP, and treated to meet standards prior to discharge.  The CTF will be covered with a welded HDPE cover, followed by fill, subsoil and topsoil (at a slope or shape designed to preclude standing water), re-grading and re-vegetation.  This plan will eliminate long-term exposure of the final lifts to oxygen and water.  The double lined CTF with drainage collection is designed to prevent discharge to surface water and groundwater.  Any water produced from the CTF sump in closure (if any) will go directly to the water treatment plant.  This will continue into closure while water quality and inflow are monitored, with gradually decreased monitoring until sufficient data is available to evidence that final closure objectives have been met (i.e., at some point in closure the water treatment plant will no longer be required).

## 2.2  Black Butte Copper Project Geology

The geology and subsurface stratigraphy within the project area has been reported by Tintina, based on geologic mapping and extensive exploratory drilling, and is summarized here.  Further hydrogeological detail is described by Hydrometrics in Appendices B and M of the MOP (Tintina, 2015).

A geologic map of the project area is shown in **Figure 2-1** and a stratigraphic section for the project area is shown in **Figure 2-2.**  The mine will be developed within dolomitic and silicic shales of the Proterozoic Newland Formation that dip gently to the southeast and are bounded to the north by a prominent northeast trending thrust fault known as the Volcano Valley Fault (VVF).

**Figure 1-3** shows the principal stratigraphic units that will be encountered during development of the Johnny Lee deposits. There are the Upper (UCZ) and Lower Copper Zones (LCZ) hosted within the Upper and Lower Sulfide Zones (USZ, LSZ, respectively) of the lower Newland Formation.  The UCZ lies approximately 250 to 600 feet below ground surface and is overlain by shale and dolostone (Ynl A), and dolomite (Ynl 0) interbeds.  The UCZ is underlain by the lower Newland shale and conglomerate (Ynl B).  These units are cut by the southward-dipping VVF to the north, shown as a heavy purple line in **Figure 1-3**. A thin slice of the lower Newland Formation lies below the VVF and contains the LCZ at a depth of approximately 1,100 to 1,500 feet below surface.  The LCZ and Lower Newland shales lie just above the contact with the Chamberlain Formation and are cut to the north by the Buttress Fault, shown as a thin purple line in **Figure 1-3**.  Lower Newland rock lying stratigraphically below the VVF are generally referred to as LZ FW (Lower Zone Footwall) rocks.

**Figure 2-1.     Black Butte Copper Site Geologic Map**
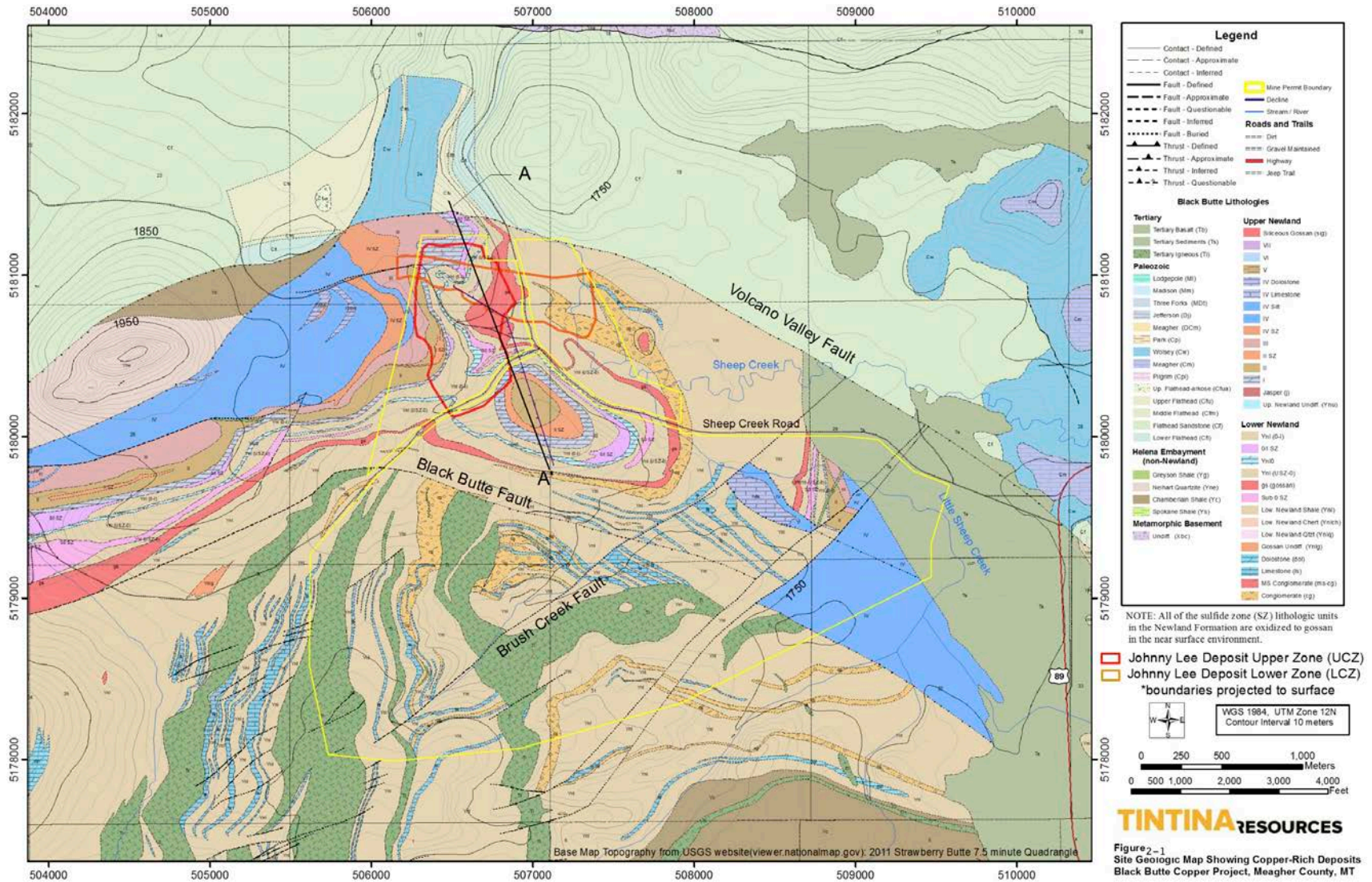
**Figure 2-2.    Black Butte Copper Stratigraphic Section**
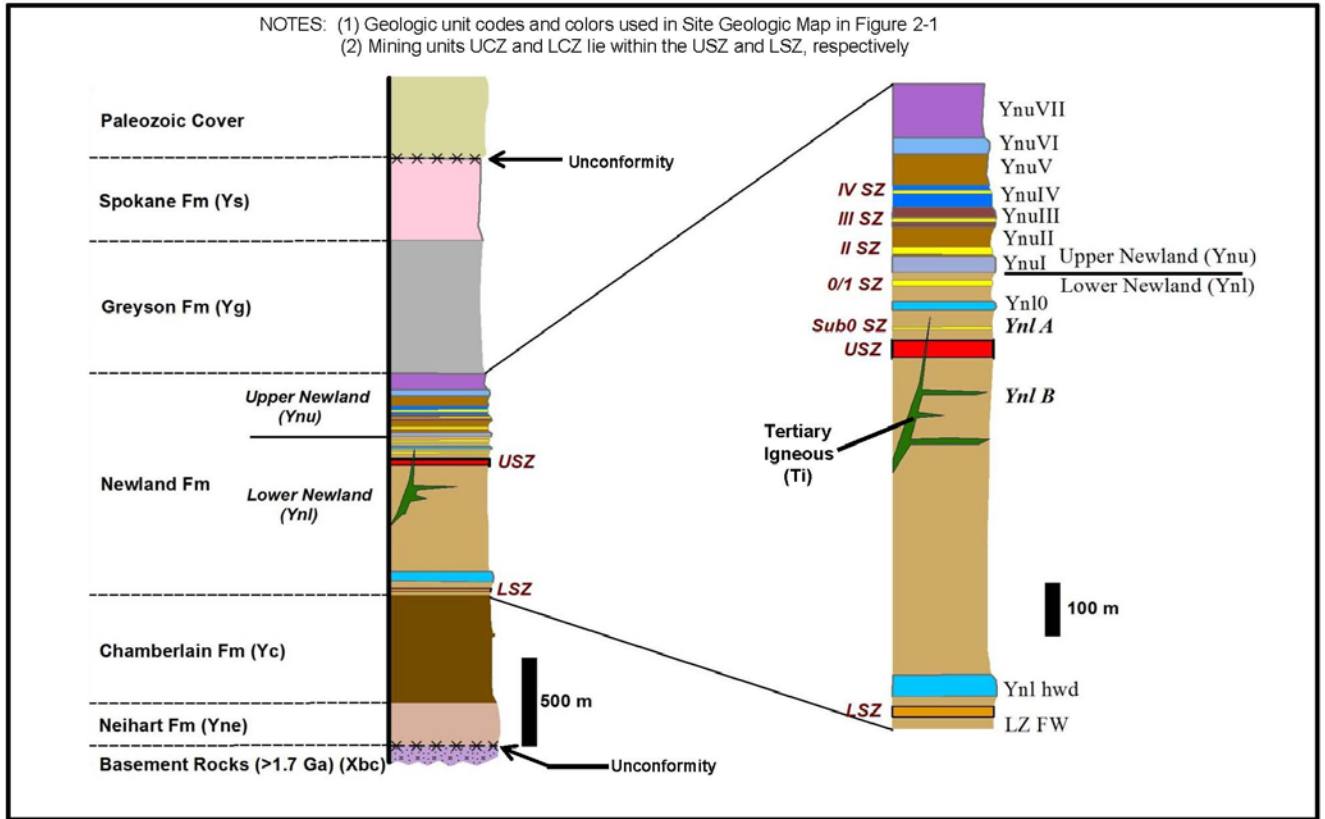
## 2.3  Groundwater Chemistry Data

The quality of groundwater flowing from exposed bedrock units is an essential component of the UG water quality model.  Groundwater monitoring for the Black Butte Copper project was initiated by Hydrometrics, Inc. in May of 2011 as part of a larger baseline study of flow, water levels, and water quality in the project area.  The groundwater baseline data can be reviewed in detail in Appendix B of the MOP.

Monitoring wells and test wells have been completed within the shallow and deep stratigraphic units described above to define baseline water levels, groundwater flow directions and groundwater quality within the project area (**Table 2-1**).  A series of paired monitoring wells (MW-1A, -1B; MW-2A, -2B; MW-4A, -4B; and MW-6A, -6B) were installed between 2011 and 2013 to document baseline conditions within the unconsolidated Quaternary/Tertiary clay-rich gravel deposits and in the underlying shallow bedrock groundwater system (**Figure 2-3**).  Monitoring well MW-3 was also completed in November 2011 near the proposed terminus of the exploration decline within the UCZ.  In 2014, an additional monitoring well, MW-9, was installed in the Ynl A zone above the sulfide and copper-enriched zones as a monitoring point to assess the effects of mine dewatering on overlying units during development.

An additional 10 test wells (PW-1 through PW-10) were installed for aquifer testing to provide hydrologic characteristics and water quality data for representative stratigraphic units.  Of these wells, problems were experienced while drilling through the VVF in well PW-7, requiring the use of drilling muds which could not be fully purged from the well during development due to very low flow conditions.  This has affected water quality data collected from this well, preventing their inclusion in the modeling work.  As a conservative replacement, the water chemistry from PW-9 is used, which has the highest dissolved concentrations of all monitored wells.

Groundwater monitoring is conducted quarterly at 12 monitoring well sites and static water levels are measured quarterly at 22 additional test wells and piezometer sites.  Water quality data have also been collected at ten test wells during site investigations; however, these wells are not routinely monitored during baseline monitoring events.  In addition to baseline monitoring, a number of groundwater investigations have been conducted to characterize hydrostratigraphic units in the project area (Hydrometrics, 2012, 2013, and 2015). **Table 2-2** summarizes the groundwater quality data collected by Hydrometrics and the period of record available for each of the monitoring wells.

**Table 2-1.    Summary of Hydrostratigraphic Units and Associated Well Completions
(from Hydrometrics, 2015)**

| Hydrostratigraphic Unit/ Structure | Monitoring Well | Test Well |
|---|---|---|
| Qa/Overburden | MW-1A MW-4A MW-6A | NA |
| Ynl (Dolostone) | MW-6B MW-7 MW-8 | NA |
| Ynl-A | MW-1B MW-2A MW-2B MW-9 | PW-1 PW-3 PW-8 |
| USZ | MW-3 | PW-2 PW-4 |
| UCZ | NA | PW-9 |
| Ynl-B | MW-4B | PW-10 |
| LCZ | NA | PW-7 |
| Yne | NA | PW-6N |
| Volcano Valley Fault | NA | PW-5 |
| Buttress Fault | NA | PW-6 |

**Figure 2-3.    Location of Black Butte Copper Groundwater Monitoring Wells
(from Hydrometrics, 2015)**
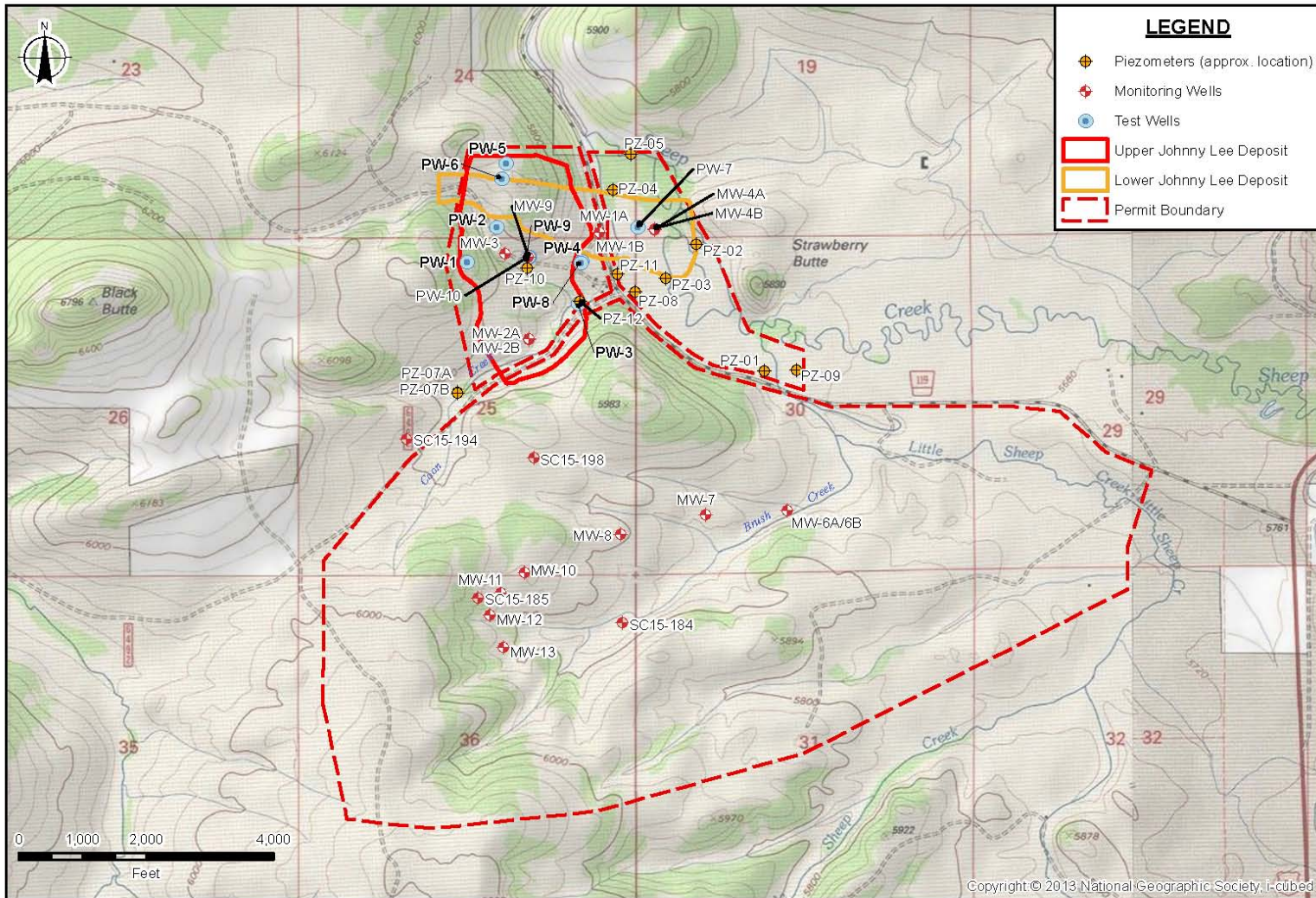
**Table 2-2.    Summary of Monitoring Wells from Groundwater Baseline Study, after Hydrometrics (2015)**

| Monitoring Site | Easting (meters) | Northing (meters) | Monitoring Frequency | Period of record | Flow or Water Level | Field Parameters | Lab Parameters | Comments |
|---|---|---|---|---|---|---|---|---|
| | UTM-WGS 1984 Zone 12 | | | | | | | |
| Monitoring Wells | | | | | | | | |
| MW-1A | 506935.22 | 5180841.5 | Quarterly | 2011-2015 | X | X | X | |
| MW-1B | 506934.19 | 5180845.5 | Quarterly | 2011-2015 | X | X | X | |
| MW-2A | 506598.18 | 5180331.93 | Quarterly | 2011-2015 | X | X | X | |
| MW-2B | 506596.96 | 5180328.73 | Quarterly | 2011-2015 | X | X | X | |
| MW-3 | 506484.1 | 5180740.2 | Quarterly | 2011-2015 | X | X | X | |
| MW-4A | 507201.5 | 5180855.4 | Quarterly | 2012-2015 | X | X | X | |
| MW-4B | 507200.1 | 5180858.5 | Quarterly | 2012-2015 | X | X | X | |
| MW-6A | 507809.2 | 5179492.9 | Quarterly | 2013-2015 | X | X | X | |
| MW-6B | 507792.8 | 5179490.7 | Quarterly | 2013-2015 | X | X | X | |
| MW-7 | 507451.7 | 5179500.7 | Quarterly | 2013-2015 | X | X | X | |
| MW-8 | 507036.0 | 5179398.3 | Quarterly | 2013-2015 | X | X | X | |
| MW-9 | 506593.0 | 5180725.5 | Quarterly | 2014-2015 | X | X | X | |
| SC15-184 | 507047.3 | 5178972.5 | Quarterly | 2015-2016 | X | X | X | first monitoring July 2015 |
| SC15-185 | 506355.5 | 5179094.2 | Quarterly | 2015-2016 | X | X | X | first monitoring July 2015 |
| SC15-194 | 506014.1 | 5179854.9 | Quarterly | 2015-2016 | X | X | X | first monitoring July 2015 |
| SC15-198 | 506621.4 | 5179854.9 | Quarterly | 2015-2016 | X | X | X | first monitoring July 2015 |

**Table 2-2.    Sampling Summary for Baseline Monitoring Sites (continued)**

| Monitoring Site | Easting (meters) | Northing (meters) | Monitoring Frequency | Period of record | Flow or Water Level | Field Parameters | Lab Parameters | Comments |
|---|---|---|---|---|---|---|---|---|
| | **UTM-WGS 1984 Zone 12** | | | | | | | |
| **Test Wells** | | | | | | | | |
| PW-1 | 506301.4 | 5180698.4 | Quarterly | 2011-2015 | X | One Time | One Time | Lab Data from Pumping Test |
| PW-2 | 506443.2 | 5180865.0 | Quarterly | 2011-2015 | X | One Time | One Time | Lab Data from Pumping Test |
| PW-3 | 506846.4 | 5180479.4 | Quarterly | 2012-2015 | X | twice | twice | Lab Data from Pumping Test |
| PW-4 | 506901.8 | 5180688.3 | Quarterly | 2012-2015 | X | One Time | One Time | Lab Data from Pumping Test |
| PW-5 | 506490.7 | 5181172.8 | Quarterly | 2013-2015 | X | -- | -- | |
| PW-6 | 506468.1 | 5181097.9 | Quarterly | 2012-2015 | X | -- | -- | Lab Data from Pumping Test |
| PW-6N | 506468.1 | 5181097.9 | Quarterly | 2015 | X | -- | -- | |
| PW-7 | 506846.2 | 5180695.5 | Quarterly | 2013-2015 | X | twice | twice | Lab Data from Pumping Test |
| PW-8 | 506598.4 | 5180721.9 | Quarterly | 2014-2015 | X | twice | twice | Lab Data from Pumping Test |
| PW-10 | 506593.6 | 5180721.9 | Quarterly | 2014-2015 | X | twice | twice | Lab Data from Pumping Test |
| **Piezometers** | | | | | | | | |
| PZ-01 | 507650.0 | 5180255.6 | Quarterly | 2012-2014 | X | -- | -- | |
| PZ-02 | 507400.7 | 5180778.8 | Quarterly | 2012-2014 | X | -- | -- | |
| PZ-03 | 507249.2 | 5180618.9 | Quarterly | 2012-2015 | X | -- | -- | |
| PZ-04 | 506991.7 | 5181110.8 | Quarterly | 2012-2015 | X | -- | -- | |
| PZ-05 | 507080.0 | 5181214.7 | Quarterly | 2012-2015 | X | -- | -- | |
| PZ-07A | 506258.4 | 5180074.7 | Quarterly | Nov-14 | X | -- | -- | |
| PZ-07B | 506258.5 | 5180075.0 | Quarterly | Nov-14 | X | -- | -- | |
| PZ-08 | 507090.3 | 5180573.8 | Quarterly | 2014-2015 | X | -- | -- | |
| PZ-09 | 507883.8 | 5180178.6 | Quarterly | 2014-2015 | X | -- | -- | |
| PZ-10 | ND | ND | One-Time | Nov-14 | X | -- | -- | PW-8 Aq Test temporary piezometers |
| PZ-11 | ND | ND | Twice | Nov-14, Mar-15 | X | -- | -- | PW-8 Aq Test temporary piezometers |
| PZ-12 | ND | ND | One-Time | Nov-14 | X | -- | -- | PW-8 Aq Test temporary piezometers |

## 2.4 Groundwater Flow Data

Hydrometrics, Inc. has developed a three-dimensional numerical groundwater model of the proposed Black Butte Copper Mine (Appendix M of the MOP). This model evaluates the effects of mine dewatering on groundwater and surface water in the vicinity of the project and estimates groundwater inflow to the mine working from different hydro-stratigraphic units that are encountered by the UG workings (**Table 2-3**). The maximum extent of drawdown at the top of the water table calculated by the model was in year 4, followed by gradual recession of the drawdown cone as stopes are backfilled with cement paste causing mine inflows to decrease. The water quality model herein uses estimated mine inflow rates at year 6 from the high storage sensitivity analysis to predict water quality during operations. These were selected as a conservative approach as the greatest inflow rates were simulated in the high storage sensitivity analysis. Groundwater flux through different hydro-stratigraphic units was provided by Hydrometrics for year 10 of post-closure. Table 2-3 summarizes the mine inflow rates at year 6 and the post closure groundwater flux through different HSUs.

**Table 2-3.      Simulated Maximum Annual Inflow to Mine Workings (from Hydrometrics, 2016b)**

| Mine Structure | Mine Inflow at Yr 6 (gpm) | Post Closure Groundwater Flux (gpm) |
|---|---|---|
| **Surface Decline Total** | **111** | **99** |
| Surface Decline (Ynl A) | 102 | 91 |
| Surface Decline (UCZ) | 9 | 8 |
| **Upper Access and Stopes Total** | **287** | **8** |
| UZ Access/Stopes (USZ/UCZ) | 274 | 5 |
| UZ Access (Ynl B) | 13 | 3 |
| **Lower Decline Total** | **119** | **3** |
| Lower Decline (Ynl B) | 119 | 3 |
| **Lower Access and Stopes Total** | **27** | **1.3 (assume 0 in model)** |
| LZ Access/Stopes (LCZ) | 10 | 0.3 |
| LZ Access (Ynl B) | 17 | 1 |
| **Total Mine Inflow** | **544** | **111** |

## 2.5 Environmental Geochemistry Data

The acid generation and metal release potential of rock and tailings have been characterized using static multi-element analysis, acid-base accounting, net acid generation potential, and kinetic methods. Results are reported through October 2015 in Appendix D of Tintina's Mine Operating Permit, but have been updated in January 2016 and again in August 2016. A final report will be issued when all ongoing testing is complete.

Waste rock from the Lower-Zone Footwall (LZ FW, 35% of waste rock tonnage), the Lower Newland shale below the USZ zone (Ynl B, 32%), the Upper Sulfide Zone (USZ, 28%), and the Lower Newland shale above the USZ (Ynl A, 4%) will be produced by the project. This rock will be exposed in underground access workings. It will also be stockpiled for up to 2

years on a lined surface pad prior to being co-disposed with cemented tailings early in mine life.  Tailings will also be produced and mixed into cemented paste, for use as backfill (4%) and placement in the surface cement tailing facility (up to 2%).

**Waste Rock Geochemistry**
A total of 8,040 whole rock samples were analyzed to characterize overall geochemical variability within multiple rock units.  Results of ABA and NAG tests indicate that the majority of Ynl A and Ynl B samples (90%) are unlikely to form acid, while many USZ and LZ FW samples have an uncertain potential or are likely to generate acid.  Metal mobility predictions have been based on kinetic test results.

Currently, kinetic tests of Ynl B (2012 and 2015), USZ (2012), and Ynl A (2012) waste rock have been completed following ASTM protocol D5744.  Tests of the LZ FW is completed at week 58 and the USZ (2015) is ongoing, in week 60.  At the time that the model was developed, varying weeks of data were available.  The averaged humidity cell effluent data (weeks 1 to 4, as well as all weeks of available data at the time of modeling, which varied for each HCT) used as model inputs are presented for each of the relevant hydrostratigraphic units in Appendices A and B.

The four main waste rock units to be mined showed evidence of sulfide oxidation in the HCT tests.  However, consistent with static test results and the presence of abundant carbonate mineralization, oxidation in the Ynl B, Ynl A, and LZ FW tests has not produced sufficient acidity to deplete alkalinity nor have these tests produced acidic pH values.  Despite indications of sulfide oxidation, depleted alkalinity and increased acidity with lower pH was only evident in the 2015 USZ test and not in the 2012 test.  This reflects the variation in sulfide mineralization within the USZ.  The 2012 test focused on samples collected from the USZ in the immediate vicinity of the Johnny Lee Decline, while the 2015 composite includes samples collected site-wide and includes copper-enriched rock access zones.

The concentrations of regulated metals were measured in humidity cell effluent from weeks 0, 1, 2, 4, and every 4 weeks thereafter.  Despite maintaining neutral pH in the test cells, the Ynl B, Ynl A, and LZ FW units have shown potential to exceed surface water quality standards for some metals in early weeks of kinetic testing, but do not exceed groundwater standards after week 2.  The 2012 USZ HCT exceeded Pb, Ni, and Tl groundwater standards in leachate from week 0, which is considered a product of sample preparation and was only included in the "all weeks" sensitivity analysis.  Only Tl in week 1 exceeded groundwater standards after week 0, and is included in the base-case model. In contrast to low metal release in the 2012 USZ HCT, the 2015 sample exceeded groundwater standards for As, Be, Cd, Cu, Pb, and Ni in week 0 (due to sample preparation, only included in "all weeks" sensitivity analysis).  Groundwater exceedances were also observed for Ni (week 1) Hg, (weeks 1 and 2) and Sr and Tl (all weeks).

**Tailings Geochemistry**
Splits of homogenized tailings reject produced in bench-scale metallurgical testing were used in static and kinetic tests.  Cement was added to provide structural strength in support of drift and fill mining methods underground, and to change the physical properties of the material to a stable, non-flowable material with low hydraulic conductivity on the order of $10^{-8}$ m/sec in both surface and underground settings.  Static ABA and NAG tests indicate that the tailings will have a strong potential to generate acid, with or without paste amendment.  The following tests have been used for the purpose of modeling, as described below.

Five conventional or modified HCTs (ASTM D5744) were conducted on cemented paste tailing cylinders and non-amended tailings, and diffusion tests (C1308) were performed on two cemented paste tailing cylinders, all of which are described in the Revised Baseline Geochemistry Report (MOP Appendix D). For modeling, the 4% paste cylinder diffusion test was used for predicting the underground conditions at closure, the 4% paste cylinder HCT was used for underground conditions during operations, and the 2% paste cylinder HCT was used for predictions in the CTF at operations and the 4% paste HCT was used for the CTF at closure.

Cemented paste tailing cylinders were tested (without crushing) using the conventional ASTM method D5744 (HCT) to simulate sub-aerial weathering in the underground (during operations) and the CTF, and in ASTM C1308 diffusion tests to simulate diffusion through backfill in saturated underground workings.

Despite the low ABA and NAG results, the 4% paste cylinder yielded largely neutral pH values, and low sulfate and metal release. This is a result of reduced surface area and limited oxidation reactions under saturated test conditions. The diffusion test data for the 4% cylinder (average of all data points) that were used as model inputs for the backfilled stopes are presented in Appendices A and B.

Rates of metal release were substantially lower in diffusion tests of saturated cement paste tailings than in unsaturated humidity cell tests of cemented paste tailings, because oxidation rates are greatly reduced under saturated conditions. Under unsaturated weathering conditions, all of the cemented paste tailings treatments have potential to oxidize after a lag time, with some release of sulfate, acidity, and metals if left exposed to air and water.

Acid and sulfate production in the HCTs varied between the cemented paste treatments, with the 2% test exhibiting greater release than the 4% test, which is reasonably attributable to rapid disaggregation. All tests began at a pH above 6. While the 2% cemented paste began to trend downward in pH between weeks 2 and 4, the 4% paste amended material held pH for several weeks, until sulfide oxidation began to increase in week 8. This suggests that the massive character and lateral support of cemented paste tailings is important in controlling sulfide exposure for oxidation.

Metal concentrations in effluent from the 4% paste cement backfill were lower, and in weeks 1-4 (used for modeling) only exceeded the groundwater quality standard for Tl in week 4. Subsequently, exceedances of As, Cr, Cu, Ni, and Tl groundwater standards were observed. Metal concentrations in effluent from the 2% cemented paste exceeded groundwater standards for As, Ni, and Tl regularly in the early weeks of testing. Concentrations of Be, Cu, U, and Zn, were also observed to exceed groundwater standards in week 4. Subsequent to week 4, frequent groundwater exceedances were observed, which is likely the result of disaggregation of the highly weathered, poorly supported cylinder geometry.

Tintina proposes to place 0.5 to 2% cemented paste tailings in its surface CTF, and to continuously collect and remove water from that impoundment. Importantly, the observed disaggregation in the 2% HCT did not occur immediately, and the rate of weathering in a HCT is recognized to be greater than in the field, particularly for the small, unconfined cylinder of paste cement with a high surface area to mass ratio as was used in the HCTs. Therefore, in the CTF, each newly added lift of cemented paste tailings will behave as a massive block of material with low transmissivity, with a thin upper surface that will be

exposed to some degree of oxidation before being covered by fresh paste tails within 60 days of placement.  If material is covered in the manner described in the mine operation plan (generally within a week but never more than 60 days), oxidation, acidity, and leaching of metals would be limited to the immediate surface of the cemented paste tailings.  Any water interacting with oxidized tailings will subsequently travel through the ramp and rock drain, where it will react with waste rock as it is collected for treatment to meet water quality standards prior to discharge in the infiltration galleries.

# 3   Modeling Approach

To predict impacts to water quality, Enviromin developed a mass-load model for i) the UG, ii) the temporary WRS pad, iii) the CTF, and iv) the combined input to the PWP and ultimately, the WTP.  We predict a mass load for each facility under a base case scenario and various sensitivity scenarios.  The model evaluates UG, CTF, WRS and PWP facilities under operational scenarios, and the UG and CTF at closure.  For each facility and time, the mass-load solution is evaluated for equilibrium solubility and sorption constraints using the USGS PHREEQC geochemical model, as discussed below.

## *3.1   Mass Load Assumptions*

The predicted water chemistries for each facility are divided by rock or material type and described using estimated water flows (Hydrometrics, 2015) and kinetic (or diffusion) test results, described in Section 2.  The models scale the mass load (i.e., release of ions, metals, and protons) from each rock unit according to the reactive mass (or surface area, for diffusion test data) and the water flow.  Scaling is appropriate because the surface area (or reactive mass) of bench scale test reactors (e.g., HCTs) differ from those anticipated under field conditions.  To provide a final mass prediction in the collection sump for each facility, the mass contributed by each rock unit is added to the groundwater chemistry at each location, and then mixed together in the sump.  This mass-load approach is conservative because it neglects phase removal at isolated, high-concentration sources.  We assume an exposure time of one week for flow calculations and release rates, and because the available test data are generally based on one week of exposure.  The models estimate water quality for each facility at future times that represent conditions during full operations and closure (if applicable).

- For the UG, we predict the water quality in the sump at year 6 of operation and at closure (i.e., >13 years).  We divide the underground workings into seven rock units with estimated surface areas (Tintina operational plans), groundwater flow rates and chemistries (Hydrometrics), and kinetic test data (Enviromin).  By design, the 4% cemented paste used underground for roof support will consume added water during the curing process; less than 1% water (by weight) will be released during the consolidation within the stopes so this is not included in the mass load model (AMEC, 2016, Appendix K7 of Tintina's MOP).  In the sump, the flow rates and chemical inputs from all seven units are mixed and allowed to precipitate and sorb according to PHREEQC.

- For the WRS, we estimate a reactive mass based on the volume of waste rock that could be saturated in a year of flow.  After one year, the average flow, based on HELP model predictions is 0.9 gpm (Hydrometrics, 2016a).  The saturated reactive mass was then converted to a surface area based on an assumed distribution of blast fragments (Hyle, 2016).  The HCT data were then scaled to the appropriate rock type using surface area data.

- For the CTF, we estimate the water quality at year 6 of mining, and at closure (i.e., >13 years).  We assume that the entire surface of the cemented tailings facility is exposed to an estimated precipitation rate of 84,000 m$^3$/yr (Knight Piesold, 2015).  The surface includes 2% paste tailings during operations with an average of 4,000 tonnes of co-deposited waste rock that is assumed to be exposed to weathering at any given time.  A portion of the runoff (10%) is also exposed to the waste rock used to construct the ramp/basin drain.  During operations, we include water that releases

from the wet paste, which has higher water content to ensure pumpability and due to atmospheric precipitation onto the CTF (see AMEC, 2016b, Appendix K7 of Tintina's MOP). Water comprising 5% of the paste deposited each week by weight (i.e., 29,029 $m^3$/yr) was represented using water chemistry measured in process water during metallurgy tests. At closure, we assume the surface to be 4% cemented paste tailings.

- For the PWP, we use the predicted chemistry for the UG at year 6 of operations and for the CTF at year 6 of tailings production. We add direct precipitation and runon, as well as water from the mill (i.e., chemistry of process water from bench metallurgical tests from Austin, 2015). We equilibrate the mixed solution with PHREEQC to estimate the chemistry of water reporting to the WTP.

## 3.2 Geochemical Modeling of Mineral Precipitation and Metal Sorption

Enviromin estimates equilibrium conditions of the mixed solutions using the USGS code PHREEQC (Parkhurst and Appelo, 1999), which has been rigorously tested and is the industry standard for aqueous geochemistry. We used the *minteq.dat* thermodynamic database supplied with version 3.1.1-8288 version of PHREEQC. Redox conditions were determined based on the recognized pe/pH conditions in natural water, as reported by Baas Becking in his time honored study of water worldwide (1960). For the UG during operations, and CTF at closure, we set pe + pH = 13, to represent moderately oxidizing conditions within the open workings. During UG closure, we set pe + pH = 7, to represent a more suboxic environment in the flooded and backfilled mine workings. In the surface facilities, i.e. WRS, PWP and CTF during operations, we set pe + pH = 15 to represent the fully oxidizing surface environment modeled for these settings. Charge is initially balanced on magnesium, and charge is maintained by balancing on pH after reactions occur. Appendix C shows an example input model, for the UG model at year 6.

At the sump of each facility, we predict the mineral phases that will precipitate and the metals that will sorb to precipitated iron oxide (specifically, ferrihydrite). In the event of supersaturation, the following phases were allowed to precipitate: alunite, celestite, gypsum, K-jarosite, barite, $Ba_3(AO_4)_2$, gibbsite, ferrihydrite, fluorite, quartz, $MnHPO_4$, $SbO_2$, and $Cr_2O_3$. These minerals were chosen based on initial supersaturation in some solutions, and general likelihood to occur in mine-affected water associated with the Black Butte Copper deposit. Understanding the saturation states of these minerals is not only important to predict water quality, but also to assess potential mineral scaling in the system.

**Table 3-1.      Mineral Phases Allowed to Precipitate in PHREEQC Modeling**

| Equilibrium Phase | Ideal Formula | Rationale for Inclusion in PHREEQC Model |
|---|---|---|
| Alunite | $K_2Al_6(SO_4)_4(OH)_{12}$ | Primary control on aluminum in mine affected water (Eary, 1999). |
| Celestite | $SrSO_4$ | Oversaturated in sump water. |
| $Ba_3(AsO_4)_2$ | $Ba_3(AsO_4)_2$ | Close to saturation in sump water |
| Barite | $BaSO_4$ | Primary control on barium (Eary, 1999). |
| K-jarosite | $KFe_3(SO_4)_2(OH)_6$ | Common secondary product of sulfide oxidation |
| $Cr_2O_3$ | $Cr_2O_3$ | Oversaturated in sump water. |
| Ferrihydrite | $5Fe_2O_3.9H_2O$ | Major control on iron. Thermodynamic properties well defined (Dzombak and Morel, 1990).  Sorption substrate for various metals and oxyanions. |
| Quartz | $SiO_2$ | Close to or saturated in sump water |
| Fluorite | $CaF_2$ | Primary control on fluoride (Eary, 1999). |
| Gibbsite | $Al(OH)_3$ | Primary control on aluminum at pH >4.5 (Eary, 1999). Oversaturated in sump water. |
| Gypsum | $CaSO_4.2H_2O$ | Primary control on sulfate in mine pit lakes (Eary, 1999). Close to saturation in sump water |
| $MnHPO_4$ | $MnHPO_4$ | Primary control on manganese at circum-neutral pH (Eary, 1999). Oversaturated in sump water |
| $SbO_2$ | $SbO_2$ | Close to saturation in sump water |

Metals are allowed to sorb to ferrihydrite precipitated from modeled solutions under oxidizing conditions using the default PHREEQC parameters for sorption site surface area and density of strong/weak sites in diffuse layer calculations (Parkhurst and Appelo, 2013).  All metals with ferrihydrite sorption isotherm data provided in the *minteq.dat* database were allowed to potentially sorb.  Sorption to sulfide minerals stable under reducing conditions (based on isotherms which are not incorporated in the PHREEQC database) were calculated using published isotherm data.

## 3.3  Sensitivity Analyses

To evaluate uncertainty in model predictions, we assessed the sensitivity of the models to key assumptions and input parameters.  These sensitivity scenarios, which vary between the UG, WRS, CTF, and PWP models, are summarized here and as Appendix D to this report, and presented in detail for each model in Sections 4, 5, 6, and 7 below.

# 4  Underground Workings Water Quality Model

## 4.1  Conceptual Model

The access tunnels, decline, access workings and stopes, will transect various rock types in the subsurface, as shown in **Figure 4-1**.  To be consistent with groundwater flow data (from Hydrometrics, 2016b), we divided the underground model into seven hydrostratigraphic units.

**Figure 4-1.     Conceptual model of the seven hydrostratigraphic units, each providing input to the sump**



| Unit | Humidity Cell | GW Chemistry | Flow at yr 6 (gpm) |
|---|---|---|---|
| Decline Ynl A | 2012 Ynl | Avg (MW-1B, -2A, -2B, -4B, -9, PW-1 and -8) | 102 |
| Decline USZ | 2012 USZ | PW-9 Avg | 9 |
| Upper Ore access/stopes USZ/UCZ | 2015 USZ 4% Binder Diff. | Avg (MW-3, PW-2, PW-4) | 274 |
| Decline Ynl B | 2015 YnlB | PW-10 | 13 |
| Lower Access Ynl B | 2015 YnlB | PW-10 | 119 |
| Lower Ore access/stopes LCZ | 2015 LZFW 4% Binder Diff. | PW-9 from UCZ, because data for PW-7 are poor | 10 |
| Lower Zone Access Ynl B | 2015 LZFW | PW-10 | 17 |

Predicted water quality in the sump

Each of the units was assigned a total flow input, a surface area (based on operational plans), and a rock type that correlates with kinetic test data.  For the model, each unit can be conceptually viewed as a large kinetic test, scaled based on surface area and flow rate.  The scaling approach is described in detail in Section 4.3.3.  The mixed solution incorporating inflow from all seven units is allowed to reach geochemical equilibrium, using PHREEQC, and then the water reports to the water treatment facility.

The quality of water in the UG was predicted during operations at year 6 and post-closure, following rebound of the groundwater to original elevation.  The assumptions and inputs used in these base cases are compared with changes made in sensitivity analyses in Appendix D.  For the UG at year 6 of operations, the sensitivity of modeled predictions was tested by halving and doubling the base case fracture density; using an average of HCT data from all weeks instead of weeks 1-4; increasing the base case oxidation rate from 6 to 40 kg/m2/yr; increasing the reactive mass zone thickness from 1 to 2 m; doubling the area

of paste backfill; and testing the combined influence of oxidation rate, rind thickness, fracture density, and backfill surface area assumptions on the reactive mass calculations. The reactive mass scenario compounds conservatism by using upper bound values for all of the assumptions together in a highly conservative prediction of water quality. In the post-closure model for the UG, factors affecting modeled sulfide oxidation (oxidation rate, fracture density, rim thickness, etc.) are no longer relevant under suboxic conditions. The sensitivity analyses for the UG closure model therefore evaluate the influence of doubling backfill surface area and tests the effect of propagating detection limits through the mass load calculations. Supporting evidence for these assumptions and inputs is provided below.

## 4.2  Data Sources

The model incorporates groundwater flow and chemistry data and geochemistry data from kinetic tests to predict future underground water quality. These data are describe below.

### 4.2.1  Groundwater Quality Data

To represent groundwater chemistries, the model uses data collected from wells, listed under GW Chemistry in **Figure 4-1**. Appendix E summarizes the groundwater chemistry provided by Hydrometrics and used to develop averages for wells and hydrostratigraphic units. These data varied in the number of samples collected per well (over time) and the number of wells completed in each lithotype. Additionally, the parameters analyzed for individual samples varied. In some cases, data were reported both above and below method detection limits, and in other instances, all results were reported below method detection limits. The reported method detection limits were used as values when analyzing the data. For all of these reasons, the data were thoroughly evaluated from a quality control standpoint. Statistical methods were used to test for the presence of outliers in the data prior to their inclusion in the water quality model. Also, well PW-7, which was contaminated by drill fluids, was excluded from use in the modeling calculations.

Enviromin evaluated the full groundwater data set to identify and possibly reject any results that failed due to statistical or quality assurance/quality control (QA/QC) criteria. The data were provided to Enviromin in a spreadsheet format by Hydrometrics, Inc. As discussed below, out of a total of 2,490 data points, only six were rejected as statistical outliers and none were rejected due to QA/QC issues.

### 4.2.1.1 Representative Data

Some rock types have larger data sets and thus narrower confidence intervals than others. This is the result of more wells used to characterize the rock type as well as more sampling events. Limited data for certain rock types relative to others does not imply the data misrepresents groundwater in those rock types, but there is greater uncertainty in the model input parameters derived from the smaller data sets.

### 4.2.1.2 Average Calculations

We evaluated seven different groundwater-bearing rock types and used data from 13 monitoring wells within those rock types, listed in **Figure 4-1**. As shown in

**Table 4-1**, the 13 monitoring wells are not evenly distributed among the seven rock types. Further, the single well (PW-7) completed in the LZ FW produced so little water that it could not be properly developed; resulting water quality issues have led to its exclusion from this analysis. Water quality data from PW-9, conservatively representing the poorest quality groundwater from the UCZ, was used to represent the LZ FW.

The number of monitoring events ranged from sixteen events for MW-1B to a single event for wells PW-1, PW-2, PW-4 and PW-10.  The number of monitoring events per well is indicated in parentheses for each well in

**Table 4-1**, which total 91 individual well-specific monitoring events.

**Table 4-1.       Wells Used for Groundwater Input Data**

(number of monitoring events per well); UA, underground access; LD, lower decline

| Ynl A | USZ/UCZ | UCZ | Ynl B-UA | Ynl B-LD | LCZ | Ynl B-LA |
|-------|---------|-----|----------|----------|-----|----------|
| MW-1B (16) | MW-3 (13) | PW-9 (5) | PW-10 (1) | PW-10 (1) | PW-9 (5) | PW-10 (1) |
| MW-2A (14) | PW-2 (1) | | | | | |
| MW-2B (14) | PW-4 (1) | | | | | |
| MW-4B (13) | | | | | | |
| MW-9 (3) | | | | | | |
| PW-1 (1) | | | | | | |
| PW-8 (5) | | | | | | |

Some 29 to 31 groundwater parameters were used as model input parameters, depending on the sampling event.  This is because phosphorus and silicon were included in only a small number of laboratory analyses from certain wells, so in many cases the number of parameters totaled only 29.  Laboratory results were below detection for a large number of many analytes, and for all censored values, the detection limit was used.

With a total of 91 well-specific monitoring events, the maximum number of data points in the evaluation is 2,821 based on 31 groundwater parameters per well per event.  However, as discussed above, because phosphorus and silicon were included in only small number of laboratory analyses, the actual number of total data points in the full data set used for groundwater input is 2,490.

For each rock type, the average value of each of the 29 to 31 input parameters was calculated using all of the statistically valid data (see below) provided by Hydrometrics.  The number of significant figures in the average calculations was determined by the value for each analyte with the fewest number of decimal places.  For most of the laboratory results, the number of significant figures remained constant for a given analyte throughout all monitoring events in a set, although there were some instances where results had a different reporting limit.

### 4.2.1.3 Three Sigma Evaluation

Enviromin performed a statistical evaluation of the data set to ensure the groundwater data set represented each of the seven hydrostratigraphic units. Groundwater input parameters consist of various parameters and analytes reported by Energy Laboratory of Billings, Montana for groundwater samples collected from multiple wells at the site by Hydrometrics. The data were provided to Enviromin by Hydrometrics as tabulated spreadsheet entries.

Enviromin used the "empirical rule" of statistics to identify outliers, which were excluded from the averages used as individual model input values.  For a normal distribution of random data points, the "three sigma test," states that 68 percent of the data in the set fall within one

standard deviation (σ) of the mean (μ) of the full set, 95 percent fall within two standard deviations (2σ), and 99.7 percent fall within three standard deviations (3σ).  Therefore, any result larger than the mean plus three standard deviations was rejected, i.e.,

$$\text{If Value} > \mu + 3\sigma, \text{ then reject.}$$

For laboratory results that were below reporting limits, the value of the reporting limit was used in the calculations.  Furthermore, in events where both a natural and duplicate sample were collected, only the natural sample was used in the calculations.

Additionally, Enviromin also looked at Energy Laboratory's internal data quality assurance/quality control evaluation and the subsequent data QA/QC evaluation conducted by Hydrometrics conducted on all laboratory groundwater data and concluded that the data used to establish model input parameters are valid.

The results of the three sigma evaluation of the groundwater data are summarized below in **Table 4-2**.  As shown in the table, only 6 out of 2,490 data points were rejected as outliers from the three-sigma evaluation.  Furthermore, all of those rejected data points came from the two largest data sets, i.e., Ynl A and USZ/UCZ which had 1,769 and 429 data points, respectively.

**Table 4-2.      Three Sigma Evaluation Results Groundwater Input Data**

|  | Ynl A | USZ/UCZ | UCZ | LCZ | Ynl B Upper Access | Ynl B Lower Decline | Ynl B Lower Access | Totals |
|---|---|---|---|---|---|---|---|---|
| Total Data Points | 1,769 | 429 | 144 | 58 | 30 | 30 | 30 | 2,490 |
| Rejects | 4 | 2 | 0 | 0 | 0 | 0 | 0 | 6 |

## 4.2.1.4 QA/QC Evaluation

Hydrometrics J-flagged many results.  None of the values failed internal laboratory quality assurance/quality control criteria, but instead the results were qualified due to issues with relative percent differences between natural and duplicate samples.  Specifically, in any event in which the RPD between a natural sample and a duplicate sample result exceeded 20 percent, not only was the result of that analyte J-flagged for that particular sample, but as a conservative measure, the results for that particular analyte were J-flagged for all samples collected during the sampling event.

However, in evaluating data quality, failure of the RPD criteria does not warrant rejection of a result, either for the natural sample for which the RPD was exceeded or for any of other results in the full data set.  Therefore, none of the J-flagged results in the data set were rejected on that or any other quality assurance/quality control criterion.

## 4.2.2  HCT Data

Chemical contributions to groundwater of each hydrostratigraphic unit are based on the baseline geochemistry testing conducted since 2011.  Specifically, these data are from seven kinetic humidity cell tests (HCTs) and one diffusion test: the Ynl A, Ynl B, and USZ HCTs from 2012, and the Ynl B, LZ FW, USZ, and 4% cement HCTs from 2015, as well as the diffusion test of tailings with 4% cement.  We used an average of HCT data for weeks 1-4.  Due to the initially high solute release rate in weeks 1 and 2 of most HCT data, data from weeks 1-4 represents a reasonable, relatively conservative approach to modeling inputs because early solute release rates are often the high relative to subsequent weeks.  To

address model sensitivity to this approach, an average of all weeks (available at the time the modeling was conducted) was also used as a sensitivity analysis for the UG model.

For the paste backfill during operations, we use data from the 4% cement HCT, averaged over weeks 1-4.  For the closure model, we use the average diffusion test data for 14 samples were collected over 11 days, to account for the saturated conditions and longer-term exposure.  The averages used as model inputs are presented in Appendix A of this report.  All original geochemical test results, used in calculating averages, have been presented in the Draft Baseline Geochemistry Report (Appendix D, MOP), and updated more recently in regulatory communications.

## 4.3  Mass Load Model Calculations

### 4.3.1  Surface Area Calculations

For each lithostratigraphic unit, Enviromin estimates open tunnel lengths based on the projected mine schedule for stope development in the upper and lower workings (Tintina MOP, 2015).  Consistent with Tintina's design, the tunnels are assumed to be 5 m across and 5 m high and provide the basis to calculate the open surface area, including the back (roof) and sill (floor) walls.  Surface areas for the year 6 underground model assume the conditions projected for the start of year 6 and are, therefore, based on surfaces exposed during years 1-5 of mine life.  At that stage, Tintina has projected that approximately 20% of the stopes will have been mined and backfilled.  Furthermore, Tintina proposes to have 0.67% of the stopes open at any given time in the mine life.  Surface areas used for the closure scenario in the underground model assume that the mining is complete and all mined stopes have been backfilled, as proposed by Tintina.  In contrast to the 2% material that will be used to fill the CTF, which will be made with excess water to ensure adequate flow during placement, the 4% cemented paste tailings used in the underground workings will be made with a limited volume of water to ensure compressive strength.  It will also cure in a warm underground stope where it will be exposed to dry ventilation air, thus promoting hydration of the binder material and ensuring that very little water (less than 1% by weight) will be discharged in the underground workings (AMEC, 2016b, Appendix K7 of Tintina's MOP).  For these reasons, dewatering water is not included in the UG model.

To calculate the reactive mass of the paste backfill, which has much lower transmissivity, Enviromin has not assumed an equivalent porous media model as was done for the fractured walls.  Rather we estimate the surface area of the backfill and scale it to the surface area of the samples used in diffusion tests.  At year 6, ~20% of the stopes will have been backfilled; at closure, 100%.  For the reactive surface of the backfilled paste, we assume that a 5-inch gap exists above 5% of the paste backfill surface; this conservatively represents the reality that backfilling process will leave some pockets where complete filling is not accomplished.  Our estimate of 5%, which is based on 3rd party observation of paste backfilling operations at an existing underground mine (where similar methods are currently in use) is likely conservative, as the proactive management contemplated by Tintina improves the completeness of backfill and subsequent filling of adjacent stopes will provide lateral secondary backfilling (AMEC, 2016a, Appendix K6 of Tintina's MOP). The size of the gap (i.e., 5") is not as relevant as the fact that it exists, and therefore exposes the reactive surfaces shown in red in **Figure 4-2**.

**Figure 4-2.    Conceptual Model of Surface Area Within Backfilled Stopes
at Year 6 (above) and at Closure (below).**
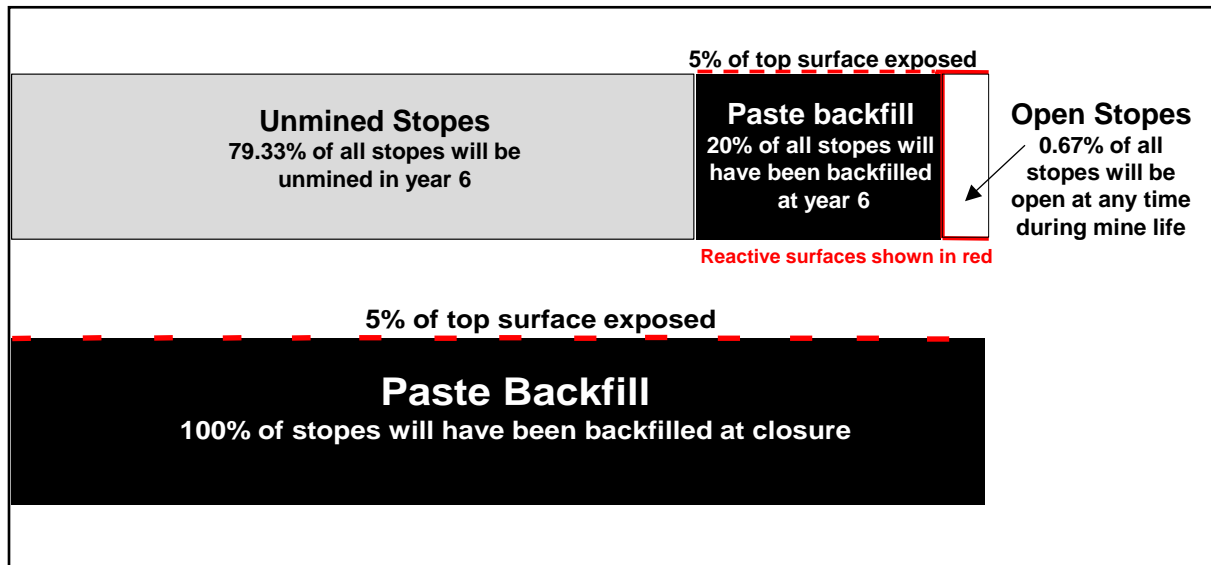


In addition to the stopes and backfills, we include the surface areas of all ramps and access tunnels, based on the primary lithologies of the workings.  The final surface areas are summarized in **Table 4-3**.

**Table 4-3.    Surface Area Values for Year 6 and Closure**

| Hydrometrics Hydrostratigraphic Categories | Contributions from Table 1 in Mine Development.pptx from Tintina | Calculated surface areas @ Year 6 | Calculated surface areas @ Closure |
|---|---|---|---|
| Surface Decline YNL A | Ynl under water table (a total of 740 meters with 495 meters below the water table) | **9,900** | **9,900** |
| Surface Decline UCZ | USZ (ramp) (60 meters) | **1,200** | **1,200** |
| UZ Access/Stopes (USZ/UCZ) + Ceiling of backfilled UZ stopes | Sum Open Access/stopes of USZ (3640 m)and linear feet of open stopes (770 m = 11 open stopes at 70 m) + 5% of the ceilings in backfilled stopes | **91,545** | **72,800** |
| UZ access Ynl B | Ynl B (UZ access (2500 meters) | **50,000** | **50,000** |
| Lower Decline Ynl B | Ynl B ramp (3170 meters) | **63,400** | **63,400** |
| Lower Zone Access, grouped with stopes in Hydrometrics classification | LZ FW (LZ access, 4720 meters) | **94,400** | *94,400* |
| LCZ Stopes (LCZ)+ ceiling of backfilled LZ stopes | Linear feet of open stopes (350 meters = 7 open stopes @ 50 m) + 5% of ceilings in backfilled stopes | **8,713** | **-** |
| Lower Zone Access (Ynl B) | LZ FW (ramp, 1240 meters) | **27,280** | *27,280* |
| Paste Tailings backfill-UZ | 5% of ceiling of backfilled block.  Ceiling dimension = total linear meters mined in USZ in years 3-5 multiplied by width of paste block. | **3,346** | **14,653** |
| Paste Tailings backfill-LZ | 5% of ceiling of backfilled block.  Ceiling dimension = total linear meters mined in USZ in years 3-5 multiplied by width of paste block. | **1,714** | *13,176* |
| *\* Lower zone surface areas have no effect at closure because the flow rate is assumed to be zero* | | | |

## 4.3.2 Calculation of Reactive Mass

Using estimated surface areas, as described in Section 4.3.1, the reactive mass ($R_m$) of each fractured wall surface was estimated according to

$$R_m = S * F_D * T_{RZ} * \rho,$$

where $S$ is the surface area (m$^2$, shown in **Table 4-3**), $F_D$ is the fracture density, $\rho$ is the rock density, (kg/m$^3$), and $T_{RZ}$ is the thickness of the reactive zone. The density of each rock type was estimated using measurements conducted by Tintina; 3,600 kg/m$^3$ for Upper and Lower Copper Zones, and 2,710 kg/m$^3$ for Ynl units, respectively.

As an equivalent porous media model (EPM), $F_D$ accounts for the difference in the surface area of a fractured volume and the surface area of unconsolidated HCT material. In other words, the finely-ground, unconsolidated material in HCT samples would have a $F_D$ of 100%. At the opposite extreme, unblasted wall rock with no natural faults or fractures would have a $F_D$ of 0%. In the base case model, we assume a $F_D$ of 10% in the upper zone, meaning that the fractures induced by the blasts have a reactive surface area that is 10% of the surface area of HCT material. A 10% $F_D$ is conservative because it is on the high end of previously reported studies of pit walls fracture densities, which would be under less lithostatic pressure than subsurface workings and would be expected to have higher fracture density. (Siskind and Fumanti, 1974; Kelsall et al., 1984). In the lower units we assume a $F_D$ of 2%, which is based on a higher lithostatic load and is supported by 2-3 lower orders of magnitude observed permeability in those units. We evaluate model sensitivity by changing $F_D$ to twice the base case (i.e., 20% for upper unit and 4% for lower unit) and to half the base case (i.e., 5% and 1%).

The base case model assumes that $T_{RZ}$ has a maximum of 1 meter. Early reports (Kelsall 1984, and Siskind and Fumanti, 1974) indicate that blast fracturing in granite and basalt walls is generally limited to a depth of 1 meter, beyond which rock porosity was unchanged by blasting. Kelsall et al. (1984) also show that typical values range from 0.3 m to 1.0 m, so our estimate is conservative. We evaluate model sensitivity to this assumption by using a 2-meter maximum $T_{RZ}$ in a sensitivity scenario.

While the maximum $T_{RZ}$ is determined by fracture penetration from blasting, the actual $T_{RZ}$, and thus the $R_m$, is a function of oxidation of the sulfide minerals. Once the initial fracturing occurs, the reactive zone grows as oxygen diffuses from inside the tunnel and oxidizes sulfide minerals. Kempton et al. (2009) point out that physical processes (i.e., oxygen diffusion) are more important than chemical processes for determining intrinsic rate coefficients for sulfide oxidation, as suggested by the "shrinking core" model (Davis et al., 1986). The oxygen profile in the rock, and thus the sulfide oxidation rate, is related to sulfide content because the conversion of sulfide to sulfate consumes oxygen (Davis, 1983).

The base case model assumes an oxidation rate of 6 kg SO$_4$/m$^2$/year, based on observations and models describing rates of oxidation in pit walls (Kempton et al., 2009). Field observations reported by Kempton and Atkins (2009) suggest a maximum of 6 kg SO$_4$/m$^2$/year, while models have indicated an initial maximum rates of sulfide oxidation of 21 kg SO$_4$/m$^2$/year, with a subsequent decline to a value of 10 kg SO$_4$/m$^2$/year. A value of 40 kg SO$_4$/m$^2$/year was reported for fresh surfaces on a pit bench. For a sensitivity analysis, we use 40 kg SO$_4$/m$^2$/year. To convert from these rates to a mass of sulfide oxidized, we assume the stoichiometry of the following reaction:

$$2FeS_2 + 7.5O_2 + 7H_2O \leftrightarrow 4SO_4^{2-} + 2\,Fe(OH)_3 + 8H^+$$
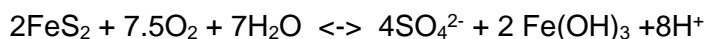
The actual calculation of Rm proceeds as follows:

$$R_m(kg) = \left(X\frac{kg\ SO4}{yr*m2}\right)\left(\frac{kmol\ SO4}{96\ kg\ SO4}\right)\left(\frac{kmol\ S}{kmol\ SO4}\right)\left(\frac{32\ kg\ S}{kmol\ S}\right)\left(\frac{kg\ rock}{Y\ kg\ S}\right)\left(\frac{2\ kmol\ S}{kmol\ FeS2}\right)\left(\frac{2\ kmol\ FeS2}{4\ kmol\ SO4}\right)*S(m^2)$$
$$*A(days)*\left(\frac{1\ yr}{365\ days}\right)$$

1. Use the sulfide oxidation rate ($X = 6$ kg $SO_4/m^2$/year in the base case) to calculate the mass $SO_4^2$ after $A$ days of exposure.
2. Convert $SO_4^2$ produced to $FeS_2$ oxidized, based on the stoichiometry above
3. Convert mass of $FeS_2$ oxidized to mass of rock oxidized, (based on $Y$, the mass fraction of sulfur in the rock)
4. Convert the mass of rock oxidized ($R_m$) to a $T_{FZ}$, based on the density of the rock, according to $R_m = S * F_D * T_{FZ} * \rho$. If the calculated $T_{FZ}$ is less than 1 meter, then we use the calculated value for $R_m$. If the calculated $T_{FZ}$ exceeds 1 meter, then we fix the $T_{FZ}$ at 1 meter and recalculate an $R_m$ based on the rock density.

**Figure 4-3** shows a cross-section of the maximum reactive zone, based on fracture penetration of one meter. The reactive zone (i.e., oxidized rind) grows over time, from the inside, as sulfide oxidizes. For the access tunnels, we assume that oxidation has occurred for 6 years, thus increasing the reactive thickness accordingly. We assume that flow infiltrates through the reactive zones on all four sides of the tunnels.

**Figure 4-3.    Schematic Cross-Section of Mine Workings with an Oxidized Zone That Grows Outward**



**Blast-induced fracture zone**
The base case maximum fracture zone is one meter. Reported values are typically 0.3-1 m (Siskind and Fumanti), although typically <0.5 m for low-charge methods (Kelsall et al.).

**Oxidized rind (reactive zone)**
The rind thickness increases as a function of time and sulfide content (i.e., oxygen consumption). The base case assumes that the rind increases according to sulfide oxidation (sulfate production),

$2FeS_2(s) + 7.5O_2 + 7H_2O \leftrightarrow 4SO_4^{2-} + 2\ Fe(OH)_{3(S)} + 8H^+$

at a rate of 6 kg $SO_4^{2-}/m^2$/yr.

## 4.3.3 Scaling of HCT Data to Reactive Mass

The model estimates the release of components in each unit based on data from humidity cell tests (HCTs). HCTs have a known volume of water, reactive mass of rock, and time of exposure. For each rock type that releases a component at a rate ($\dot{r}$), we scale HCT results based on the assumption that the concentration, $C_i$, of the released component (e.g.,

metals, protons, etc.) is proportional to the ratio of reactive mass (or surface area) to the volume of water per time (i.e., flux, $Q$). That is,

$$C_i \;=\; \frac{Reactive\ mass\ (R_m)}{Volume\ of\ water\ per\ time\ (Q)} \; \dot{r}.$$

Because ($\dot{r}$) is an intensive property of the material, we can use the proportionality ($C_i\ \alpha\ R_m/Q$) to estimate the concentration of each constituent ($i$) released from the rock in the field ($C_{rock,i}$), according to

$$C_{rock,i} = \frac{\left(R_m/Q\right)_{rock}}{\left(R_m/Q\right)_{HCT}} C_{HCT,i}.$$

**Figure 4-4** provides a visual description of how inflow ($Q$) into each known mass ($R_m$), then reacts to produce a concentration ($C$).

**Figure 4-4.    Schematic Showing Scaling of HCT Data to Predict Chemistry in the Wall Rock**
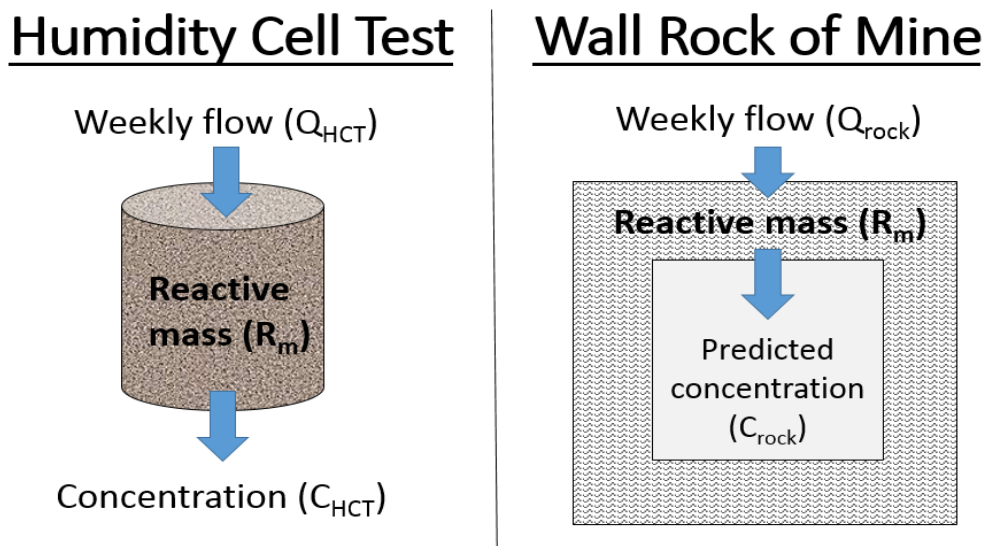


In the model, the ratio of $(R_m/Q)_{rock}$ to $(R_m/Q)_{HCT}$ is referred to as the "scaling factor" because it provides a value that directly scales the field "reactor" to the lab "reactor". After estimating the contribution of the rock from the scaling factor, we add the baseline groundwater contributions (data Appendix E), according to

$$C_{predicted,i}\left(\frac{mg}{L}\right) = C_{rock,i}\left(\frac{mg}{L}\right) + C_{groundwater,i}\left(\frac{mg}{L}\right).$$

Finally, we combine the contributions from all seven units to predict the mass load in the final solution in the sump. This mixed solution is then modeled using PHREEQC to evaluate the potential for precipitation and sorption.

## 4.4  Geochemical Modeling of Underground Water

For each solution that collects in the sump, the model allows precipitation of the following phases: alunite, celestite, gypsum, K-jarosite, barite, quartz, $Ba_3(AsO_4)_2$, gibbsite, ferrihydrite, fluorite, $MnHPO_4$, $SbO_2$, and $Cr_2O_3$.  These phases were chosen based on supersaturation in calculated solutions, as well as general likelihood of occurrence in mine-affected water.  If the solution is not supersaturated in one of the identified phases, then there is no effect on the solution.  Dissolution of precipitated minerals or bedrock is not allowed in the model; these reactions are represented empirically by the accelerated weathering environment of the HCT.

If ferrihydrite is supersaturated, then sorption of metals is allowed on the surface using the default parameters for ferrihydrite surface area and sorption site density and isotherm data provided with the PHREEQC *minteq.dat* database (Parkhurst and Appelo 2013, Appendix C).  Under reduced conditions, as would exist following saturation of the bedrock and cemented paste fill in the UG at closure, sorption to iron sulfide is calculated using published sorption isotherm data and mineralogy (Appendix F).  This mechanism is included because pyrite is known to adsorb a variety of metals common to mining environments (Doyle et al., 2004; Borah and Senapati, 2006; Oxverdi and Erdem, 2006) and has been proposed for use in reactive barrier technology to remove metals from contaminated groundwater (Brown et al. 1979).

## 4.5  Water Quality Prediction for Year 6 Operations

For year 6 of operations, **Table 4.4** shows the predicted chemistry of the base case and all sensitivity analyses.  We also provide the baseline groundwater chemistry and groundwater standards according to MT DEQ.  We estimated a $NO_3^-$ concentration of 18 ppm (as N) based on values from an effectively managed underground Montana mine currently in operation.  This is because $NO_3^-$ release will depend on future blasting practices and is difficult to predict in advance.  The use of these data as a proxy for Tintina's planned blasting practices is reasonable.  The mass loads calculated for each input source are shown in Appendix G.

The base case model predicts neutral to mildly acidic water during UG operations.  The mass load calculations suggest that the greatest load of metals, acidity, and sulfate comes from the UCZ unit.  As the groundwater flow rate from the UCZ is lower, this contribution is substantially diluted by cleaner water from the Ynl A and Ynl B units. Furthermore, the load contributed by the UCZ unit would decrease if the model allowed supersaturated phases to precipitate prior to mixing in the sump.  While this is the more likely "real world" scenario, thermodynamic modeling of individual inputs prior to mixing would be time consuming for multiple sensitivity scenarios. By accounting for mineral precipitation and metal sorption after mixing, we have been conservative in our approach to predicting mass load, as all solute input to the model reports to the sump.

The predicted water quality for the year 6 underground base case suggests a slight decline in alkalinity to 183 mg/L, with an associated decrease in pH from 7.09 to 6.86.  These changes are in response to sulfide oxidation during mining operations, as indicated by a 50% increase in sulfate to a predicted concentration of 304 mg/L.  The abundant carbonate mineralization in the exposed lithotypes clearly provides neutralization potential in buffering acidity resulting from sulfide oxidation, and the extent of predicted oxidation is low at neutral pH. Alunite, $Ba_3(AsO_4)_2$, ferrihydrite, and quartz are predicted to be supersaturated in the base case, providing substrate for sorption of As, Be, Cu, Mn, Ni, Sr. Se, and Tl.  In the oxidizing environmental of the active workings, no sorption to sulfide minerals was allowed.

The resulting predicted chemistry shows little change for many metals.  The concentrations of Al, Fe, Ba, and As are reduced as a result of mineral precipitation.  The concentrations of $NO_3^-$, Cu, F, Mn, Ni, Sb, Se, Tl, U and Zn in the sump water are predicted to increase (above background concentrations) prior to collection for treatment to meet non-degradation standards.  Of these, only $NO_3^-$, As, and U are predicted to exceed Montana DEQ groundwater quality standards in the operational base case and multiple sensitivity scenarios (Table 4.4).  Arsenic also exceeds the standard in groundwater under background conditions, however, and only rises above the background concentration in the reactive mass sensitivity scenario.  Likewise, the background concentration of Sr in groundwater is elevated above the MT DEQ standard of 4 mg/L; predicted concentrations under elevated oxidation rate and high reactive mass sensitivity scenarios are higher than background. Thallium is predicted to exceed the standard in the conservative elevated sulfide oxidation and reactive mass scenarios, while Sb is predicted to exceed the groundwater standard only in the combined high reactive mass scenario.  In general, the assumptions about fracture density and reactive-zone thickness have the greatest effect on predicted metal release, and the inclusion of all week HCT data has the greatest effect on the pH. The predicted value of 18 mg/L nitrate (as N) assumes that no denitrification occurs during operations, when the workings will be fully ventilated.  As noted, this value will depend considerably on operational blasting practices.  Because all water will be collected during operational dewatering for treatment to meet non-degradation criteria prior to discharge, these predicted changes will not affect downgradient water quality.

The various sensitivity analyses show relatively minor variation in predicted pH (4.89 - 6.88), alkalinity (180-207), and sulfate (262-672 mg/L) across a range of changes: fracture density; HCT input; increasing the sulfate production rate to a maximum value of 40 kg/m$^2$/yr; doubling of the oxidation zone to 2 meters; and doubling of the backfill surface area.  Metal concentrations vary somewhat between sensitivity analyses (**Table 4-4**), and appear to be more sensitive to surface area assumptions (fracture density and reactive zone thickness) than to sulfide oxidation, which more directly influences pH and sulfate concentrations. Even in the high reactive mass sensitivity scenario (right side of Table 4-4), which incorporates conservative sensitivity values for multiple parameters, including the maximum oxidation rate, a 2 m rim thickness, and twice the backfill surface area and fracture density, pH is predicted to be 6.56, with 207 mg/L alkalinity and 672 mg/L sulfate.  Metals are elevated in this latter scenario, with U, Tl, Sr, Sb, and As exceeding groundwater standards, although it is highly unlikely that all of these parameters would concurrently increase to theoretical maximum values in the underground workings at year 6.  Regardless, these results show that any attendant uncertainty associated with the base case UG water quality predictions is modest.  Despite these predicted changes in water quality, they are not material because water will be collected during operational dewatering of the workings for reverse-osmosis treatment to meet non-degradation criteria.

## *4.6  Water Quality at Closure*

During initial flushing of stored oxidation products (which will have accumulated on some exposed surfaces during operations) as the mine floods, Tintina proposes to treat water until steady state conditions develop in the saturated and backfilled workings.  Reduced groundwater flowing through remaining voids will react with the exposed paste and bedrock surfaces, as described in **Section 4.3.2**.  This model predicts chemistry under saturated, post-filling conditions.

Several parameters change in the closure model.  We assume that all stopes are closed and backfilled, and that groundwater recovers to its original elevation.  The decline and a

portion of the access development will remain open, but it will be flooded creating suboxic conditions so that sulfide oxidation will not occur.  At the relatively neutral pH of the system, iron oxide will precipitate, so oxidation by ferric iron is not a concern.  Further, because the hydrostratigraphic units below the Volcano Valley Fault are predicted to contribute very little if any water in closure, and will be isolated from the upper workings by a hydraulic plug, they are not considered to function as aquifers post-closure (Hydrometrics, 2016b).  They are therefore not included in the closure model.  Changes in flow and flow ratios shift background groundwater quality slightly, compared to operating conditions.  The estimated flow rates are shown in **Table 2-3**.  **Table 4-5** shows the predicted water chemistry at steady state closure for the base case, as well as an analysis of model sensitivity to doubling backfill surface area.  The mass load calculated for each input term is shown in Appendix H. Background groundwater chemistry, MT DEQ standards for groundwater quality and estimated non-degradation criteria for groundwater are included in Table 4-5 (Hydrometrics, 2016, in Appendix N1 of Tintina's MOP). We estimated an $NO_3^-$ concentration of 0.18 ppm (as N) based on the assumption that 99% of the nitrate would be removed via denitrification under sub-oxic conditions within the flooded workings at closure. Denitrification (the conversion of $NO_3^-$ to $NO_2^-$ and $N_2$ gas**)** by native heterotrophic bacteria, is a common and highly efficient process under low oxygen conditions when carbon is available.  Due to the low diffusivity of oxygen in water and low predicted flow of water in the mine post-closure, as well as the elevated carbon content of the lower Newland shales, denitrification is very likely to occur at a high level of efficiency, removing virtually all nitrate.  As noted previously, the actual concentration of nitrate will be determined by blasting practices.

**Table 4-4.    Model Predictions for Underground Water Quality at Year 6 of Operations**

| | | Mixed Groundwater with No Mine Influence | Underground model predictions at yr 6, after PhreeqC | | | | | | | | Groundwater Standards (MT DEQ-7) |
|---|---|---|---|---|---|---|---|---|---|---|---|
| | | | BASECASE (HCT wk1-4, 1 m max rind, Fracture density 10% in UZ and 2% in LZ, Oxid. Rate = 6 kg/m2/yr) | Fracture density one half basecase | Fracture density twice basecase | All HCT data of wall rock | Oxid. Rate = 40 kg/m2/y | 2 m max reactive zone thickness | Paste backfill surface area doubled | Combined High Reactive Mass Parameters (Oxid Rate 40, 2-meter rind, fracture density x2, backfill SAx2) | |
| pH | s.u. | 7.09 | 6.86 | 6.88 | 6.82 | 4.89 | 6.67 | 6.82 | 6.79 | 6.56 | na* |
| Al | mg/L | 0.014 | 0.010 | 0.012 | 0.009 | 0.229 | 0.008 | 0.009 | 0.010 | 0.024 | na |
| Alkalinity | mg/L CaCO₃ | 218 | 183 | 180 | 188 | 182 | 184 | 188 | 183 | 207 | na* |
| As | mg/L | 0.051 | 0.004 | 0.002 | 0.009 | 0.068 | 0.004 | 0.009 | 0.004 | 0.101 | 0.01 |
| Ba | mg/L | 0.049 | 0.00086 | 0.00117 | 0.00053 | 0.00883 | 0.00140 | 0.00053 | 0.00097 | 0.00022 | 1 |
| Be | mg/L | 0.0008 | 0.0005 | 0.0004 | 0.0006 | 0.0011 | 0.0006 | 0.0006 | 0.0005 | 0.0020 | 0.0040 |
| Ca | mg/L | 76 | 89 | 83 | 100 | 90 | 103 | 100 | 89 | 141 | na |
| Cd | mg/L | 0.000045 | 0.000045 | 0.000045 | 0.000045 | 0.000045 | 0.000045 | 0.000045 | 0.000045 | 0.000045 | 0.005000 |
| Cl | mg/L | 1.29 | 1.38 | 1.34 | 1.44 | 1.43 | 1.64 | 1.44 | 1.40 | 1.86 | na* |
| Cr | mg/L | 0.007 | 0.00046 | 0.00044 | 0.00050 | 0.01044 | 0.00068 | 0.00050 | 0.00052 | 0.00091 | 0.1 |
| Cu | mg/L | 0.0019 | 0.0005 | 0.0004 | 0.0007 | 0.3448 | 0.0009 | 0.0007 | 0.0006 | 0.0067 | 1.3 |
| F | mg/L | 0.64 | 0.96 | 0.82 | 1.26 | 0.83 | 0.99 | 1.26 | 0.97 | 2.12 | 4 |
| Fe | mg/L | 1.81 | 0.0016 | 0.0015 | 0.0017 | 0.0057 | 0.0024 | 0.0017 | 0.0018 | 0.0024 | na** |
| Hg | mg/L | 0.000006 | 0.000006 | 0.000006 | 0.000006 | 0.000006 | 0.000006 | 0.000006 | 0.000006 | 0.000006 | 0.002000 |
| K | mg/L | 3.4 | 11 | 8 | 17 | 10 | 12 | 17 | 11 | 37 | na |
| Mg | mg/L | 47 | 57 | 51 | 69 | 52 | 72 | 69 | 57 | 109 | na |
| Mn | mg/L | 0.146 | 0.165 | 0.162 | 0.172 | 0.180 | 0.313 | 0.172 | 0.165 | 0.334 | na** |
| NO₃ | ppm as N | 0.02 | 18.0 | 18.0 | 18.0 | 18.0 | 18.0 | 18.0 | 18.0 | 18.0 | 1 |
| Na | mg/L | 11 | 14.7 | 13.1 | 17.8 | 14.7 | 15.0 | 17.8 | 14.7 | 27.9 | na |
| Ni | mg/L | 0.004 | 0.006 | 0.005 | 0.009 | 0.049 | 0.010 | 0.009 | 0.007 | 0.017 | 0.1 |
| P | mg/L | 0.011 | 0.004 | 0.003 | 0.006 | 0.012 | 0.003 | 0.006 | 0.003 | 0.021 | na |
| Pb | mg/L | 0.001 | 0.00002 | 0.00002 | 0.00004 | 0.00099 | 0.00002 | 0.00004 | 0.00002 | 0.00255 | 0.015 |
| SO₄ | mg/L | 205 | 304 | 262 | 388 | 285 | 398 | 388 | 305 | 672 | na** |
| Sb | mg/L | 0.0015 | 0.0032 | 0.0025 | 0.0046 | 0.0024 | 0.0033 | 0.0046 | 0.0032 | 0.0089 | 0.006 |
| Se | mg/L | 0.0005 | 0.0039 | 0.0024 | 0.0069 | 0.0018 | 0.0042 | 0.0069 | 0.0039 | 0.0151 | 0.05 |
| Si | mg/L | 8.78 | 1.55 | 1.55 | 1.55 | 1.54 | 1.55 | 1.55 | 1.55 | 1.54 | na |
| Sr | mg/L | 10.5 | 10.5 | 10.4 | 10.8 | 10.4 | 11.4 | 10.8 | 10.5 | 12.1 | 4 |
| Tl | mg/L | 0.001 | 0.002 | 0.002 | 0.002 | 0.002 | 0.005 | 0.002 | 0.002 | 0.006 | 0.002 |
| U | mg/L | 0.005 | 0.037 | 0.021 | 0.069 | 0.029 | 0.038 | 0.069 | 0.037 | 0.133 | 0.03 |
| Zn | mg/L | 0.029 | 0.029 | 0.028 | 0.032 | 0.040 | 0.031 | 0.032 | 0.030 | 0.041 | 2 |

Supersaturated phases in basecase: Alunite, Ba3(AsO4)2, Cr2O3, ferrihydrite, quartz          empirical prediction of endpoint, not based on modeling

See discussion of sensitivity scenarios in Section 4.1.                    *narrative standards may exist          **secondary standard

*Results include the mass load from the seven lithological units, precipitation of supersaturated phases and sorption on ferrihydrite, based on PHREEQC models.*

**Table 4-5.     Model Predictions for Underground Water Quality at Closure**

| | | Mixed Groundwater with No Mine Influence | Underground model predictions at closure, after PhreeqC | | | Groundwater Standards (MT DEQ-7) | Estimated Groundwater Non-degradation Criteria |
|---|---|---|---|---|---|---|---|
| | | | BASECASE | Paste backfill surface area doubled | Detection limits = 0 | | |
| pH | s.u. | 6.97 | 6.91 | 6.86 | 6.91 | na* | 6.0-7.8 |
| Al | mg/L | 0.015 | 0.015 | 0.015 | 0.015 | na | 0.058 |
| Alkalinity | mg/L CaCO$_3$ | 193 | 151 | 153 | 151 | na* | na |
| As | mg/L | 0.0262 | 0.0002 | 0.0004 | 0.0002 | 0.01 | 0.064 |
| Ba | mg/L | 0.055 | 0.0042 | 0.0035 | 0.0042 | 1 | 0.1928 |
| Be | mg/L | *0.0008* | *0.0005* | *0.0007* | *0.0004* | 0.004 | 0.00095 |
| Ca | mg/L | 61 | 64 | 71 | 64 | na | na |
| Cd | mg/L | 0.000042 | 0.000042 | 0.000042 | 0.000042 | 0.005000 | 0.0008 |
| Cl | mg/L | 1.40 | 1.7 | 2.0 | 1.7 | na* | na |
| Cr | mg/L | 0.00653 | 0.00041 | 0.00044 | 0.00041 | 0.1 | 0.025 |
| Cu | mg/L | *0.0017* | *0.0008* | *0.0010* | *0.0005* | 1.3 | 0.1970 |
| F | mg/L | *0.35* | *0.36* | *0.40* | *0.33* | 4 | 1.2 |
| Fe | mg/L | 5.13 | 3.66 | 3.68 | 3.65 | na** | na |
| Hg | mg/L | 0.000006 | 0.000006 | 0.000006 | 0.000006 | 0.002 | 0.000010 |
| K | mg/L | 2.2 | 2.9 | 3.8 | 2.9 | na | na |
| Mg | mg/L | 31 | 21.5 | 20.3 | 21.5 | na | na |
| Mn | mg/L | 0.053 | 0.052 | 0.054 | 0.051 | na** | na |
| NO$_3$ | ppm as N | 0.06 | 0.18 | 0.18 | 0.18 | 1 | 7.5 |
| Na | mg/L | 4.5 | 4.8 | 5.3 | 4.8 | na | na |
| Ni | mg/L | *0.0045* | *0.0050* | *0.0057* | *0.0043* | 0.1 | 0.025 |
| P | mg/L | 0.015 | 0.006 | 0.009 | 0.006 | na | na |
| Pb | mg/L | 0.00147 | 0.00004 | 0.00005 | 0.00003 | 0.015 | 0.0028 |
| SO$_4$ | mg/L | 111 | 115 | 124 | 115 | na** | 250** |
| Sb | mg/L | 0.0028 | 0.0001 | 0.0001 | 0.0001 | 0.006 | 0.002 |
| Se | mg/L | *0.0005* | *0.0009* | *0.0012* | *0.0005* | 0.05 | 0.0085 |
| Si | mg/L | 9.97 | 1.55 | 1.55 | 1.55 | na | na |
| Sr | mg/L | 2.1 | 2.1 | 2.2 | 2.1 | 4 | 6.48 |
| Tl | mg/L | 0.0037 | 0.0037 | 0.0038 | 0.0037 | 0.002 | 0.0039 |
| U | mg/L | 0.00522 | 0.00504 | 0.00511 | 0.00497 | 0.03 | 0.008 |
| Zn | mg/L | *0.022* | *0.022* | *0.025* | *0.019* | 2 | 0.317 |

*Italicized predictions affected by detection limit propogation in the model*          *narrative standards may exist
prediction of endpont, not based on modeling          **secondary standard
Supersaturated phases in basecase: Ba3(AsO4), Cr2O3, ferrihydrite, quartz

*Results include precipitation of supersaturated phases and sorption to ferrihydrite and sulfide.*

Diminished oxidation due to flooding, completion of backfilling, and reduced inflow of water from below the VVF produces the base case chemistry shown in **Table 4-5**. While the predicted pH and alkalinity are lower than background groundwater quality, and a bit lower than the quality predicted underground during operations, predicted pH is 6.91 with 151 mg/L alkalinity and a sulfate concentration of 115 mg/L. No parameters fail to meet MT groundwater standards or non-degradation criteria in post-closure groundwater. Our sensitivity analysis shows that propagation of detection limits for censored (less than detect) values results in overestimation of increased concentrations for Be, Cu, F, Ni and Zn. This is shown in Table 4-5 where the italicized values illustrate the predicted value when the detection limits are removed and replaced with zero.

The minerals Ba$_3$(AsO$_4$)$_2$, Cr$_2$O$_3$, ferrihydrite, and quartz, are predicted to be oversaturated, and their precipitation influences the water quality prediction as shown in **Table 4-5**. Sorption of several metals, notably As, Cu, Ni, Sr, Tl, U and Zn, to precipitated ferrihydrite reduces their concentrations, as does sorption of Cd and Hg to pyrite.

# 5  Waste Rock Storage Facility Water Quality Model

## 5.1  Conceptual Model

Approximately 411,537 tonnes (453,642 tons) of waste rock will have been be generated from the Ynl A, USZ, and Ynl B at the end of year 2 of mining operations.  This rock will be stockpiled on a temporary, lined waste rock storage (WRS) facility before it can be placed in or co-disposed with tailings in the cemented tailings facility (CTF).  The WRS will be constructed in three 16-ft lifts, with 8-foot benches, up to a maximum height of 50 ft (15 m) above a 100 mil thick HDPE-lined pad (**Figure 5-1**).  Additional waste rock to be produced from the LZ FW and LCZ after CTF construction begins will report directly to that facility and will not be placed on the stockpile. The waste rock has potential for acid generation and metal leaching (see Section 2.4.2 of the Tintina Operating Permit Application).

The model assumes that three types of waste rock will be stored on the WRS facility: Ynl A will be deposited first, followed by USZ and then Ynl B, based on the order they will be encountered during mine development **(Figure 5-1**).  The LZ FW will not be produced for placement on the WRS pad. Therefore the model incorporates the relative tonnages of the remaining rock types that will be present on the WRS pad, i.e., 6.25% Ynl A, 43.75% USZ, and 50% Ynl B.  However, all of this mass is not assumed to be reactive: rather, we estimate the reactive mass based on the maximum material that could be saturated by 1 year of water flow at the estimated flow rate (0.9 gpm).  Precipitation is assumed to flow preferentially through the partially saturated waste rock after an initial year of wetting and collects in a drain system that then reports to the water treatment facility.  The purpose of this model is to predict the chemistry of water that collects in the drain prior to treatment.

**Figure 5-1.    Conceptual Model of Waste Rock Storage Facility (from Knight Piesold)**
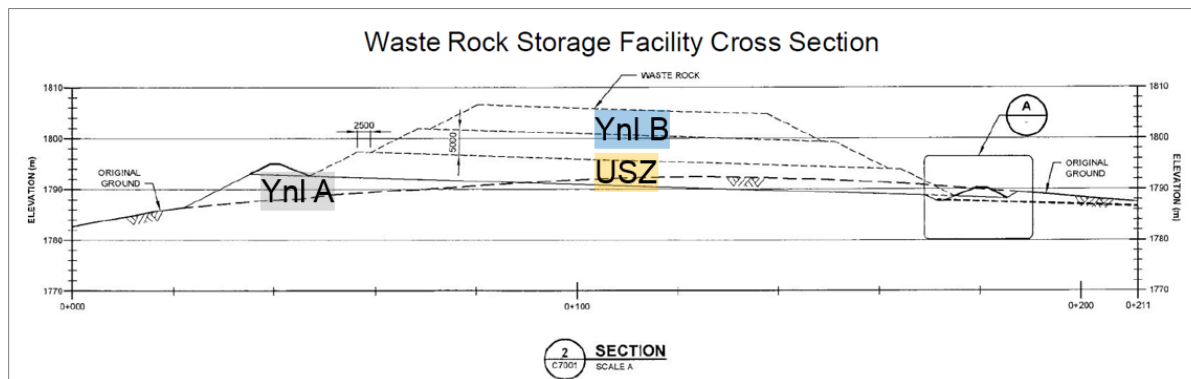


The assumptions and inputs used in the WRS base case are compared with changes made by halving the reactive mass in the sensitivity analyses described in Appendix D. Functionally, these changes also represent the effect of halving duration of infiltration, doubling the porosity, or halving the waste rock surface area. Supporting evidence for these assumptions and inputs is provided below.

## 5.2  Data Sources

### 5.2.1  Waste Rock HCT Data

The environmental geochemistry testing methods and assumptions were described in section 2.5.  For the WRS facility, we use HCT data from 2012 Ynl to describe the Ynl A portion, 2015 USZ to describe the USZ portion, and 2015 Ynl B to describe the Ynl B

portion.  For consistency with other models, data from week 1 to 4 were averaged for use in the model. Due to the short operating life of the WRS, use of the early weeks of testing is particularly appropriate.  Appendix A shows these data.

## 5.2.2  Water Balance

Hydraulic behavior at the proposed WRS facility was modeled by Hydrometrics, Inc., using the Hydrologic Evaluation of Landfill Performance (HELP) model, developed by the Army Corps of Engineers (Hydrometrics 2016a; Shroeder et al., 1994).  The HELP model uses climate data to predict one-dimensional moisture flow through a soil profile, accounting for evapotranspiration, snow removal, solar radiation, and average precipitation.  The HELP model predicts an average flow rate of 4.31 L/min (0.9 gpm) through the WRS facility, once steady state saturated flow is achieved after year 1.

## *5.3  Mass Load Model Calculations*

## 5.3.1  Calculation of Reactive Mass and Surface Area

The flow rate (4.31 L/min) is very low in relation to the size of the WRS facility, so it is not reasonable to assume that all of the waste rock surface will be saturated and exposed to infiltration at the end of year 2.  To account for this, we conservatively estimate a reactive mass by calculating the amount of rock that can be saturated by 4.31 L/min of flow for one year.  We chose one year as a calculation time frame based on the approximate time that it takes to establish a steady-state seepage, according to the HELP model.

To calculate the reactive mass, we start with the yearly water flow, 1,785,551 L/yr based on 4.31 L/min.  We assume that the unconsolidated rock pile has 40% porosity to calculate the volume of rock that could be saturated.  Lastly, using the density of the rock, we calculate the reactive mass for each rock type *(i)*.  The overall equation is

$$R_{m,i}(tons) = \frac{L_{H2O}}{yr} * \frac{1000\ cm^3_{H2O}}{L_{H2O}} * \frac{6\ cm^3_{rock}}{4\ cm^3_{H2O}} * \frac{g_{rock}}{cm^3_{rock}} * \frac{ton_{rock}}{10^6 g_{rock}} * \frac{ton_i}{ton_{rock}}$$
.

The resulting calculation suggests that ~2% of the total WRS material is exposed to infiltrating meteoric water and is thus reactive.  Using $R_m$, we then calculate a reactive surface area $R_{SA}$ of each rock type by using a published gradation of run of mine waste rock from the underground workings of the Ashanti mine (**Figure 1-2**, from Hyle, 2016, Appendix D2 of Tintina's MOP) to predict the surface area of future waste rock for Black Butte Copper.  This rock size gradation is representative of particle size distributions in rock mined using typical blasting practices.  While some changes will exist between the gradation for Ashanti and the Black Butte Copper mine, this uncertainty that has been addressed through sensitivity analysis, by doubling and halving the surface area.

**Figure 5-2.    Waste Rock Gradation from Ashanti Mine (Hyle, 2016)**



| Diameter (inch) | Mass % |
|---|---|
| 7.87 | 27.4 |
| 3.9 | 28.6 |
| 2.1 | 23.8 |
| 1.1 | 8.3 |
| 0.5 | 6 |
| 0.3 | 3.6 |
| 0.07 | 2.4 |

Assuming that the particles are spherical, the specific surface area is calculated to be 0.0559 $m^2$/kg for the USZ and 0.0743 $m^2$/kg for the Ynl B and Ynl A.  The difference is based on the different rock densities (all calculations shown in the model).  The spherical assumption underestimates true surface areas but is consistent with the spherical assumption in the surface area estimate for the humidity cell test material.  Assuming that the sphericity of the particles is similar in the two cases, this assumption balances out when we scale the surface area between the two HCT samples and the blasted waste rock.

For the waste rock samples in the humidity cell tests, the reactive surface area was estimated from sieved analyses.  From these calculations, assuming spherical particles, the specific surface areas are 2.01 $m^2$/kg for USZ, 2.94 $m^2$/kg for Ynl A and 3.01 $m^2$/kg for Ynl B.

## 5.3.2  Scaling of HCT Data to Reactive Surface Area

For the waste rock water quality prediction, we use an approach to scaling that is similar to the UG model (Section 4.3.3) to predict mass load.  Rather than scaling to a reactive mass within a fractured, equivalent porous media (EPM) model, we scale the WRS material to reactive surface area.  We do this because the WRS material is unconsolidated and particle sizes (i.e., surface areas) control reactivity; fracture-density and rind-thickness estimates are thus not applicable.

The model estimates the release of components in each unit based on data from humidity cell tests (HCTs).  HCTs have a known volume of water, reactive mass of rock, and time of exposure.  For each rock type that releases a component at a rate ($\dot{r}$), we scale HCT results based on the assumption that the concentration, $C_i$, of the released component (e.g.,

metals, protons, etc.) is proportional to the ratio of reactive surface area to the volume of water per time (i.e., flux, $Q$). That is,

$$C_i \;\;=\;\; \frac{Reactive\ surface\ area\ (R_{SA})}{Volume\ of\ water\ per\ time\ (Q)}\ \dot{r}.$$

Because $(\dot{r})$ is an intensive property of the material, we can use the proportionality $(C_i\ \alpha\ R_{SA}/Q)$ to estimate the concentration of each constituent ($i$) released from the rock in the field ($C_{WRS,i}$), according to

$$C_{rock,i} = \frac{\left(R_{SA}/Q\right)_{WRS}}{\left(R_{SA}/Q\right)_{HCT}} C_{HCT,i}.$$

In the model, the ratio of $(R_{SA}/Q)_{WRS}$ to $(R_{SA}/Q)_{HCT}$ is referred to as the "scaling factor" because it provides a value that directly scales the field "reactor" to the lab "reactor."  The final solution after mass-load estimation is input into PHREEQC to allow for precipitation and sorption to ferrihydrite.

## *5.4 Predicted Water Quality at Year 2 of Mining*

**Table 5-1** shows the predicted chemistry of water draining from the WRS facility at year 2, in addition to the baseline groundwater chemistry and the MT DEQ groundwater standards for comparison.  The sensitivity analysis (i.e., 0.5x) can be interpreted in a few ways: if the model assumes a 0.5x value for surface area, the effect is identical to assuming 0.5x infiltration time or 0.5x reactive mass.  Because we base the estimate of reactive mass on water infiltration over one year, then a change in the precipitation would have no effect – i.e., the higher surface area is negated by the proportional water for dilution. The mass loads calculated for each input source are shown in Appendix I.

The model predicts a pH of 5.49 for the base case, where saturated flow occurs in 2% of the waste rock.  Predicted sulfate concentration is high, at 3,780 ppm in the base case.  This is likely conservative, due to dissolution of solutes from the HCT (with higher surface area and a higher water:rock ratio) into a very small predicted volume of water.  We estimated a $NO_3^-$ concentration of 18 ppm (as N) based on values from another underground Montana mine, although the actual concentration will vary with blasting practices.  The predicted pH is 5.79 in the sensitivity scenarios.The model is very sensitive to rock/water ratio (e.g., changes in infiltration relative to surface area), which explains the very conservative base case result.  When the reactive mass is halved, e.g., if porosity were to be doubled or surface area was halved, the sulfate concentrations drop and pH increases.  Minerals predicted to precipitate include barite, celestite, fluorite, gypsum, jarosite, $MnHPO_4$, and quartz, based on PHREEQC predictions.  No sorption was predicted due to the absence of ferrihydrite.  Several metals increase in proportion to infiltration/surface area, together with $SO_4,$ but of these, only $NO_3$, Ni and Tl exceed the MT DEQ groundwater standard in the base case.

The waste rock on the temporary WRS pad will be stored on a liner with a small estimated volume of water reporting from the WRS pad liner drainage system to the lined contact water pond (CWP) where it will be collected for treatment until rock is placed into the CTF. Waste rock leachate will be treated to meet non-degradation criteria.

**Table 5-1.          Year 2 Results for Waste Rock Storage Facility**

| | | Model predictions for WRS at Yr 2 | | Groundwater Standards (MT DEQ-7) |
|---|---|---|---|---|
| | | Basecase | Reactive mass halved (<u>OR</u> 6 mo infiltration <u>OR</u> half surface area <u>OR</u> 80% porosity) | |
| pH | s.u. | 5.49 | 5.79 | na* |
| Al | mg/L | 0.172 | 0.069 | na |
| Alkalinity | mg/L CaCO$_3$ | 47 | 24 | na* |
| As | mg/L | 0.008 | 0.004 | 0.01 |
| Ba | mg/L | 0.002 | 0.002 | 1 |
| Be | mg/L | 0.002 | 0.001 | 0.004 |
| Ca | mg/L | 404 | 333 | na |
| Cd | mg/L | 0.00061 | 0.00031 | 0.00500 |
| Cl | mg/L | 10 | 4.93 | na* |
| Cr | mg/L | 0.028 | 0.014 | 0.1 |
| Cu | mg/L | 0.065 | 0.032 | 1.3 |
| F | mg/L | 2.49 | 1.43 | 4 |
| Fe | mg/L | 0.002 | 0.003 | na** |
| Hg | mg/L | 0.0020 | 0.0010 | 0.0020 |
| K | mg/L | 60 | 30 | na |
| Mg | mg/L | 685 | 344 | na |
| Mn | mg/L | 6.7 | 3.4 | na** |
| NO$_3$ | ppm as N | 18.0 | 18.0 | 1 |
| Na | mg/L | 24 | 12.2 | na |
| Ni | mg/L | 0.144 | 0.072 | 0.1 |
| P | mg/L | 0.014 | 0.008 | na |
| Pb | mg/L | 0.0068 | 0.0034 | 0.0150 |
| SO$_4$ | mg/L | 3780 | 2211 | na** |
| Sb | mg/L | 0.004 | 0.002 | 0.006 |
| Se | mg/L | 0.017 | 0.009 | 0.05 |
| Si | mg/L | 1.13 | 0.62 | na |
| Sr | mg/L | 9.3 | 11.0 | 4 |
| Tl | mg/L | 0.165 | 0.083 | 0.002 |
| U | mg/L | 0.002 | 0.001 | 0.03 |
| Zn | mg/L | 0.042 | 0.021 | 2 |

prediction of endpoint, not based on modeling

<u>Supersaturated phases in basecase</u>: Barite, celestite, fluorite, gysum, jarosite, MnHPO4, quartz

*narrative standards may exist      **secondary standard

*Results include precipitation of supersaturated phases and sorption*

# 6 Cement Tailings Facility Water Quality Model

## 6.1 Conceptual Model

In year 3, the cement tailings facility (CTF) will become operational and will store both cemented paste tailings and waste rock from UG development workings and the temporary WRS pad.  After construction, Tintina will begin mining and milling copper-enriched rock to produce copper concentrate, and cement pasted tailings will be co-deposited with end-dumped waste rock in the lined CTF, as shown in **Figure 6-1** (Tintina MOP, 2015).  A drain system designed to prohibit standing water and promote direct runoff to a rock-lined sump will be constructed of waste rock.  Approximately every week, but not longer than every 60 days, a new paste layer will be deposited across the CTF surface.  Water from precipitation (84,000 m³/yr) is assumed to contact the surface of the dried paste in addition to the co-deposited waste rock.  Water will additionally be introduced through dewatering of the wet 2% cement paste tailings. Unlike the 4% cement pasted tailings, which will be mixed to provide strength in roof support underground, the 2% cement paste tailings will have water added to ensure flow during deposition. Every day the mine will generate 2,900 tonnes of paste; on average, 55% will be deposited in the CTF and the remainder will go underground. From the deposited paste, as much as 5% of the mass will seep out as water, producing 29,029 m³/yr (AMEC, 2016b Appendix K7 of Tintina's MOP).

**Figure 6-1.    Conceptual Model of CTF Showing Waste Rock Ramp and Local Placement of Waste Rock Mined from UG, Year 6 of Tailings Production**
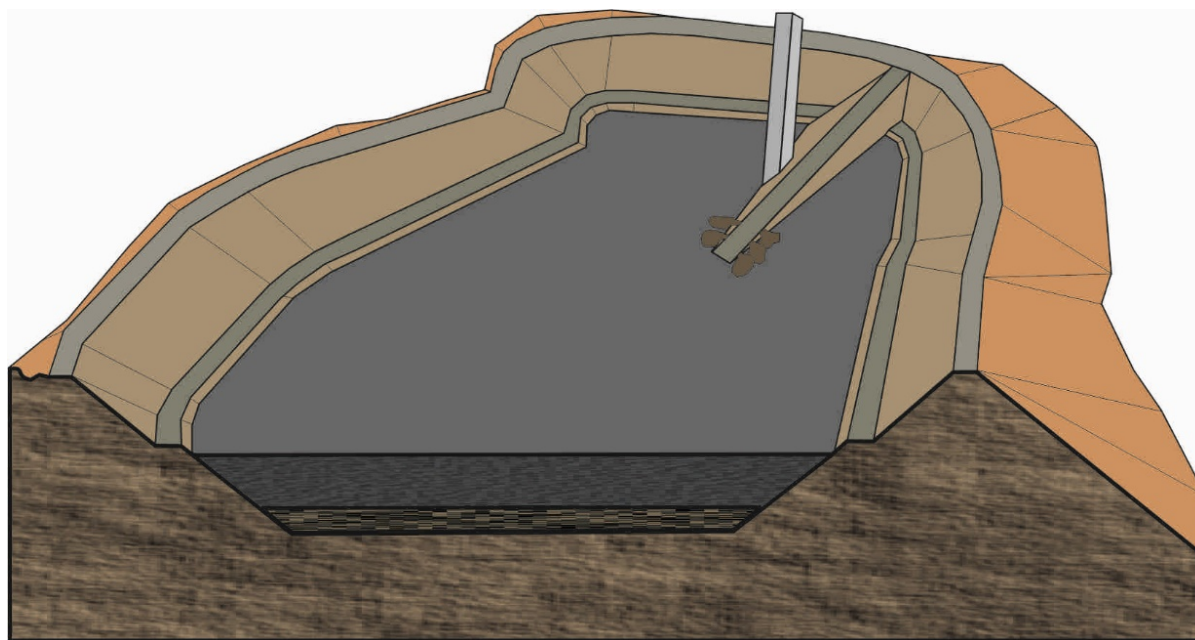


Using the estimated surface areas of the paste and the waste rock, we estimate mass-load inputs by scaling to the appropriate humidity cell test of pasted tailings, ultimately predicting water quality in the sump.  The model further evaluates the predicted sump water quality with a PHREEQC geochemical model, allowing precipitation of supersaturated phases and sorption to ferrihydrite surfaces if ferrihydrite is supersaturated.

Water quality at year 6 of tailings production, and in early closure (when all tailings have been deposited) has been estimated as part of this study. In closure, all water from the sump will be pumped to the water treatment facility until the volume declines to acceptable closure levels (determined by DEQ) following placement of a composite geomembrane and fill / soil cover.

The quality of water in the CTF was predicted at year 6 of tailings production and in early closure, prior to placement of the geosynthetic cap and construction of the vegetated cover. The assumptions and inputs used in these base cases are compared with changes made in sensitivity analyses in Appendix D. The sensitivity of the model was tested by doubling the waste rock and cement surfaces. The cement surface was also halved. Supporting evidence for these assumptions and inputs is provided below.

## *6.2 Data Sources*

The model assumes two sources of water input: precipitation (i.e., rain/snow water) and water seeping from the wet paste. Precipitation water is assumed to be distilled water, and the wet paste seepage is estimated from water quality measured in process water from metallurgical tests (Appendix J, from Austin, 2015). The metallurgical data did not report alkalinity; therefore we estimated total alkalinity values of in the mass-load model of 400 ppm (as $CaCO_3$), which slightly exceeded the calculated alkalinity input from other dissolved species that were measured, and thus allowed the PHREEQC model to run and close.

### 6.2.1 Cemented Paste HCT Data

Because the runoff water will contact the cemented-paste surface for a short time (i.e., the material will not be saturated like the cemented pasted backfill in the underground), we used humidity cell test data for the 2% paste to estimate a mass load on a weekly basis for the year 6 model and 4% paste for the closure model.

## *6.3 Mass Load Calculations*

To calculate the mass load, we apply an approach similar to that used for the WRS facility, where we estimate the surface area and water flow, then scale according to a proportionality between flow and surface area. In other words, the concentration, $C_i$, of the released component (e.g., metals, protons, etc.) is proportional to the ratio of reactive surface area to the volume of water per time (i.e., flux, $Q$). That is,

$$C_i = \frac{Reactive\ surface\ area\ (R_{SA})}{Volume\ of\ water\ per\ time\ (Q)}\ \dot{r}.$$

### 6.3.1 Estimation of Paste Material Surface Area

The reactive surface area of pasted tailings will increase over time. We estimate relative surface areas of the CTF surface and kinetic tests based on different extents of weathering. The 2% cemented paste cylinder showed visible evidence of disaggregation in the HCT; this was true to a lesser extent for the 4% cement. HCTs are designed and intended to expedite weathering, so it most likely that the CTF surface will weather at a slower rate; however, we do not have field data for a CTF to use and therefore cannot speculate as to how much slower the field rate will be. Further, the extent of disaggregation is strongly influenced by the amount of cement paste amendment, with incremental increases in cylinder disaggregation over changing time frames (e.g., weeks 1 and 4 in the HCT), but we only have surface area measurements at the start and end of testing (weeks 0 and 28).

We therefore account for the fact that the HCT data come from material that has been weathered for 1-4 weeks at the test cell scale, whereas the CTF will weather on a timeline of 1-8 weeks at full scale, which we represent with 1 week of equivalent test cell weathering.

The CTF mass-load model assumes that solute release is proportional to surface area and thus weathering. The HCT data support this assumption, in that the release of a conserved solute such as sulfate increased exponentially during early weeks of weathering, when progressive disaggregation was observed. We therefore use the HCT sulfate data to estimate the relationship between time and weathering on the relevant scale (i.e., compare the HCT surface area with the predicted CTF surface area). This requires that we assume that the intrinsic rates of reaction are the same in the HCT as they would be in the field; this is a strongly conservative assumption that is required in the absence of field scale data.

If we look at the 4% and 2% paste HCT data for the initial time frame when disaggregation occurs, both visibly and according to sulfate data, and we assume that sulfate production is proportional to surface area (as assumed in the UG mass-load model), both data sets are well described by a physical model of surface area that increases at an exponential rate with time, to the power of 1.6. Physically, this is explained by small particle disaggregating and exposing progressively more surface to disaggregate. The time frame of exponential disaggregation was approximately 4 weeks in the 2% HCT and 14 weeks in the 4% HCT (i.e., the 4% HCT crumbled exponentially at a slower rate). While the intrinsic rates are different between 2% and 4% material, both scale similarly with time. The data are shown below, and the fitted curves are sulfate = $390*t^{1.6}$ for 2% binder and $15*t^{1.6}$ for 4% binder, where t is time (weeks).

**Figure 6-2.    Polynomial Fit for Sulfate Data, Used to Estimate Surface Area**
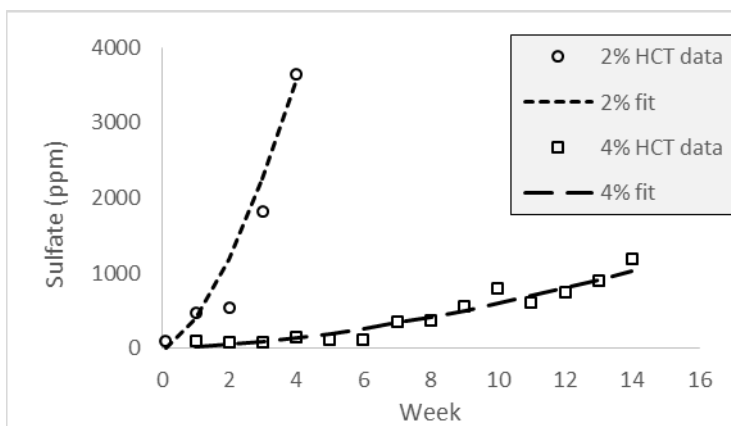


Using this correlation with sulfate release (and thus, surface area) over time, we compared 1 week of weathering to 2, 3, and 4 weeks of weathering, in terms of relative increase in surface area. According to $t^{1.6}$ increase, material at two weeks has weathered 3.03 times as much as material at one week. Similarly, material has weathered 5.8 times as much at 3 weeks and 9.19 times at 4 week. We estimate that the amount of weathering that occurred in the HCT data collected at weeks 1, 2, 3, and 4 was 4.75 times as much as the data collected at week 1. Therefore, we estimate that the CTF surface, which will weather for approximately 1 week, will have a surface area that is 4.75 times less than the surface area of the HCT samples that were used to provide the data to scale.

We believe this estimate to be conservative for a few reasons: 1) We assume the same rate of weathering, when HCT tests are designed to increase weather rates and are recognized to yield as much as an order or magnitude higher rates of oxidation when compared to field

scale weathering processes, 2), the HCT weathering of cylinders occurred in a non-confined space, promoting disaggregation, which will not be the case in the CTF facility (tailings are laterally confined), and 3) fine, unconsolidated particles, with high surface areas were kept in the HCT, while they would likely be transported off of the CTF surface.

## 6.3.2 Estimations of Waste Rock Reactive Surface

At any given time during the filling of the CTF, approximately 4,000 tonnes of co-disposed waste rock will be exposed.  This material will be comprised of 40% USZ, 21% Ynl B, and 39% LZ FW.  We assume that all of this mass is reactive and the surface area per mass is given by the particle sizes in the blast fragmentation of waste rock at the Ashanti mine (shown in **Figure 5-2**).

Additionally, the access ramp will be constructed of 390,000 tonnes of waste rock, composed of Ynl A (14.5%), USZ (1.5%), Ynl B (50%), and LZ FW (30%).  Also, sub 3/8 inch screened fragments of Ynl B (4%) will first be deposited as an initial lift (cushion layer) to prevent punctures to the liner.  Because this mass is large and it is unlikely or impossible that all surfaces would react with water, we used the same approach taken for the Waste Rock Storage Facility by calculating a reactive mass for the fraction of rock that could be saturated by water flow in one week, assuming a 30% porosity.  The lower porosity compared to the WRS (40% porosity) is assumed because of compaction from use of the ramp.  For a sensitivity analysis, we also assume that all mass in the waste rock drain is reactive.

For waste rock samples in the humidity cell tests, the reactive surface area was estimated from sieve analyses.  From these calculations, assuming spherical particles, the specific surface areas are 2.01 $m^2$/kg for USZ, 2.94 $m^2$/kg for Ynl A and 3.01 $m^2$/kg for Ynl B.

## 6.3.3 Water Balance

Given the footprint of the CTF, the model assumes 84,000 $m^3$/year of precipitation and runoff, based on data collected by Knight Piesold (2015).  This value accounts for snow accumulation, plowing, etc.  All of this water is assumed to contact and react with the top surface of the CTF and the co-deposited waste rock at year 6.

At year 6, while paste continues to be deposited, the model assumes that 29,029 $m^3$/year of water comes from the wet paste dewatering.  This estimate is based on 5% dewatering (by mass) of the 1,595 tonnes of paste (55% of 2,900 tonnes) deposited per day on an annualized basis (AMEC, 2016, Appendix K7 of Tintina's MOP).  Combined with the runoff water, this means that 113,029 $m^3$/year of water reports to the sump. At closure, the dewatering contribution is removed, and only 84,000 $m^3$/year of precipitation reports to the sump.

The model assumes that 10% of the runoff and the dewatered paste water also flows through the waste rock drain (access ramp) and receives additional load from the waste rock.  This is based on the drain occupying 10% of the CTF surface area in year 6.

## *6.4 Predicted Water Quality at Year 6*

Modeling results suggest that the water reporting to the CTF sump at year 6 will be acidic, with a pH of 4.13 in the base case (**Table 6-1**).  Sulfate concentration is moderately high (765 mg/L) and several metals (e.g., As, Cu, Ni, Pb, Sb, and Tl) will exceed groundwater quality standards, requiring treatment.  The minerals alunite, barite, jarosite and quartz are predicted to precipitate; the precipitation of these sulfate minerals explains the relatively

lower sulfate concentrations under the more acidic conditions.  No sorption is predicted. The mass loads calculated for each input sources are shown in Appendix K.

The sensitivity analyses suggest that the pH and some metal concentrations (e.g., Al, Cu, Fe, Se, Sr, and Tl) are linked to the estimation of paste surface area.  Values for $SO_4^{-2}$, As, F, Sb, U, and Zn are more strongly linked to the estimation of the waste rock contribution. The sensitivity analysis which uses solute concentrations from the 4% cement paste HCT (in place of the 2% cement paste HCT) suggests that use of 4% cement paste could be an effective contingency for interim closure management.

**Table 6-1.    Predicted Water Quality in the CTF Sump at Year 6, Including Sensitivity Analyses**

| | | Model predictions for CTF at yr 6 of mining | | | | | Groundwater Standards (MT DEQ-7) |
|---|---|---|---|---|---|---|---|
| | | Base Case | Waste Rock Surface Area Doubled | Paste Cement Surface Area Doubled | Paste Cement Surface Area Halved | 4% paste cement surface | |
| pH | s.u. | 4.13 | 4.11 | 3.80 | 4.38 | 5.89 | na* |
| Al | mg/L | 17.70 | 16.15 | 38.26 | 4.78 | 0.02 | na |
| Alkalinity | mg/L CaCO₃ | 97 | 92 | 93 | 86 | 111 | na* |
| As | mg/L | 0.031 | 0.033 | 0.048 | 0.016 | 0.002 | 0.01 |
| Ba | mg/L | 0.004 | 0.003 | 0.003 | 0.005 | 0.014 | 1 |
| Be | mg/L | 0.0051 | 0.0051 | 0.0102 | 0.0026 | 0.0008 | 0.004 |
| Ca | mg/L | 132 | 137 | 246 | 75 | 42 | na |
| Cd | mg/L | 0.00141 | 0.00142 | 0.00281 | 0.00071 | 0.00004 | 0.0050 |
| Cl | mg/L | 34.3 | 34.3 | 38.0 | 32.4 | 31.7 | na* |
| Cr | mg/L | 0.012 | 0.013 | 0.023 | 0.007 | 0.006 | 0.1 |
| Cu | mg/L | 61.3 | 61.3 | 121.8 | 31.0 | 0.7 | 1.3 |
| F | mg/L | 0.66 | 0.70 | 1.22 | 0.38 | 0.22 | 4 |
| Fe | mg/L | 0.636 | 0.518 | 1.955 | 0.513 | 0.013 | na** |
| Hg | mg/L | 0.000127 | 0.000141 | 0.000240 | 0.000071 | 0.000041 | 0.002000 |
| K | mg/L | 0.00003 | 0.00005 | 0.00001 | 0.00004 | 3.45189 | na |
| Mg | mg/L | 92 | 97 | 145 | 65 | 32 | na |
| Mn | mg/L | 2.68 | 2.73 | 5.29 | 1.36 | 0.05 | na** |
| NO₃ | ppm as N | nd | nd | nd | nd | nd | 1 |
| Na | mg/L | 13 | 13.6 | 15.9 | 12.1 | 12.6 | na |
| Ni | mg/L | 8.5 | 35.0 | 17.1 | 4.3 | 0.0 | 0.1 |
| P | mg/L | 0.26 | 0.26 | 0.49 | 0.05 | 0.02 | na |
| Pb | mg/L | 0.027 | 0.028 | 0.030 | 0.025 | 0.024 | 0.015 |
| SO₄ | mg/L | 765 | 797 | 1481 | 406 | 97 | na** |
| Sb | mg/L | 0.015 | 0.015 | 0.016 | 0.014 | 0.014 | 0.006 |
| Se | mg/L | 0.003 | 0.003 | 0.005 | 0.002 | 0.001 | 0.050 |
| Si | mg/L | 1.142 | 1.142 | 1.129 | 0.74 | 0.12 | na |
| Sr | mg/L | 2.62 | 2.92 | 4.67 | 1.59 | 0.86 | 4 |
| Tl | mg/L | 0.016 | 0.017 | 0.030 | 0.009 | 0.003 | 0.002 |
| U | mg/L | 0.012 | 0.015 | 0.021 | 0.008 | 0.003 | 0.03 |
| Zn | mg/L | 0.826 | 0.826 | 1.650 | 0.413 | 0.008 | 2 |

nitrate removed by flotation                                              *narrative standards may exist

supersaturated phases in basecase: alunite, barite, jarosite, quartz          **secondary standard

*Results include precipitation of supersaturated phases*

## *6.5  Predicted Water Quality at Closure*

The CTF closure model accounts for the increased surface area of the cemented paste and removes the contribution from dewatered paste.  The final paste lift will be constructed with 4% cement paste.  However, Tintina also proposes to cover the CTF with a welded HDPE cover, followed by fill, subsoil and topsoil (at a slope designed to preclude standing water), regraded and re-vegetated.  This plan will eliminate long-term exposure to oxygen and water.  The closure predictions shown here represent water quality at the end of tailing production, prior to placement of the cover, when the entire surface remains exposed to oxygen and water.  The mass loads for each input source are shown in Appendix K.

Although the surface area of the CTF is higher at closure (210,000 $m^2$) compared to year 6 (132,000 $m^2$), the lower predicted acidity and metals result in better water quality due to the planned use of a cemented paste tailings lift containing 4% cement immediately prior to placement of the cover.

At closure, the water reporting to the CTF sump is predicted to be moderately acidic, with a pH of 5.57 in the base case (**Table 6-2**).  Sulfate concentration is predicted to be much lower (90 mg/L) and the base case meets groundwater standards except for Tl, and As under the scenario where reactive surface area of paste on the CTF is doubled.  Sensitivity results indicate that metal concentrations are more sensitive to increases in reactive paste surface area than waste rock surface area.  Barite, jarosite, and $Ba_3(AsO_4)_2$ are predicted to precipitate. No sorption was calculated due to the lack of ferrihydrite precipitation. The mass loads calculated for each input sources are shown in Appendix L.

The cement pasted tailings will be placed on a double liner until a composite geomembrane / soil cover is constructed to eliminate infiltration at closure, and water will be collected from the sump for treatment until no standing water remains and the cover has eliminated any seepage.  Water with the quality predicted at closure will be of limited duration, due to the elimination of run-on and precipitation by the cover at closure, and there will be no standing inventory of water on the liner.  Because the surface area of the impoundment is an important factor, water quality should be expected to drop gradually as the facility approaches complete buildout with maximum reactive surface area, followed by improvement with the construction of the final 4% tailings lift and placement of the cover.  The drain should be also managed to avoid plugging with secondary minerals.  However, the drain is unlikely to be fully saturated with the predicted (215 L/min) flow of seepage, leaving multiple paths for water flow.

**Table 6-2.    Predicted Water Quality in the CTF Sump at Closure, Including Sensitivity Analyses**

| | | Model predictions for CTF at closure | | | | Groundwater Standards (MT DEQ-7) |
|---|---|---|---|---|---|---|
| | | Base Case | Waste Rock Surface Area Doubled | Paste Cement Surface Area Doubled | Paste Cement Surface Area Halved | |
| pH | s.u. | 5.57 | 5.57 | 5.27 | 5.87 | na* |
| Al | mg/L | 0.020 | 0.020 | 0.039 | 0.010 | na |
| Alkalinity | mg/L CaCO₃ | 53 | 53 | 106 | 53 | na* |
| As | mg/L | 0.0044 | 0.0046 | 0.0160 | 0.0010 | 0.01 |
| Ba | mg/L | 0.017 | 0.017 | 0.011 | 0.019 | 1 |
| Be | mg/L | 0.0016 | 0.0016 | 0.0031 | 0.0008 | 0.004 |
| Ca | mg/L | 54 | 54 | 108 | 27 | na |
| Cd | mg/L | 0.000059 | 0.000060 | 0.000118 | 0.000030 | 0.005000 |
| Cl | mg/L | 2.6 | 2.6 | 5.1 | 1.3 | na* |
| Cr | mg/L | 0.010 | 0.010 | 0.020 | 0.005 | 0.1 |
| Cu | mg/L | 0.0039 | 0.0040 | 0.0078 | 0.0020 | 1.3 |
| F | mg/L | 0.27 | 0.28 | 0.53 | 0.14 | 4 |
| Fe | mg/L | 0.012 | 0.011 | 0.007 | 0.014 | na** |
| Hg | mg/L | 0.000056 | 0.000057 | 0.000112 | 0.000028 | 0.002000 |
| K | mg/L | 4.2 | 4.4 | 8.3 | 2.2 | na |
| Mg | mg/L | 0.6 | 1.0 | 0.4 | 7.0 | na |
| Mn | mg/L | 0.010 | 0.011 | 0.020 | 0.006 | na** |
| NO₃ | ppm as N | nd | nd | nd | nd | 1 |
| Na | mg/L | 4.0 | 4.1 | 7.9 | 2.1 | na |
| Ni | mg/L | 0.019 | 0.019 | 0.037 | 0.009 | 0.1 |
| P | mg/L | 0.021 | 0.021 | 0.042 | 0.010 | na |
| Pb | mg/L | 0.00041 | 0.00042 | 0.00079 | 0.00019 | 0.015 |
| SO₄ | mg/L | 90 | 93 | 177 | 46 | na** |
| Sb | mg/L | 0.0011 | 0.0011 | 0.0021 | 0.0006 | 0.006 |
| Se | mg/L | 0.0020 | 0.0021 | 0.0040 | 0.0011 | 0.050 |
| Si | mg/L | 0.11 | 0.12 | 0.22 | 0.06 | na |
| Sr | mg/L | 0.65 | 0.66 | 1.29 | 0.33 | 4 |
| Tl | mg/L | 0.0022 | 0.0022 | 0.0044 | 0.0011 | 0.002 |
| U | mg/L | 0.0011 | 0.0018 | 0.0015 | 0.0009 | 0.03 |
| Zn | mg/L | 0.016 | 0.016 | 0.031 | 0.008 | 2 |

nitrate removed by flotation                          *narrative standards may exist

supersaturated phases in basecase: barite, jarosite, Ba3(AsO4)2          **secondary standard

*Results include precipitation of supersaturated phases*

# 7  Process Water Pond Water Quality Model

All water from the CTF and some of the water from the UG workings will report to the PWP where it will mix with water from the mill (i.e., thickener overflow), direct precipitation and runon.  In the PWP model, we mix these solutions and equilibrate the solution using PHREEQC.  **Figure 1-2** shows the facilities map.  The water balance is provided by Knight Piesold (2016) for year 6.

The quality of water in the PWP was predicted during operations at year 6.  Model sensitivity was not tested as this is a straightforward mixing model which relies on assumptions tested for the UG and CTF models. Supporting evidence for this approach is provided below.

## 7.1  Process Water Pond Water Balance

**Figure 7-1** shows the overall water balance in the PWP, including the sources and annual flow rates.

**Figure 7-1.     Water Balance for Process Water Pond**
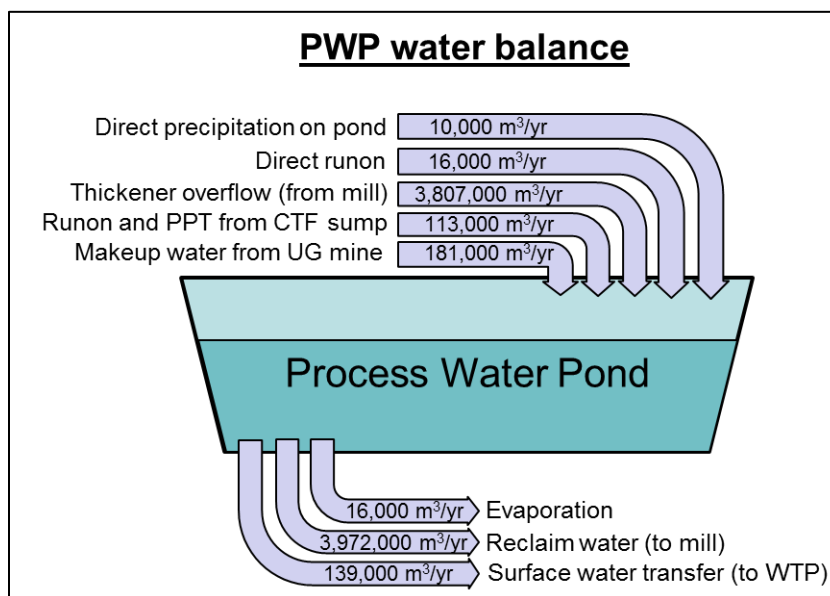


We use results from Sections 4.5 and 6.4 to predict the water chemistries from the UG and CTF facilities, respectively.  For the thickener overflow (from mill), we use metallurgical chemistry provided by Jeff Austin (2015).  In addition to these solutions, we add runon and direct precipitation (assumed to be dionized water) and remove water for evaporation. These three fluxes of dionize water add up to a net influx of 10,000 m³/yr of water, which dilutes the system by only a small amount.  The final mixed solution is equilibrated in PHREEQC to predict the PWP chemistry that will report to the WTP.

## 7.2  Predicted Water Quality in PWP

**Table 7-1** shows the results of the mixing and equilibration in the process water pond. The predicted pH is 5.69, with an alkalinity of 386 and sulfate of 110.  The mass-load model is shown in Appendix M. PHREEQC predicts precipitation of alunite, $Ba_3(AsO_4)_2$, barite, and ferrihydrite, with sorption of several metals including Cu, Pb, and As.  The model predicts

that Cu, NO$_3$, Ni, Pb, Sb, and Tl will exceed groundwater standards prior to treatment to meet non-degradation criteria. Tintina plans to treat all of the water inventory in the PWP prior to removal and reclamation of the pond at closure.

**Table 7-1.       Predicted Water Quality in PWP at Year 6**

|  |  | **Model prediction of PWP** | **Groundwater Standards (MT DEQ-7)** |
|---|---|---|---|
| **pH** | s.u. | 5.69 | na* |
| **Al** | mg/L | 0.049 | na |
| **Alkalinity** | mg/L CaCO$_3$ | 386 | na* |
| **As** | mg/L | 0.003 | 0.01 |
| **Ba** | mg/L | 0.019 | 1 |
| **Be** | mg/L | 0.0002 | 0.0040 |
| **Ca** | mg/L | 51 | na |
| **Cd** | mg/L | 0.00008 | 0.00500 |
| **Cl** | mg/L | 110.7 | na* |
| **Cr** | mg/L | 0.004 | 0.1 |
| **Cu** | mg/L | 4.3 | 1.3 |
| **F** | mg/L | 0.320 | 4 |
| **Fe** | mg/L | 0.022 | na** |
| **Hg** | mg/L | 0.000010 | 0.002000 |
| **K** | mg/L | 3 | na |
| **Mg** | mg/L | 104 | na |
| **Mn** | mg/L | 0.1 | na** |
| **NO$_3$** | ppm as N | 1.3 | 1 |
| **Na** | mg/L | 39 | na |
| **Ni** | mg/L | 0.251 | 0.1 |
| **P** | mg/L | 0.05 | na |
| **Pb** | mg/L | 0.090 | 0.015 |
| **SO$_4$** | mg/L | 110 | na** |
| **Sb** | mg/L | 0.049 | 0.006 |
| **Se** | mg/L | 0.001 | 0.05 |
| **Si** | mg/L | 0.207 | na |
| **Sr** | mg/L | 1.46 | 4 |
| **Tl** | mg/L | 0.004 | 0.002 |
| **U** | mg/L | 0.002 | 0.03 |
| **Zn** | mg/L | 0.027 | 2 |

prediction based on assumed 18 ppm from underground

*narrative standards may exist                    **secondary standard

Supersaturated phases: Alunite, Ba3(AsO4)2, barite, ferrihydrite

*Results include precipitation of supersaturated phases and sorption.*

# 8  Conclusions and Recommendations

Enviromin has predicted water quality for the proposed i.) underground workings (i.e., access, declines, and stopes), UG; ii.) temporary waste rock storage facility, WRS; iii.) cemented tailings facility, CTF; and iv.) the downgradient water treatment plant, WTP.  For all models, Enviromin provides base case scenarios for likely and foreseeable conditions, which include inherent elements of conservatism.  For the important parameters in the models, sensitivity analyses show variations from the base case parameters, which may over- or under-estimate true values.  In general, the predicted changes are not extreme, even in the case of the compound conservative analysis, suggesting that the models provide a solid analysis of future water quality for the facilities.

In the UG, we estimate water quality at year 6 of mining operations and at post-closure conditions, when groundwater has rebounded fully.  For the WRS facility, we estimate water quality only at the end of year 2, when it will begin to be dismantled and the material moved to the CTF for permanent storage.  For the CTF, we estimate water quality at year 6 of production and at the start of closure, prior to placement of the cover which will eliminate all subsequent seepage to the CTF sump.  Except for the groundwater in the underground workings at closure (following cessation of dewatering), water from each of the modeled facilities will report directly to the water treatment facility for treatment prior to discharge.  This water is predicted to meet non-degradation criteria prior to discharge to shallow groundwater via the infiltration galleries.

- **UG:** For the UG model, we predict water quality in year 6 of operations to be neutral, with a pH of 6.86, abundant alkalinity (183 mg/L) and a moderate increase in sulfate concentration (over background) to 304 mg/L.  The highest contributions of acidity, metals, and sulfate come from the UCZ, but the rate of groundwater flow from the UCZ is very low so the net effect is minor.  Enviromin predicts precipitation of alunite, $Ba_3(AsO_4)_2$, $Cr_2O_3$, ferrihydrite, and quartz, based on PHREEQC predictions of supersaturation in the mixed influent water in the sump, with sorption of metals Ba, Be, Zn, Cu, Pb, and As to ferrihydrite.  Concentrations of $NO_3^-$, Cu, F, Mn, Ni, Sb, Se, Tl, U and Zn are predicted to increase in the resulting solution above background concentrations.  Of these parameters, $NO_3^-$ and U are predicted to exceed Montana DEQ groundwater quality standards in the operational base case and multiple sensitivity scenarios.  Arsenic and Sr have a low potential to exceed their elevated background concentrations in groundwater.  If a higher rate of sulfide oxidation or a greater reactive mass of rock were to be encountered, Tl and Sb could also exceed standards.  Because all water will be collected during operational dewatering for treatment to meet non-degradation criteria prior to discharge, these predicted exceedances are not material and they are not expected to affect water quality.

  The model includes several sensitivity analyses of the predicted underground water quality, addressing uncertainty in model inputs for i.) HCT data (i.e., all data vs. weeks 1-4), ii.) fracture density, iii.) fracture zone thickness, iv.) estimated surface area, and v.) sulfide oxidation rate.  Alkalinity is abundant in all sensitivity scenarios, including the compound conservative analysis which combines several conservative assumptions; predicted pH ranges from 4.89 to 6.88 and sulfate ranges from 262 to 672 mg/L in this combined scenario.  In general, the assumptions about fracture density and reactive-zone thickness have the greatest effect on predicted metal release, and the sulfide oxidation rate has the most dominant, though minor effect, on the pH.  The scenario which includes HCT data for all weeks yields a lower pH, due to acidity produce later in the USZ HCT test.

At closure, following completion of mining, backfilling, and groundwater rebound, the water is predicted to have slightly higher pH (6.91) and lower alkalinity (151 mg/L) and sulfate (115 mg/L), due to changes in groundwater flow and an increase in paste cement surface area when compared to the operational predicted water quality. Concentrations of metals are also predicted to be lower. This model is most sensitive to the estimate of reactive surface area for the cemented backfill. Enviromin predicts potential precipitation of $Ba_3(AsO_4)_2$, $Cr_2O_3$, ferrihydrite, and quartz, based on PHREEQC predictions of supersaturation in the mixed water.

As mine water will be collected during dewatering operations for on-site treatment, but not when mine dewatering ceases, the predicted chemistry at closure is important. The predicted changes at closure represent minor changes in water quality, relative to the background water quality (pH of 6.97, with alkalinity of 193 mg/L and sulfate 111 mg/L). Concentrations of $NO_3$, $SO_4$, P, Se, Sr, and Zn are predicted to increase modestly above background levels, but none exceed Montana DEQ groundwater quality standards or groundwater non-degradation criteria. The limited variation between the base case and sensitivity scenarios reflects the robust design and plan for management of the UG, which limits open stope area and provides for water treatment during operations and early closure; concurrent backfilling with a low transmissivity material; flooding with RO treated water at closure, and placement of hydraulic plugs.

- **WRS:** Water quality predicted for the WRS base case at the end of year 2 of mining is moderately acidic (pH 5.49) and high in sulfate (3,780 ppm), with some elevated metals. This prediction is conservative, as a result of the very small amount of water into which the mass of solutes released from the aggressively weathered HCT is scaled. Regardless, the volume of WRS seepage is small (473,000 gallons/year; 1,790 $m^3$/year at a rate of 0.9 gpm) and water will be collected on a lined pad and discharged to the PWP prior to treatment. Our model predicts potential precipitation of barite, celestite, fluorite, gypsum, and jarosite. Sensitivity analyses show that the model is sensitive to the rock water ratio and surface area assumptions. Because the WRS will be removed in years 2 to 3, no closure evaluation was needed.

- **CTF:** For the CTF, the predicted quality of water that will collect in the sump at year 6 of tailings placement is acidic (pH 4.13) with 765 mg/L sulfate and elevated metal concentrations. More acidity and metals are contributed by the surface of cemented tailings than the co-deposited waste rock or access ramp/rock drain, while most sulfate comes from the paste dewatering and waste rock. The minerals predicted to form during operations include alunite, barite, jarosite, and quartz. At closure, following placement of a 4% lift immediately prior to cover placement, a more neutral solution (pH 5.57) is predicted. The planned reclamation procedures (e.g., composite welded HDPE /soil cover, revegetation, etc.) are not accounted for in the model, as they will eliminate seepage. At closure, the minerals predicted by PHREEQC to form include barite, jarosite, and $Ba_3(AsO_4)_2$.

Results for the CTF show that the finely ground, sulfide-rich tailing will generate higher acidity and metals, but lower sulfate due to precipitation of sulfate-rich minerals, e.g. alunite, barite and jarosite. Water quality predictions for the CTF are sensitive to the calculated surface area, implying that the surface area should be managed to limit weathering through frequent placement of fresh lifts of paste tailings. In the event of an interim closure, Tintina may elect to increase the cement content to 4%, to improve the stability of the upper paste cement during a lag in placement of fresh tailings.

- **<u>PWP:</u>** All water from the CTF sump and some water from the UG sump will report to the Process Water Pond (PWP).  These inflows mix with thickener overflow from the mill and direct precipitation.  Results of the model predict that the overall chemistry of the PWP is dominated by the thickener overflow, which provides 93% of the flow.  The predicted solution has a pH of 5.69, low sulfate (110 mg/L), and high concentrations of Cu, $NO_3$, Ni, Pb, Sb, and Tl.  PHREEQC predicts that alunite, $Ba_3(AsO_4)_2$, barite, and ferrihydrite could form, with sorption of metals including Cu, Pb and As to ferrihydrite.  Excess water from the PWP will be sent to the WTP for treatment and discharged operationally to offset consumptive use; all water on the PWP will be treated prior to closure of the facility.

# 9  References

AMEC, 2016a. *Examples of Existing Paste Backfill.*  Memo prepared for Tintina Montana, 4 pp.  31 August 2016.

AMEC, 2016b.  Paste Tailings for Johnny Lee Mine, Tintina Resources.  Memo prepared for Tintina Montana, 2 pp.  2 September 2016.

Austin, J, 2015. AMEC metallurgical testing for BBC project.

Baas-Becking, L., Kaplan, I.R., Moore, D., 1960. Limits of the natural environment in terms of pH and oxidation-reduction potentials. Geology. Vol. 68, No. 3, pp. 243-284.

Behra, P., P. Bonnissel-Gissinger, M. Alnot, R. Revel and J. J. Ehrhardt, 2001. "XPS and XAS study of the sorption of Hg(II) onto pyrite." Langmuir 17(13): pp. 3970-3979.

Bethke, C.M., 2008.  Geochemical and Biogeochemical Reaction Modeling.  Cambridge, 2nd ed.

Borah, D. and K. Senapati, 2006. Adsorption of Cd(II) from aqueous solution onto pyrite. Fuel, 85: 1929-1934.

Bower, J., Savage, K.S., Weinman, B., and Harper, W., 2008. Immobilization of mercury by pyrite ($FeS(2)$). Environmental Pollution 156(2):504-14.

Brown, J. R., G. M. Bancroft, W. S. Fyfe and R. A. N. McLean, 1979. "Mercury Removal from Water by Iron Sulfide Minerals - Electron-Spectroscopy for Chemical-Analysis (Esca) Study." Environmental Science & Technology 13(9): pp. 1142-1144.

Davis, G.B., 1983. Mathematical modelling of rate-limiting mechanisms of pyretic oxidation in overburden dumps. Doctor of Philosophy thesis, Department of Mathematics, University of Wollonggong, N.S.W., Australia.

Davis, G.B., Doherty, G, and Ritchie, A.I.M. 1986. A model of oxidation in pyritic mine waters: Part 2: Comparison of numerical and approximate solutions. *Appl. Math. Model.* 10:323-339.

Doyle, CS: Kendelewicz, T; Bostick, BC, and Brown, G, 2004. Soft X-ray spectroscopic studies of the reaction of fractured pyrite surfaces with Cr(VI)-containing aqueous solutions. *Geochimica et Cosmochimica Acta.*  Vol 68, issue 21, pp. 4287-4299.

Enviromin, Inc, 2015. *Baseline Environmental Geochemistry Evaluation 2015 Operating Permit.* November 2015. Report prepared for Tintina Resources, Inc.

Hydrometrics, Inc., 2012. *Tintina Resources Black Butte Copper Project Water Resources Monitoring 2011 Annual Report.* Report prepared for Tintina Resources, January 2012.

Hydrometrics, 2013. *Hydrological and Geochemical Assessment of Proposed Underground LAD Area, Black Butte Copper Project.* November 2013.

Hydrometrics, 2015. *Groundwater Modeling Assessment for the Black Butte Copper Project Meagher County MT.* Report prepared for Tintina Resources, Inc. November 2015.

Hydrometrics, 2016a. *Memorandum for Black Butte Copper Temporary Waste Rock Storage Facility Percolation Model.* Prepared for Geomin Resources Inc. and Enviromin, Inc. February 18, 2016.

Hydrometrics, 2016b. *Memorandum for Simulated Mine Inflow and Groundwater Flux at Closure.* Prepared for Geomin Resources Inc. and Enviromin, Inc. May 2, 2016.

Hyle, C., 2016. *Typical Underground Fragmentation.* Memo from Orca Mining Services prepared for Tintina Montana, 2 pp. 2 June 2016.

Kelsall, P.C., J.B. Case and CR Chabannes, 1984. Evaluation of Excavation-induced changes in Rock Permeability. International Journal of Rock Mechanics and Mining Sciences & Geomechanics Abstracts, Vol 21, N. 3, pp. 123-135.

Kempton, H. and D. Atkins, 2009. Direct Measurement of Sulfide Mineral Oxidation Rates and Acid Rock Drainage in Wall Rock of Open Pit Mines. Proceeds of the 8th International Conference on Acid Rock Drainage, June 23-29, 2009, Sweden.

Knight Piesold, 2015. Black Butte Copper Project Meteorology Data Analysis Update. Memo from Brendan Worral to Bob Jacko, May 27, 2015.

Knight Piesold, 2016. *Black Butte Copper Project Water Balance – Surface Water transfer to Water Treatment Plant,* Memorandum prepared for Tintina Resources, Inc. April 28, 2016. 10 pages. (File No. VA 101-00460/03-A.01.

Oxverdi, A., Erdem, M. 2006. Cu2+, Cd2+ and Pb2+ adsorption from aqueous solutions by pyrite and synthetic iron sulphide. Journal of Hazardous Materials, 137, 1: 626-632.

Parkhurst, D.L., and Appelo, C.A.J., 2013, Description of input and examples for PHREEQC version 3—A computer program for speciation, batch-reaction, one-dimensional transport, and inverse geochemical calculations: U.S. Geological Survey Techniques and Methods, book 6, chap. A43, 497 p., available only at http://pubs.usgs.gov/tm/06/a43/.

Siskind, D., & Fumanti, R. (1974). *Blast-produced fractures in Lithonia granite.* U.S. Bureau of Mines, Report of investigations 7901.

Tintina Resources, Inc., 2015. Mine Operating Permit Application - Black Butte Copper Project, Meagher County, MT. Submitted to the Department of Environmental Quality, December 15, 2015. 312 p.

Tintina Resources, Inc., 2016, Mine Operating Permit Application - Black Butte Copper project, Meagher County, MT. Submitted to the Montana Department of Environmental Quality, August 2016.

# APPENDIX A: Average HCT data for weeks 1-4 (from Enviromin, 2015)

| | | Corresponding lithotype | YNL-A | UCZ | USZ/UCZ | YNLB-UA | YNLB-LD | LCZ | YNLB-LA | Paste backfill (closure) |
|---|---|---|---|---|---|---|---|---|---|---|
| | | HCT (avg of wks 1-4) or  DIFF TEST (avg of all pulls) | HCT - 2012 Ynl | HCT - 2012 USZ | HCT - 2015 USZ | HCT - 2012 Ynl B | HCT - 2015 Ynl B | HCT - 2015 LZFW | HCT - 2015 LZFW | DIFF TEST - 2015 4% binder |
| **Parameter** | **Units** | | | | | | | | | |
| Mass of rock | kg | | 2.00800 | 1.99500 | 2.00170 | 1.99500 | 1.99500 | 2.01540 | 2.01540 | 1.31750 |
| Volume | L | | 0.89050 | 0.87875 | 0.87900 | 0.90600 | 0.85450 | 0.87200 | 0.87200 | 4.40000 |
| specific surface area | m2/kg | | 2.94119 | 2.01073 | 2.01073 | 3.01078 | 3.01078 | 2.01073 | 2.01073 | |
| total surface area | m2 | | 5.90590 | 4.01141 | 4.02488 | 6.00651 | 6.00651 | 4.05243 | 4.05243 | 0.04370 |
| pH | s.u. | | 7.29100 | 6.82645 | 5.62132 | 7.99711 | 7.40326 | 7.29068 | 7.29068 | 7.40145 |
| activity of hydrogen | - | | 5.12E-08 | 1.49E-07 | 2.39E-06 | 1.01E-08 | 3.95E-08 | 5.12E-08 | 5.12E-08 | 3.97E-08 |
| Temperature | °C | | 23.0 | 23.0 | 23.0 | 23.0 | 23.0 | 23.0 | 23.0 | 22.9 |
| Alkalinity | mg/L as CaCO$_3$ | | 14.75 | 12.50 | 16.50 | 27.00 | 27.75 | 23.00 | 23.00 | 10.57 |
| Aluminum | mg/L | | 0.012 | 0.009 | 0.059 | 0.039 | 0.072 | 0.058 | 0.058 | 0.311 |
| Antimony | mg/L | | 0.001 | 0.001 | 0.001 | 0.005 | 0.002 | 0.008 | 0.008 | 0.001 |
| Arsenic | mg/L | | 0.001 | 0.001 | 0.002 | 0.003 | 0.004 | 0.134 | 0.134 | 0.018 |
| Barium | mg/L | | 0.023 | 0.016 | 0.014 | 0.006 | 0.028 | 0.027 | 0.027 | 0.050 |
| Beryllium | mg/L | | 0.001 | 0.001 | 0.001 | 0.001 | 0.001 | 0.001 | 0.001 | 0.001 |
| Cadmium | mg/L | | 0.000 | 0.000 | 0.000 | 0.000 | 0.000 | 0.000 | 0.000 | 0.000 |
| Calcium | mg/L | | 81.7 | 117.7 | 475.3 | 17.3 | 27.0 | 32.3 | 32.3 | 18.1 |
| Chloride | mg/L | | 0.330 | 7.670 | 7.670 | 0.001 | 0.001 | 0.330 | 0.330 | 1.000 |
| Chromium | mg/L | | 0.010 | 0.010 | 0.010 | 0.010 | 0.010 | 0.010 | 0.010 | 0.005 |
| Copper | mg/L | | 0.003 | 0.003 | 0.046 | 0.002 | 0.003 | 0.002 | 0.002 | 0.002 |
| Fluoride | mg/L | | 0.600 | 0.233 | 0.267 | 0.900 | 1.850 | 0.931 | 0.931 | 0.100 |
| Iron | mg/L | | 0.020 | 0.020 | 10.953 | 0.020 | 0.020 | 0.020 | 0.020 | 0.020 |
| Lead | mg/L | | 0.000 | 0.000 | 0.002 | 0.000 | 0.003 | 0.002 | 0.002 | 0.000 |
| Magnesium | mg/L | | 49.7 | 181.7 | 439.0 | 15.0 | 32.7 | 48.3 | 48.3 | 0.5 |
| Manganese | mg/L | | 0.064 | 0.905 | 5.187 | 0.005 | 0.008 | 0.014 | 0.014 | 0.005 |
| Mercury | mg/L | | 0.000 | 0.000 | 0.002 | 0.000 | 0.000 | 0.000 | 0.000 | 0.000 |
| Nickel | mg/L | | 0.004 | 0.026 | 0.108 | 0.002 | 0.002 | 0.013 | 0.013 | 0.002 |
| Nitrate | mg/L as N | | 0.000 | 0.000 | 0.000 | 0.000 | 0.000 | 0.000 | 0.000 | 0.000 |
| Phosphorus | mg/L | | 0.006 | 0.005 | 0.005 | 0.005 | 0.006 | 0.013 | 0.013 | 0.026 |
| Potassium | mg/L | | 11.7 | 22.0 | 22.0 | 25.0 | 25.0 | 26.3 | 26.3 | 2.4 |
| Selenium | mg/L | | 0.006 | 0.008 | 0.004 | 0.007 | 0.008 | 0.015 | 0.015 | 0.001 |
| Silicon | mg/L | | 1.103 | 0.590 | 1.383 | 1.510 | 1.710 | 2.767 | 2.767 | 0.312 |
| Sodium | mg/L | | 12.33 | 3.00 | 3.00 | 13.67 | 13.67 | 10.00 | 10.00 | 1.46 |
| Strontium | mg/L | | 0.850 | 0.800 | 30.767 | 0.143 | 1.470 | 0.600 | 0.600 | 0.286 |
| Sulfate | mg/L | | 410.7 | 894.0 | 3116.7 | 86.7 | 263.0 | 295.7 | 295.7 | 27.5 |
| Thallium | mg/L | | 0.002 | 0.002 | 0.127 | 0.000 | 0.001 | 0.001 | 0.001 | 0.000 |
| Uranium | mg/L | | 0.001 | 0.000 | 0.001 | 0.001 | 0.001 | 0.223 | 0.223 | 0.000 |
| Zinc | mg/L | | 0.008 | 0.008 | 0.024 | 0.008 | 0.008 | 0.008 | 0.008 | 0.008 |
| | | | | | detection limits | | | | | |
| | | | | | not measured | | | | | |

## APPENDIX B: Average HCT Data for All Weeks (from Enviromin, 2015)

| Parameter | Units | Corresponding lithotype / HCT (avg of all wks or DIFF TEST (avg of all pulls) | YNL-A / HCT - 2012 Ynl | UCZ / HCT - 2012 USZ | USZ/UCZ / HCT - 2015 USZ | YNLB-UA / HCT - 2012 Ynl B | YNLB-LD / HCT - 2015 Ynl B | LCZ / HCT - 2015 LZFW | YNLB-LA / HCT - 2015 LZFW | Paste backfill / DIFF TEST - 2015 4% binder | Paste backfill (operations) / HCT TEST - 2015 4% binder |
|---|---|---|---|---|---|---|---|---|---|---|---|
| Mass of rock | kg | | 2.00800 | 1.99500 | 2.00170 | 1.99500 | 1.99500 | 2.01540 | 2.01540 | 1.31750 | 1.37 |
| Volume | L | | 0.89050 | 0.87875 | 0.87900 | 0.90600 | 0.85450 | 0.87200 | 0.87200 | 4.40000 | 3.148 |
| specific surface area | m2/kg | | 2.94119 | 2.01073 | 2.01073 | 3.01078 | 3.01078 | 2.01073 | 2.01073 | | |
| total surface area | m2 | | 5.90590 | 4.01141 | 4.02488 | 6.00651 | 6.00651 | 4.05243 | 4.05243 | 0.04370 | 0.04370 |
| pH | s.u. | | 7.26987 | 6.94551 | 5.43285 | 7.63406 | 7.37165 | 7.36590 | 7.36590 | 7.40145 | 3.14 |
| activity of hydrogen | - | | 5.37E-08 | 1.13E-07 | 3.69E-06 | 2.32E-08 | 4.25E-08 | 4.31E-08 | 4.31E-08 | 3.97E-08 | 7.24E-04 |
| Temperature | °C | | 23.0 | 23.0 | 23.0 | 23.0 | 23.0 | 23.0 | 23.0 | 22.9 | 21.64482759 |
| Alkalinity | mg/L as CaCO$_3$ | | 19.03 | 18.24 | 9.64 | 27.71 | 30.73 | 25.42 | 25.42 | 10.57 | 1.33 |
| Aluminum | mg/L | | 0.010 | 0.037 | 0.450 | 0.022 | 0.034 | 0.033 | 0.033 | 0.311 | 11.7443 |
| Antimony | mg/L | | 0.001 | 0.001 | 0.001 | 0.002 | 0.001 | 0.004 | 0.004 | 0.001 | 0.001 |
| Arsenic | mg/L | | 0.001 | 0.002 | 0.007 | 0.001 | 0.002 | 0.099 | 0.099 | 0.018 | 0.2424 |
| Barium | mg/L | | 0.009 | 0.013 | 0.014 | 0.007 | 0.016 | 0.023 | 0.023 | 0.050 | 0.0246 |
| Beryllium | mg/L | | 0.001 | 0.001 | 0.001 | 0.001 | 0.001 | 0.001 | 0.001 | 0.001 | 0.003 |
| Cadmium | mg/L | | 0.000 | 0.001 | 0.001 | 0.001 | 0.000 | 0.000 | 0.000 | 0.000 | 0.001 |
| Calcium | mg/L | | 69.0 | 119.8 | 443.4 | 40.8 | 50.4 | 24.0 | 24.0 | 18.1 | 21.55172414 |
| Chloride | mg/L | | 0.330 | 7.670 | 7.670 | 0.001 | 0.001 | 0.330 | 0.330 | 1.000 | 4.220 |
| Chromium | mg/L | | 0.010 | 0.010 | 0.010 | 0.010 | 0.010 | 0.010 | 0.010 | 0.005 | 0.05094 |
| Copper | mg/L | | 0.002 | 0.002 | 1.869 | 0.002 | 0.002 | 0.002 | 0.002 | 0.002 | 19.031 |
| Fluoride | mg/L | | 0.284 | 0.211 | 0.225 | 0.407 | 0.791 | 0.788 | 0.788 | 0.100 | 0.434 |
| Iron | mg/L | | 0.516 | 12.462 | 96.560 | 0.020 | 0.028 | 0.021 | 0.021 | 0.020 | 94.74 |
| Lead | mg/L | | 0.000 | 0.005 | 0.008 | 0.000 | 0.002 | 0.002 | 0.002 | 0.000 | 0.001 |
| Magnesium | mg/L | | 36.9 | 116.6 | 252.4 | 21.8 | 41.1 | 24.6 | 24.6 | 0.5 | 20.11724138 |
| Manganese | mg/L | | 0.042 | 0.952 | 4.367 | 0.009 | 0.010 | 0.011 | 0.011 | 0.005 | 1.129 |
| Mercury | mg/L | | 0.000 | 0.000 | 0.00030 | 0.000 | 0.00001 | 0.00001 | 0.00001 | 0.000 | 0.000 |
| Nickel | mg/L | | 0.008 | 0.141 | 0.313 | 0.002 | 0.004 | 0.013 | 0.013 | 0.002 | 2.364 |
| Nitrate | mg/L as N | | 0.000 | 0.000 | 0.000 | 0.000 | 0.000 | 0.000 | 0.000 | 0.000 | 0.000 |
| Phosphorus | mg/L | | 0.006 | 0.006 | 0.011 | 0.006 | 0.007 | 0.012 | 0.012 | 0.026 | 0.075 |
| Potassium | mg/L | | 11.7 | 22.0 | 22.0 | 25.0 | 25.0 | 26.3 | 26.3 | 2.4 | 1.217 |
| Selenium | mg/L | | 0.002 | 0.004 | 0.002 | 0.002 | 0.005 | 0.005 | 0.005 | 0.001 | 0.0011 |
| Silicon | mg/L | | 0.674 | 0.552 | 3.219 | 1.000 | 4.370 | 5.431 | 5.431 | 0.312 | 0.864 |
| Sodium | mg/L | | 12.33 | 3.00 | 3.00 | 13.67 | 13.67 | 10.00 | 10.00 | 1.46 | 1.223 |
| Strontium | mg/L | | 0.293 | 0.557 | 23.531 | 0.132 | 1.108 | 0.278 | 0.278 | 0.286 | 0.298 |
| Sulfate | mg/L | | 304.6 | 742.8 | 2446.9 | 163.9 | 307.4 | 154.1 | 154.1 | 27.5 | 517 |
| Thallium | mg/L | | 0.001 | 0.003 | 0.082 | 0.000 | 0.001 | 0.000 | 0.000 | 0.000 | 0.0024 |
| Uranium | mg/L | | 0.001 | 0.000 | 0.001 | 0.001 | 0.001 | 0.163 | 0.163 | 0.000 | 0.004 |
| Zinc | mg/L | | 0.011 | 0.050 | 0.170 | 0.011 | 0.007 | 0.008 | 0.008 | 0.008 | 0.408 |

detection limits

not measured

**\* Data taken from weeks 1-4 because data not available for all weeks**

# APPENDIX C:  PHREEQC Input for Underground Operations at Year 6

```
#ASSUMPTIONS
#starting pe + pH set to 13, to simulate a moderately opens system
#The following precipitates are allowed to form and reach equilibrium:
#Alunite, Celestite, Gypsum, K-Jarosite, Barite, Ba3(AsO4)2, Gibbsite, Ferrihydrite, Fluorite, MnHPO4, SbO2,
Cr2O3
#These phases were chosen based on supersaturation and general likelihood in mine-affected water. Goethite and
hematite were not allowed to precipitate because they are not likely to form at low temperatures in mine-
affected water (Bethke, Geochemical and Biogeochemical Reaction Modeling, 2008)

TITLE Groundwater base case Yr6

#solution predicted from mass loading model
SOLUTION 1
    temp      9.52
    pH        6.88
    pe        6.12
    redox     pe
    units     mg/kgw
    density   1
    Al        0.0335547
    Alkalinity 225.5543058
    As        0.0693722
    Ba        0.0536521
    Be        0.0010995
    Ca        88.9408254
    Cd        8.32e-005
    Cl        1.39512
    Cr        0.0096426
    Cu        0.0028121
    F         0.9646121
    Fe        1.8627779
    Hg        1.61e-005
    K         10.8784163
    Mg        60.3967574 charge
    Mn        0.1652109
    N(5)      0.2903226 mMol/kgw
    Na        14.6610865
    Ni        0.0064961
    P         0.0110735
    Pb        0.0010091
    S(6)      3.1657251 mMol/kgw
    Sb        0.0031677
    Se        0.0038824
    Si        6.7318916
    Sr        10.4846032
    Tl        0.0019636
    U         0.037117
    Zn        0.0319166
    -water    1 # kg
EQUILIBRIUM_PHASES 1
    Alunite    0 0 precipitate_only
    Ba3(AsO4)2 0 0 precipitate_only
    Barite     0 0 precipitate_only
    Celestite  0 0 precipitate_only
    Cr2O3      0 0 precipitate_only
    Ferrihydrite 0 0
    Fluorite   0 0 precipitate_only
    Gibbsite(C) 0 0 precipitate_only
    Gypsum     0 0 precipitate_only
    Jarosite-K 0 0 precipitate_only
    MnHPO4(C) 0 0 precipitate_only
    Quartz     0 0 precipitate_only
    SbO2       0 0 precipitate_only
SURFACE 1
    Hfo_sOH Ferrihydrite    equilibrium_phase 0.005  64200
    Hfo_wOH Ferrihydrite    equilibrium_phase 0.2
    -donnan 1e-008

END
```

# APPENDIX D: Base Case and Sensitivity Scenarios for UG, WRS, CTF, and PWP Models

| | | Parameters | | | | | NOTES |
|---|---|---|---|---|---|---|---|
| **Underground at Year 6** | | Fracture Density | Weeks of HCT data used | Sulfide Oxidation Rate (kg SO4/m2/yr) | Maximum Fracture Zone Thickness | Paste Backfill Surface Area (m2) | |
| | Base case | 10% in UZ, 2% in LZ | Weeks 1-4 | 6 | 1 meter | 3346 for UZ, 1714 for LZ | Likely and forseeable scenario for UG working sump water at year 6 |
| Sensitivity | Fracture Density Halved | 5% in UZ, 1% in LZ | Bc | Bc | Bc | Bc | Model sensitivity to high fracture density estimate |
| | Fracture Density Doubled | 20% in UZ, 4% in LZ | Bc | Bc | Bc | Bc | Model sensitivity to low fracture density estimate |
| | All HCT Data | Bc | All Weeks | Bc | Bc | Bc | Model sensitivity to HCT data selection |
| | Oxidation Rate 40 kg SO4/m2/yr | Bc | Bc | 40 | Bc | Bc | Model sensitivity to sulfide oxidation rate |
| | Two Meter Max Reactive Zone | Bc | Bc | Bc | 2 meter | Bc | Model sensitivity to fracture zone thickness |
| | Paste Backfill Surface Area Doubled | Bc | Bc | Bc | Bc | 6692 for UZ, 3428 for LZ | Model sensitivity to paste backfill surface area |
| | Combined Highest Reactive Mass Parameters | 20% in UZ, 4% in LZ | Bc | 40 | Bc | 6692 for UZ, 3428 for LZ | Model sensitivity to estimates of multiple parameters affecting reactive mass. This scenario compounds affect of multiple conservative estimates. |
| **Underground at Closure** | | Paste Backfill Surface Area (m2) | Assumed values for non-detects | | | | |
| | Base case | 14,653 for UZ and 13176 for LZ | Detection limit | | | | Likely and forseeable scenario for UG post-closure |
| Sensitivity Analyses | Paste Backfill Surface Area Doubled | 29306 for UZ, 26353 for LZ | Bc | | | | Model sensitivity to paste backfill surface area |
| | Detection Limits = 0 | BC | Zero | | | | Influence of detection limit propagation in model calculations (replace d.l. values with 0). |

| | | Parameters | | | | | NOTES |
|---|---|---|---|---|---|---|---|
| **CTF at Year 6** | | Waste Rock Surface Area (m2) | Paste Cement Surface Area (m2) | Kinetic Test Used for Paste (m2) | | | |
| Base case | | 267,590 on surface, 111,012 in ramp/drain | 13200 | 2% Paste HCT | | | Likely and forseeable prediction of WRS seepage in year 2. Conservative application of HCT results for wk 1-4, based on higher surface area and water flux of HCT, to very low volume of predicted seepage. |
| Sensitivity Analyses | Waste Rock Surface Area Doubled | 535180 for surface 222,025 for ramp/drain | Bc | Bc | | | Uncertainty about future BBC particle size gradation. |
| | Paste Cement Surface Area Doubled | Bc | 264000 | Bc | | | Influence of low paste cement surface area |
| | Paste Cement Surface Area Halved | Bc | 66000 | Bc | | | Influence of high paste cement surface area |
| | 4% Paste Cement Surface | Bc | Bc | 4% Paste HCT | | | Evaluates use of 4% cement paste in place of 2% |
| **CTF at Closure** | | Waste Rock Surface Area (m2) | Paste Cement Surface Area (m2) | | | | |
| Base case | | 82,501 in ramp/drain | 210000 | | | | Likely and forseeable scenario for CTF at closure |
| Sensitivity Analyses | Waste Rock Surface Area Doubled | 165,003 | Bc | | | | Influence of underestimating waste rock surface area |
| | Paste Cement Surface Area Doubled | Bc | 420000 | | | | Influence of low waste rock surface area |
| | Paste Cement Surface Area Halved | Bc | 105000 | | | | Influence of high waste rock surface area |
| **WRS at Year 2** | | Reactive Mass (tonnes) | | | | | |
| Base case | | 8301 | | | | | Likely and forseeable scenario for WRS in year 2 |
| Sensitivity Analyses | Reactive Mass Halved | 4150 | | | | | Influence of high estimate of reactive mass (also, proportional to surface area and flow). |

# APPENDIX E: Groundwater Chemistry Model Inputs, from Hydrometrics Inc. (2015)

| Parameter | Units* | Groundwater contribution | | | | | | | AVERAGE OF ALL GW |
|---|---|---|---|---|---|---|---|---|---|
| | | surface decline | | upper access/stopes | | lower decline | lower access/stopes | | |
| | | YNL-A | USZ | USZ/UCZ | YNLB-UA | YNLB-LD | LCZ & LZFW | YnIB-LA | |
| | | Avg (MW-1B, -2A, -2B, -4B, -9, PW-1 and -8) | PW-9 Avg | Avg (MW-3, PW-2, PW-4) | PW-10 | PW-10 | From PW-9 in UCZ (worst case), because data for PW-7 are poor | PW-10 | |
| Flow rate | L/min | 386 | 34 | 1037 | 49 | 450 | 37.85 | 64 | 2059 |
| | L/week | 3891997 | 343411 | 10454972 | 496039 | 4540663 | 381568 | 648666 | 20757317 |
| Fraction of total flow | - | 0.188 | 0.017 | 0.504 | 0.024 | 0.219 | 0.018 | 0.031 | 1 |
| Surface area | m2 | | | | | | | | |
| Rock density | kg/m3 | | | | | | | | |
| Mass fraction sulfide (as S) | - | | | | | | | | |
| Exposure time (days) | days | | | | | | | | |
| Reactive mass (kg) | kg | | | | | | | | |
| Oxidized rind thickness (m) | m | | | | | | | | |
| Scaling factor w.r.t. HCT | - | | | | | | | | |
| pH | s.u. | 7.03 | 6.56 | 7.06 | 7.39 | 7.39 | 6.56 | 7.39 | 7.086 |
| Activity of hydrogen | - | 9.43E-08 | 2.75E-07 | 8.66E-08 | 4.07E-08 | 4.07E-08 | 2.75E-07 | 4.07E-08 | 8.21E-08 |
| Temperature | °C | 7.1 | 10.3 | 9.3 | 8.5 | 8.5 | 10.3 | 8.5 | 8.7 |
| Total Alkalinity | mg/L as CaCO₃ | 189 | 204 | 223 | 230 | 230 | 204 | 230 | 218 |
| Aluminum | mg/L | 0.015 | 0.009 | 0.016 | 0.009 | 0.009 | 0.009 | 0.009 | 0.014 |
| Antimony | mg/L | 0.003 | 0.001 | 0.002 | 0.001 | 0.001 | 0.001 | 0.001 | 0.001 |
| Arsenic | mg/L | 0.018 | 0.086 | 0.063 | 0.048 | 0.048 | 0.086 | 0.048 | 0.051 |
| Barium | mg/L | 0.059 | 0.014 | 0.014 | 0.111 | 0.111 | 0.014 | 0.111 | 0.049 |
| Beryllium | mg/L | 0.001 | 0.001 | 0.001 | 0.001 | 0.001 | 0.001 | 0.001 | 0.001 |
| Cadmium | mg/L | 0.00004 | 0.00003 | 0.00005 | 0.00004 | 0.00004 | 0.00003 | 0.00004 | 0.00005 |
| Calcium | mg/L | 58 | 83 | 84 | 74 | 74 | 83 | 74 | 76 |
| Chloride | mg/L | 1.41 | 1.40 | 1.40 | 1.00 | 1.00 | 1.40 | 1.00 | 1.29 |
| Chromium | mg/L | 0.007 | 0.005 | 0.005 | 0.010 | 0.010 | 0.005 | 0.010 | 0.007 |
| Copper | mg/L | 0.002 | 0.002 | 0.002 | 0.002 | 0.002 | 0.002 | 0.002 | 0.002 |
| Fluoride | mg/L | 0.290 | 0.600 | 0.693 | 0.800 | 0.800 | 0.600 | 0.800 | 0.644 |
| Iron | mg/L | 5.77 | 2.18 | 1.12 | 0.340 | 0.340 | 2.18 | 0.340 | 1.81 |
| Lead | mg/L | 0.002 | 0.000 | 0.000 | 0.000 | 0.000 | 0.000 | 0.000 | 0.001 |
| Magnesium | mg/L | 28 | 48 | 53 | 47 | 47 | 48 | 47 | 47 |
| Manganese | mg/L | 0.043 | 0.041 | 0.034 | 0.437 | 0.437 | 0.041 | 0.437 | 0.146 |
| Mercury | mg/L | 0.000007 | 0.000005 | 0.000007 | 0.000005 | 0.000005 | 0.000005 | 0.000005 | 0.00001 |
| Nickel | mg/L | 0.005 | 0.001 | 0.005 | 0.001 | 0.001 | 0.001 | 0.001 | 0.004 |
| Nitrate + Nitrite | mg/L as N | 0.069 | 0.016 | 0.010 | 0.010 | 0.010 | 0.016 | 0.010 | 0.021 |
| Phosphorus | mg/L | 0.015 | | 0.010 | | | | | 0.011 |
| Potassium | mg/L | 2.007 | 3.000 | 3.143 | 5.000 | 5.000 | 3.000 | 5.000 | 3.43 |
| Selenium | mg/L | 0.001 | 0.000 | 0.001 | 0.000 | 0.000 | 0.000 | 0.000 | 0.000 |
| Silicon | mg/L | 10.060 | | 8.300 | | | | | 8.78 |
| Sodium | mg/L | 3.059 | 11.800 | 14.267 | 11.000 | 11.000 | 11.800 | 11.000 | 11.18 |
| Strontium | mg/L | 0.566 | 8.654 | 13.480 | 11.900 | 11.900 | 8.654 | 11.900 | 10.5 |
| Sulfate | mg/L | 88 | 250 | 253 | 190 | 190 | 250 | 190 | 205 |
| Thallium | mg/L | 0.004 | 0.001 | 0.0004 | 0.0002 | 0.0002 | 0.001 | 0.0002 | 0.001 |
| Uranium | mg/L | 0.005 | 0.002 | 0.004 | 0.008 | 0.008 | 0.002 | 0.008 | 0.005 |
| Zinc | mg/L | 0.019 | 0.056 | 0.046 | 0.002 | 0.002 | 0.056 | 0.002 | 0.029 |

# APPENDIX F:  Prediction of Metal Attenuation by Sulfide in Bedrock Post-Closure

At closure, the water table will rebound to the pre-mining level.  Any solutes stored in the mined out workings will dissolve into groundwater and be collected for treatment during the initial flooding of the mine at closure.  Under steady state, post-closure groundwater flow and chemistry conditions, the submerged wall rock will be exposed to reduced groundwater typical of the natural background environment.  Sulfide oxidation and associated metal release from exposed rock in the mine back will drop to low levels.   We assume groundwater flowing through remaining voids between the paste backfill and the back will continue to acquire solutes from the exposed paste surface and react with the fractured bedrock surface.  At closure, pyrite within the relatively high-surface-area zone around the workings will be stable under reducing conditions.

Pyrite is known to adsorb a variety of metals common to mining environments, including Pb, Hg, Cu, Cd, Cr, and As (Doyle et al., 2004; Borah and Senapati, 2006; Oxverdi and Erdem, 2006).  In fact, pyrite has been proposed for use in reactive barrier technology to remove metals from contaminated groundwater (Brown et al. 1979).  Of these metals, only Cd and Hg were predicted in post-closure groundwater.  We therefore calculated the capacity for their sorption to pyrite in the USZ using this analytical model.  Using the USZ pyrite concentration (46 wt %) reported by CAMP, and surface area-adjusted isotherm data for comparable pH and metal concentrations (Borah and Senapati (2006) for Cd, and Bower et al. (2008) for Hg), we estimate that Hg will be completely removed via sorption to pyrite, with an attenuation capacity of over 20 thousand years.  Likewise, we estimate that capacity exists for Cd will be completely attenuated within the bedrock fracture zone for millions of years.

The concentration of metals used in these calculations are scaled, from surface area and water flux rates typical of the laboratory diffusion tests to  conditions relevant to the post-closure mine setting.  The concentrations measured in diffusion tests are scaled up due to the increased paste backfill surface area and reduce flow of groundwater post-closure.

These calculations conservatively rely on constant, long term release of metals by paste backfill (which are likely to decline over time) and rates published for experiments that were conducted at higher concentrations of Cd and Hg. Data are not available for experiments conducted at lower concentrations, because Cd and Hg removal efficiency is 100% and therefore, lower metal concentrations are not quantifiable in solution.

Assumptions:

* 1 m fracture zone above back                    See section 4.3.2

* mass of rock in 1 m zone above the back is calculated from the density of the upper sulfide zone

* fracture density of 10% in the upper zone implies that the specific surface area is 10% of the humidity cell test material

Calculations:

| | | | |
|---|---|---|---|
| Top surface area of backfilled paste in USZ | 293060 | m2 | |
| Volume of fracture zone above back (1-m thick) | 293060 | m3 | |
| Mass of fracture zone above back | 1.06E+09 | kg | *based on 3600 kg/m3 in USZ) |
| Surface area of HCT (used for Fd scaling) | 2.0107 | m2/kg | *based on calculation from seived material |
| Surface area of fracture zone | 2.12E+08 | m2 | *based on 10% of the specific surface area of the HCT |
| Surface area of FeS2 in fracture zone | 9.76E+07 | m2 | *assumes that 46% of the surface area is pyrite, i.e. that the relative surface area is proportional to mass of pyrite reported by CAMP (Enviromin, 2016b) |
| Intrinsic attenuation capacity per mass | 0.0002 | g Hg/g FeS2 | *based on data collected by Bower et al. (2008) at lowest concentration of Hg, where 100% removal was attained in 2 days |
| Intrinsic attenuation capacity per surface area | 0.0004762 | g Hg/m2 FeS2 | *based on BET data from Bower et al., 2008, 0.42 m2/g in samples. [1] |
| Total attenuation capacity of fracture zone | 46468 | g Hg | |
| Flow rate through USZ at post-closure | 190784 | L/week through the USZ/UCZ | |

Duration of attenuation capacity = Hg

| | | |
|---|---|---|
| Assuming 230 ppt Hg released from scaled paste surface, prior to diluton | **2.03E+04** | years of attenuation capacity |

| | | | |
|---|---|---|---|
| Intrinsic attenuation capacity per mass | 0.1676 | g Cd/g FeS2 | *based on data collected by Borah and Senapati, 2006 at lowest Cd concentration, where 100% removal was attained in 2 days |
| Intrinsic attenuation capacity per surface area | 0.69833 | g Cd/m2 FeS2 | *based on BET data from Borah and Senapati, 2006, 0.24 m2/g in samples. [1] |
| Total attenuation capacity of fracture zone | 68145006 | g Cd | |
| Flow rate through USZ at post-closure | 190784 | L/week through the USZ/UCZ | |

Duration of attenuation capacity - Cd

| | | |
|---|---|---|
| Assuming 282 ppt Cd released from scaled paste surface | **2.43E+07** | years of attenuation capacity |

[1] Note that BET, which probably overestimates surface area compared to the geometric assumption used above, is conservative.

# APPENDIX G: Mass-Load Inputs from the Base Case Underground Model at Year 6

Column groups:
- **Groundwater contribution (GW)**: surface decline (YNL-A, USZ), upper access/stopes (USZ/UCZ, YNLB-UA), lower decline (YNLB-LD), lower access/stopes (LCZ & LZFW, YnlB-LA)
- **Oxidized surface contribution (OX)**: surface decline (YNL-A, USZ), upper access/stopes (USZ/UCZ, Backfill, YNLB-UA), lower decline (YNLB-LD), lower access/stopes (LCZ, LZFW, Backfill, YNLB-LA)
- **Combined input (GW + rock/stope) (CI)**: surface decline (YNL-A, USZ), upper access/stopes (USZ/UCZ, YNLB-UA), lower decline (YNLB-LD), lower access/stopes (LCZ, YnlB-LA)

Source descriptions (GW): YNL-A = Avg (MW-1B, -2A, -2B, -4B, -9, PW-1 and -8); USZ = PW-9 Avg; USZ/UCZ = Avg (MW-3, PW-2, PW-4); YNLB-UA = PW-10; YNLB-LD = PW-10; LCZ & LZFW = From PW-9 in UCZ (worst case), because data for PW-7 are poor; YnlB-LA = PW-10.

Source descriptions (OX): YNL-A = HCT - 2012 Ynl; USZ = HCT - 2012 USZ; USZ/UCZ = HCT - 2015 USZ; Backfill = 2015 4% binder cyl. Diff. test; YNLB-UA = HCT - 2012 Ynl B; YNLB-LD = HCT - 2015 Ynl B; LCZ = HCT - 2015 LZFW; LZFW = HCT - 2015 LZFW; Backfill = 2015 4% binder cyl. Diff. test; YNLB-LA = HCT - 2015 LZFW.

**Assumptions:** *Upper zone fracture density = 0.1 (applies to surface decline and upper access/stopes); *Lower zone fracture density = 0.02 (applies to lower decline and lower access/stopes); *Oxidation rate (kg SO4/y/m2) = 6.

| Parameter | Units* | GW YNL-A | GW USZ | GW USZ/UCZ | GW YNLB-UA | GW YNLB-LD | GW LCZ & LZFW | GW YnlB-LA | OX YNL-A | OX USZ | OX USZ/UCZ | OX Backfill | OX YNLB-UA | OX YNLB-LD | OX LCZ | OX LZFW | OX Backfill | OX YNLB-LA | CI YNL-A | CI USZ | CI USZ/UCZ | CI YNLB-UA | CI YNLB-LD | CI LCZ | CI YnlB-LA |
|---|---|---|---|---|---|---|---|---|---|---|---|---|---|---|---|---|---|---|---|---|---|---|---|---|---|
| Flow rate | L/min | 386 | 34 | 1037 | 49 | 450 | 37.85 | 64 | | | | | | | | | | | 386 | 34 | 1037 | 49 | 450 | 37.85 | 64 |
| Flow rate | L/week | 3891997 | 343411 | 10454972 | 496039 | 4540663 | 381568 | 648666 | | | | | | | | | | | 3891997 | 343411 | 10454972 | 496039 | 4540663 | 381568 | 648666 |
| Fraction of total flow | - | 0.188 | 0.017 | 0.504 | 0.024 | 0.219 | 0.018 | 0.031 | | | | | | | | | | | 0.188 | 0.017 | 0.504 | 0.024 | 0.219 | 0.018 | 0.031 |
| Surface area | m2 | | | | | | | | 9900 | 1200 | 91545 | 3346 | 50000 | 63400 | 8713 | 94400 | 1714 | 27280 | | | | | | | |
| Rock density | kg/m3 | | | | | | | | 2710 | 3600 | 3600 | - | 2710 | 2710 | 3600 | 3600 | - | 3600 | | | | | | | |
| Mass fraction sulfide (as S) | - | | | | | | | | 0.016 | 0.200 | 0.200 | - | 0.011 | 0.011 | 0.113 | 0.019 | - | 0.019 | | | | | | | |
| Exposure time (days) | days | | | | | | | | 2160 | 2160 | 90 | - | 2160 | 2160 | 90 | 90 | - | 90 | | | | | | | |
| Reactive mass (kg) | kg | | | | | | | | 2682900 | 71209 | 226347 | - | 2247752 | 3436280 | 38298 | 6796800 | - | 710006 | | | | | | | |
| Oxidized rind thickness (m) | m | | | | | | | | 1.000 | 0.165 | 0.007 | - | 0.166 | 1.000 | 0.061 | 1.000 | - | 0.361 | | | | | | | |
| Scaling factor w.r.t. HCT | - | | | | | | | | 0.31 | 0.09 | 0.02 | 0.02 | 2.06 | 0.32 | 0.04 | 7.71 | 0.32 | 0.47 | | | | | | | |
| pH | s.u. | 7.03 | 6.56 | 7.06 | 7.39 | 7.39 | 6.56 | 7.39 | 7.81 | 7.87 | 7.64 | 7.50 | 7.68 | 7.89 | 8.65 | 6.40 | 6.35 | 7.62 | 6.96 | 6.54 | 6.85 | 7.21 | 7.27 | 5.95 | 7.19 |
| Activity of hydrogen | - | 9.43E-08 | 2.75E-07 | 8.66E-08 | 4.07E-08 | 4.07E-08 | 2.75E-07 | 4.07E-08 | 1.6E-08 | 1.4E-08 | 2.3E-08 | 3.2E-08 | 2.1E-08 | 1.3E-08 | 2.2E-09 | 3.9E-07 | 4.4E-07 | 2.4E-08 | 1.10E-07 | 2.89E-07 | 1.41E-07 | 6.15E-08 | 5.35E-08 | 1.11E-06 | 6.50E-08 |
| Temperature | °C | 7.1 | 10.3 | 9.3 | 8.5 | 8.5 | 10.3 | 8.5 | 7.1 | 10.3 | 9.3 | 9.3 | 8.5 | 9.3 | 9.3 | 9.3 | 9.3 | 8.5 | 7.1 | 10.3 | 9.3 | 8.5 | 8.5 | 9.3 | 8.5 |
| Total Alkalinity | mg/L as CaCO3 | 189 | 204 | 223 | 230 | 230 | 204 | 230 | 4.51 | 1.14 | 0.16 | 0.03 | 56 | 9 | 1 | 177 | 0.481 | 11 | 193 | 205 | 223 | 286 | 239 | 383 | 241 |
| Aluminum | mg/L | 0.015 | 0.009 | 0.016 | 0.009 | 0.009 | 0.009 | 0.009 | 0.004 | 0.001 | 0.001 | 0.007 | 0.080 | 0.023 | 0.003 | 0.447 | 0.003 | 0.027 | 0.019 | 0.010 | 0.024 | 0.089 | 0.032 | 0.462 | 0.036 |
| Antimony | mg/L | 0.003 | 0.001 | 0.002 | 0.001 | 0.001 | 0.001 | 0.001 | 0.000 | 0.000 | 0.000 | 0.000 | 0.011 | 0.001 | 0.000 | 0.064 | 0.000 | 0.004 | 0.004 | 0.001 | 0.002 | 0.011 | 0.001 | 0.065 | 0.004 |
| Arsenic | mg/L | 0.018 | 0.086 | 0.063 | 0.048 | 0.048 | 0.086 | 0.048 | 0.000 | 0.000 | 0.000 | 0.000 | 0.005 | 0.001 | 0.006 | 1.030 | 0.001 | 0.063 | 0.018 | 0.087 | 0.063 | 0.053 | 0.049 | 1.124 | 0.111 |
| Barium | mg/L | 0.059 | 0.014 | 0.014 | 0.111 | 0.111 | 0.014 | 0.111 | 0.007 | 0.001 | 0.000 | 0.001 | 0.012 | 0.009 | 0.001 | 0.206 | 0.009 | 0.013 | 0.066 | 0.015 | 0.015 | 0.123 | 0.120 | 0.230 | 0.124 |
| Beryllium | mg/L | 0.001 | 0.001 | 0.001 | 0.001 | 0.001 | 0.001 | 0.001 | 0.000 | 0.000 | 0.000 | 0.000 | 0.002 | 0.000 | 0.000 | 0.006 | 0.000 | 0.000 | 0.001 | 0.001 | 0.001 | 0.002 | 0.001 | 0.007 | 0.001 |
| Cadmium | mg/L | 0.00004 | 0.00003 | 0.00005 | 0.00004 | 0.00004 | 0.00003 | 0.00004 | 0.000 | 0.000 | 0.000 | 0.000 | 0.000 | 0.000 | 0.000 | 0.001 | 0.000 | 0.000 | 0.000 | 0.000 | 0.000 | 0.000 | 0.000 | 0.001 | 0.000 |
| Calcium | mg/L | 58 | 83 | 84 | 74 | 74 | 83 | 74 | 25 | 11 | 5 | 0 | 36 | 9 | 1.4 | 249 | 9 | 15 | 83 | 94 | 89 | 110 | 83 | 342 | 89 |
| Chloride | mg/L | 1.41 | 1.40 | 1.40 | 1.00 | 1.00 | 1.40 | 1.00 | 0.101 | 0.70 | 0.073 | 0.023 | 0.002 | 0.000 | 0.014 | 3 | 0.427 | 0.16 | 1.513 | 2.101 | 1.496 | 1.002 | 1.000 | 4.385 | 1.156 |
| Chromium | mg/L | 0.007 | 0.005 | 0.005 | 0.010 | 0.010 | 0.005 | 0.010 | 0.003 | 0.001 | 0.000 | 0.000 | 0.021 | 0.003 | 0.000 | 0.077 | 0.002 | 0.005 | 0.010 | 0.006 | 0.005 | 0.031 | 0.013 | 0.084 | 0.015 |
| Copper | mg/L | 0.002 | 0.002 | 0.002 | 0.002 | 0.002 | 0.002 | 0.002 | 0.001 | 0.000 | 0.000 | 0.000 | 0.004 | 0.001 | 0.000 | 0.015 | 0.001 | 0.001 | 0.003 | 0.002 | 0.002 | 0.006 | 0.003 | 0.018 | 0.003 |
| Fluoride | mg/L | 0.29 | 0.60 | 0.69 | 0.80 | 0.80 | 0.60 | 0.80 | 0.18 | 0.02 | 0.00 | 0.002 | 1.85 | 0.60 | 0.04 | 7.2 | 0.043 | 0.44 | 0.47 | 0.62 | 0.70 | 2.65 | 1.40 | 7.86 | 1.24 |
| Iron | mg/L | 5.77 | 2.18 | 1.12 | 0.340 | 0.340 | 2.18 | 0.340 | 0.006 | 0.002 | 0.104 | 0.000 | 0.041 | 0.006 | 0.001 | 0.154 | 0.006 | 0.009 | 5.78 | 2.18 | 1.22 | 0.381 | 0.346 | 2.337 | 0.349 |
| Lead | mg/L | 0.002 | 0.000 | 0.000 | 0.000 | 0.000 | 0.000 | 0.000 | 0.000 | 0.000 | 0.000 | 0.000 | 0.001 | 0.001 | 0.000 | 0.013 | 0.000 | 0.001 | 0.002 | 0.000 | 0.000 | 0.001 | 0.001 | 0.014 | 0.001 |
| Magnesium | mg/L | 28 | 48 | 53 | 47 | 47 | 48 | 47 | 15 | 17 | 4 | 0.01 | 31 | 11 | 2 | 373 | 0.328 | 23 | 43 | 65 | 58 | 78 | 58 | 423 | 70 |
| Manganese | mg/L | 0.043 | 0.041 | 0.034 | 0.437 | 0.437 | 0.041 | 0.437 | 0.020 | 0.083 | 0.049 | 0.000 | 0.010 | 0.002 | 0.001 | 0.105 | 0.002 | 0.006 | 0.062 | 0.123 | 0.083 | 0.447 | 0.439 | 0.148 | 0.443 |
| Mercury | mg/L | 0.000007 | 0.000005 | 0.000007 | 0.000005 | 0.000005 | 0.000005 | 0.000005 | 0.000003 | 0.000001 | 0.000015 | 0.000001 | 0.000017 | 0.000002 | 0.000000 | 0.000039 | 0.000009 | 0.000002 | 0.000009 | 0.000006 | 0.000022 | 0.000022 | 0.000007 | 0.000053 | 0.000007 |
| Nickel | mg/L | 0.005 | 0.001 | 0.005 | 0.001 | 0.001 | 0.001 | 0.001 | 0.001 | 0.002 | 0.001 | 0.000 | 0.000 | 0.001 | 0.000 | 0.100 | 0.003 | 0.006 | 0.006 | 0.004 | 0.006 | 0.005 | 0.002 | 0.105 | 0.007 |
| Nitrate + Nitrite | mg/L as N | 0.069 | 0.016 | 0.010 | 0.010 | 0.010 | 0.016 | 0.010 | 0.000 | 0.000 | 0.000 | 0.000 | 0.000 | 0.000 | 0.000 | 0.000 | 0.000 | 0.000 | 0.069 | 0.016 | 0.010 | 0.010 | 0.010 | 0.016 | 0.010 |
| Phosphorus | mg/L | 0.015 | | 0.010 | | | | | 0.002 | 0.000 | 0.000 | 0.001 | 0.010 | 0.002 | 0.000 | 0.098 | 0.003 | 0.006 | 0.017 | 0.000 | 0.011 | 0.010 | 0.010 | 0.102 | 0.006 |
| Potassium | mg/L | 2.0 | 3.0 | 3.1 | 5.0 | 5.0 | 3.0 | 5.0 | 3.6 | 2.0 | 0.2 | 0.055 | 51.4 | 8.1 | 1.1 | 203 | 0.7 | 12.5 | 5.6 | 5.0 | 3.4 | 56.4 | 13.1 | 207.7 | 17.5 |
| Selenium | mg/L | 0.001 | 0.000 | 0.001 | 0.000 | 0.000 | 0.000 | 0.000 | 0.002 | 0.001 | 0.000 | 0.000 | 0.014 | 0.003 | 0.001 | 0.116 | 0.000 | 0.007 | 0.002 | 0.001 | 0.001 | 0.014 | 0.003 | 0.117 | 0.007 |
| Silicon | mg/L | 10.1 | | 8.3 | | | | | 0.3 | 0.1 | 0.0 | 0.007 | 3.1 | 0.6 | 0.1 | 21.3 | 0.060 | 1.3 | 10.4 | 0.1 | 8.3 | 3.1 | 0.6 | 21.5 | 1.3 |
| Sodium | mg/L | 3.1 | 11.8 | 14.3 | 11.0 | 11.0 | 11.8 | 11.0 | 3.8 | 0.3 | 0.0 | 0.033 | 28.1 | 4.4 | 0.4 | 77.1 | 0.646 | 4.7 | 6.8 | 12.1 | 14.3 | 39.1 | 15.4 | 90.0 | 15.7 |
| Strontium | mg/L | 0.6 | 8.7 | 13.5 | 11.9 | 11.9 | 8.7 | 11.9 | 0.3 | 0.1 | 0.3 | 0.007 | 0.3 | 0.5 | 0.0 | 4.6 | 0.10 | 1.3 | 0.8 | 8.7 | 13.8 | 12.2 | 12.4 | 13.4 | 12.2 |
| Sulfate | mg/L | 88 | 250 | 253 | 190 | 190 | 250 | 190 | 126 | 82 | 30 | 1 | 178 | 85 | 13 | 2279 | 14.4 | 140 | 214 | 332 | 283 | 368 | 275 | 2556 | 330 |
| Thallium | mg/L | 0.004 | 0.001 | 0.0004 | 0.0002 | 0.0002 | 0.001 | 0.0002 | 0.001 | 0.000 | 0.001 | 0.000 | 0.000 | 0.000 | 0.000 | 0.005 | 0.000 | 0.000 | 0.005 | 0.001 | 0.002 | 0.001 | 0.000 | 0.006 | 0.000 |
| Uranium | mg/L | 0.005 | 0.002 | 0.004 | 0.008 | 0.008 | 0.002 | 0.008 | 0.000 | 0.000 | 0.000 | 0.000 | 0.002 | 0.000 | 0.010 | 1.7 | 0.000 | 0.105 | 0.006 | 0.002 | 0.004 | 0.010 | 0.008 | 1.728 | 0.113 |
| Zinc | mg/L | 0.019 | 0.056 | 0.046 | 0.002 | 0.002 | 0.056 | 0.002 | 0.002 | 0.001 | 0.000 | 0.000 | 0.016 | 0.003 | 0.000 | 0.062 | 0.003 | 0.004 | 0.021 | 0.057 | 0.046 | 0.018 | 0.005 | 0.121 | 0.006 |

not measured
detection limits

For the paste backfill, results from HCTs are scaled to surface area rather than Rm, because this material is not a fractured porous media like the walls. Secondly, the ASTM method recommends normalization to the diffusion tests based on diffusion through the surface.
Surface area calculations in supporting document *Workings_SA_Calc_LS_final_4walls*

The calculation of Rm is based on sulfide oxidation rate (i.e., sulfate production), which depends on rock density, sulfide content, and exposure time. Including unit conversions, the equation is described by:

The stoichiometry of the calculation is based on the oxidation reaction   $2FeS_2(s) + 7.5O_2 + 7H_2O \leftrightarrow 4SO_4^{2-} + 2\,Fe(OH)_3(s) + 8H^+$

Purple indicates that oxidized rind has maxed out at the extent of blast-induced fractures (i.e., 1 m), so we recalculate the reactive mass based on the max thickness
For pH, we convert to H activity, and scale, and then recalculate after scaling.

# APPENDIX H: Mass-Load Inputs from the Base Case Underground Model at Closure

| Parameter | Units* | Groundwater contribution | | | | | | | Oxidized surface contribution | | | | | | | | | | Combined input (GW + rock/stope) | | | | | | |
|---|---|---|---|---|---|---|---|---|---|---|---|---|---|---|---|---|---|---|---|---|---|---|---|---|---|
| | | surface decline | | upper access/stopes | | lower decline | lower access/stopes | | surface decline | | upper access/stopes | | | lower decline | lower access/stopes | | | | surface decline | | upper access/stopes | | lower decline | lower access/stopes | |
| | | YNL-A | USZ | USZ/UCZ | YNLB-UA | YNLB-LD | LCZ & LZFW | YnIB-LA | YNL-A | USZ | USZ/UCZ | Backfill | YNLB-UA | YNLB-LD | LCZ | LZFW | Backfill | YNLB-LA | YNL-A | USZ | USZ/UCZ | YNLB-UA | YNLB-LD | LCZ | YnIB-LA |
| | | Avg (MW-1B, -2A, -2B, -4B, -9, PW-1 and -8) | PW-9 Avg | Avg (MW-3, PW-2, PW-4) | PW-10 | PW-10 | From PW-9 in UCZ (worst case), because data for PW-7 are poor | PW-10 | HCT - 2012 Ynl | HCT - 2012 USZ | HCT - 2015 USZ | 2015 4% binder cyl. Diff. test | HCT - 2012 Ynl B | HCT - 2015 Ynl B | HCT - 2015 LZFW | HCT - 2015 LZFW | 2015 4% binder cyl. Diff. test | HCT - 2015 LZFW | | | | | | | |
| Flow rate (L/min) | L/min | 344 | 30 | 19 | 11 | 15 | 4 | 1 | | | | | | | | | | | 344 | 30 | 19 | 11 | 0 | 0 | 0 |
| Flow rate (L/week) | L/week | 3472272 | 305255 | 190784 | 114470 | 152627 | 38157 | 11447 | | | | | | | | | | | 3472272 | 305255 | 190784 | 114470 | 0 | 0 | 0 |
| Fraction of total flow | - | 0.810 | 0.071 | 0.045 | 0.027 | 0.036 | 0.009 | 0.003 | | | | | | | | | | | 0.810 | 0.071 | 0.045 | 0.027 | 0.000 | 0.000 | 0.000 |
| Surface area | m2 | | | | | | | | | | | 14653 | | | | | 13176 | | | | | | | | |
| Rock density | kg/m3 | | | | | | | | | | | - | | | | | - | | | | | | | | |
| Mass fraction sulfide (as S) | - | | | | | | | | | | | - | | | | | - | | | | | | | | |
| Exposure time (days) | days | | | | | | | | | | | - | | | | | - | | | | | | | | |
| Reactive mass (kg) | kg | | | | | | | | | | | - | | | | | - | | | | | | | | |
| Oxidized rind thickness (m) | m | | | | | | | | | | | - | | | | | - | | | | | | | | |
| Scaling factor w.r.t. HCT | - | | | | | | | | | | | 7.733 | | | | | 34.769 | | | | | | | | |
| pH | s.u. | 7.03 | 6.56 | 7.06 | 7.39 | 7.39 | 6.56 | 7.39 | | | | 6.513 | | | | | 5.860 | | 7.03 | 6.56 | 6.41 | 7.39 | 7.39 | 5.78 | 7.39 |
| Activity of hydrogen | - | 9.43E-08 | 2.75E-07 | 8.66E-08 | 4.07E-08 | 4.07E-08 | 2.75E-07 | 4.07E-08 | | | | 0.000 | | | | | 0.000 | | 9.43E-08 | 2.75E-07 | 3.93E-07 | 4.07E-08 | 4.07E-08 | 1.65E-06 | 4.07E-08 |
| Temperature | °C | 7.1 | 10.3 | 9.3 | 8.5 | 8.5 | 10.3 | 8.5 | | | | 9.34 | | | | | 9.33 | | 7.1 | 10.3 | 9.3 | 8.5 | 8.5 | 9.3 | 8.5 |
| Total Alkalinity | mg/L as CaCO$_3$ | 189 | 204 | 223 | 230 | 230 | 204 | 230 | | | | 81.8 | | | | | 367.6 | | 189 | 204 | 304 | 230 | 230 | 572 | 230 |
| Aluminum | mg/L | 0.015 | 0.009 | 0.016 | 0.009 | 0.009 | 0.009 | 0.009 | | | | 2.403 | | | | | 10.806 | | 0.015 | 0.009 | 2.420 | 0.009 | 0.009 | 10.8 | 0.009 |
| Antimony | mg/L | 0.003 | 0.001 | 0.002 | 0.001 | 0.001 | 0.001 | 0.001 | | | | 0.009 | | | | | 0.041 | | 0.003 | 0.001 | 0.011 | 0.001 | 0.001 | 0.042 | 0.001 |
| Arsenic | mg/L | 0.018 | 0.086 | 0.063 | 0.048 | 0.048 | 0.086 | 0.048 | | | | 0.140 | | | | | 0.628 | | 0.018 | 0.086 | 0.202 | 0.048 | 0.048 | 0.7 | 0.048 |
| Barium | mg/L | 0.059 | 0.014 | 0.014 | 0.111 | 0.111 | 0.014 | 0.111 | | | | 0.390 | | | | | 1.753 | | 0.059 | 0.014 | 0.404 | 0.111 | 0.111 | 1.8 | 0.111 |
| Beryllium | mg/L | 0.001 | 0.001 | 0.001 | 0.001 | 0.001 | 0.001 | 0.001 | | | | 0.006 | | | | | 0.028 | | 0.001 | 0.001 | 0.007 | 0.001 | 0.001 | 0.029 | 0.001 |
| Cadmium | mg/L | 0.00004 | 0.00003 | 0.00005 | 0.00004 | 0.00004 | 0.00003 | 0.00004 | | | | 0.000232 | | | | | 0.00104 | | 0.000 | 0.000 | 0.000 | 0.000 | 0.000 | 0.001 | 0.000 |
| Calcium | mg/L | 58 | 83 | 84 | 74 | 74 | 83 | 74 | | | | 139.75 | | | | | 628.32 | | 58 | 83 | 224 | 74 | 74 | 711 | 74 |
| Chloride | mg/L | 1.41 | 1.40 | 1.40 | 1.00 | 1.00 | 1.40 | 1.00 | | | | 7.733 | | | | | 34.769 | | 1.4 | 1.4 | 9.1 | 1.0 | 1.0 | 36 | 1.0 |
| Chromium | mg/L | 0.007 | 0.005 | 0.005 | 0.010 | 0.010 | 0.005 | 0.010 | | | | 0.039 | | | | | 0.174 | | 0.007 | 0.005 | 0.044 | 0.010 | 0.010 | 0.179 | 0.010 |
| Copper | mg/L | 0.002 | 0.002 | 0.002 | 0.002 | 0.002 | 0.002 | 0.002 | | | | 0.015 | | | | | 0.070 | | 0.002 | 0.002 | 0.017 | 0.002 | 0.002 | 0.072 | 0.002 |
| Fluoride | mg/L | 0.290 | 0.600 | 0.693 | 0.800 | 0.800 | 0.600 | 0.800 | | | | 0.773 | | | | | 3.477 | | 0.290 | 0.600 | 1.467 | 0.800 | 0.800 | 4.077 | 0.800 |
| Iron | mg/L | 5.77 | 2.18 | 1.12 | 0.340 | 0.340 | 2.18 | 0.340 | | | | 0.155 | | | | | 0.695 | | 5.8 | 2.2 | 1.3 | 0.3 | 0.3 | 2.9 | 0.3 |
| Lead | mg/L | 0.002 | 0.000 | 0.000 | 0.000 | 0.000 | 0.000 | 0.000 | | | | 0.002 | | | | | 0.007 | | 0.002 | 0.000 | 0.002 | 0.000 | 0.000 | 0.007 | 0.000 |
| Magnesium | mg/L | 28 | 48 | 53 | 47 | 47 | 48 | 47 | | | | 3.867 | | | | | 17.384 | | 28 | 48 | 57 | 47 | 47 | 66 | 47 |
| Manganese | mg/L | 0.043 | 0.041 | 0.034 | 0.437 | 0.437 | 0.041 | 0.437 | | | | 0.039 | | | | | 0.174 | | 0.043 | 0.041 | 0.072 | 0.437 | 0.437 | 0.215 | 0.437 |
| Mercury | mg/L | 0.000007 | 0.000005 | 0.000007 | 0.000005 | 0.000005 | 0.000005 | 0.000005 | | | | 0.0000387 | | | | | 0.000174 | | 0.000007 | 0.000005 | 0.000045 | 0.000005 | 0.000005 | 0.000179 | 0.000005 |
| Nickel | mg/L | 0.005 | 0.001 | 0.005 | 0.001 | 0.001 | 0.001 | 0.001 | | | | 0.015 | | | | | 0.070 | | 0.005 | 0.001 | 0.020 | 0.001 | 0.001 | 0.071 | 0.001 |
| Nitrate + Nitrite | mg/L as N | 0.069 | 0.016 | 0.010 | 0.010 | 0.010 | 0.016 | 0.010 | | | | 0.000 | | | | | 0.000 | | 0.069 | 0.016 | 0.010 | 0.010 | 0.010 | 0.016 | 0.010 |
| Phosphorus | mg/L | 0.015 | | 0.010 | | | | | | | | 0.204 | | | | | 0.919 | | 0.015 | 0.000 | 0.214 | 0.000 | 0.000 | 0.919 | 0.000 |
| Potassium | mg/L | 2.007 | 3.000 | 3.143 | 5.000 | 5.000 | 3.000 | 5.000 | | | | 18.725 | | | | | 84.190 | | 2.01 | 3.00 | 21.87 | 5.00 | 5.00 | 87.19 | 5.00 |
| Selenium | mg/L | 0.001 | 0.000 | 0.001 | 0.000 | 0.000 | 0.000 | 0.000 | | | | 0.008 | | | | | 0.035 | | 0.001 | 0.000 | 0.008 | 0.000 | 0.000 | 0.035 | 0.000 |
| Silicon | mg/L | 10.060 | | 8.300 | | | | | | | | 2.414 | | | | | 10.853 | | 10.060 | 0.000 | 10.714 | 0.000 | 0.000 | 10.9 | 0.000 |
| Sodium | mg/L | 3.059 | 11.800 | 14.267 | 11.000 | 11.000 | 11.800 | 11.000 | | | | 11.252 | | | | | 50.589 | | 3.1 | 12 | 26 | 11 | 11 | 62 | 11 |
| Strontium | mg/L | 0.566 | 8.654 | 13.480 | 11.900 | 11.900 | 8.654 | 11.900 | | | | 2.215 | | | | | 9.959 | | 0.6 | 8.7 | 15.7 | 11.9 | 11.9 | 18.6 | 11.9 |
| Sulfate | mg/L | 88 | 250 | 253 | 190 | 190 | 250 | 190 | | | | 212.661 | | | | | 956.144 | | 88 | 250 | 465 | 190 | 190 | 1206 | 190 |
| Thallium | mg/L | 0.004 | 0.001 | 0.0004 | 0.0002 | 0.0002 | 0.001 | 0.0002 | | | | 0.004 | | | | | 0.016 | | 0.0043 | 0.0008 | 0.0040 | 0.0002 | 0.0002 | 0.0168 | 0.0002 |
| Uranium | mg/L | 0.005 | 0.002 | 0.004 | 0.008 | 0.008 | 0.002 | 0.008 | | | | 0.002 | | | | | 0.007 | | 0.0054 | 0.0024 | 0.0058 | 0.0080 | 0.0080 | 0.0094 | 0.0080 |
| Zinc | mg/L | 0.019 | 0.056 | 0.046 | 0.002 | 0.002 | 0.056 | 0.002 | | | | 0.062 | | | | | 0.278 | | 0.019 | 0.056 | 0.108 | 0.002 | 0.002 | 0.335 | 0.002 |

**ASSUMPTIONS**
- All oxidized wall-rock terms shut off and paste backfill becomes the only input
- Surface area of stopes increases because 100% of stopes have been mined
- At closure, all sides of the cement backfill are reactive

It is assumed that fractured surfaces go anoxic once the underground water table rebounds, and thus do not add to the groundwater concentrations

not measured in groundwater wells
detection limits

Removed these units that are not connected to the aquifer

## APPENDIX I: Mass-Load Inputs from the Base Case Model for the WRS at Year 2

| Parameter | Units* | Contribution from exposed rock | | | Water to sump (pre-Phreeq) | |
|---|---|---|---|---|---|---|
| | | USZ | YnlB | YnlA | FINAL MIX | |
| | | HCT - 2015 USZ | HCT -2015 YnlB | HCT - 2012 Ynl | | |
| Flow rate | gpm | 0.9 | 0.9 | 0.9 | 0.9 | Percolation value comes from the HELP model (Hydrometrics, 2016), |
| | L/week | 34338 | 34338 | 34338 | | which considers evapotransipiration (e.g., wind), snow removal, solar radiation, and average precipitation. |
| | L/yr | 1785551 | 1785551 | 1785551 | 1785551 | |
| Surface area | m2 | 203093 | 308333 | 38542 | | |
| specific gravity | g/cm3 | 3.60 | 2.71 | 2.71 | | Average density of WR mix     3.099375 |
| surface area per mass | m2/kg | 0.0559 | 0.0743 | 0.0743 | | |
| Total mass in WRS (tonne = 1000 k | tonnes | 180047 | 205769 | 25721 | | Assumes total WR on pile (411,537 tonnes) to be 4% YnlA, 28% USZ, 32% YnlB, and 35% LZFW. |
| Calcuated Rm (from H2O saturation) | tonnes | 3632 | 4151 | 519 | | Assumes 40% porosity, calculates the mass of waste rock that can be saturated by the water flow in 1 yr, according to |
| Scaling factor w.r.t. HCT | - | 1.29 | 1.28 | 0.24 | | |
| pH | s.u. | 5.51 | 7.30 | 7.91 | 5.50 | $R_{m,i}(tonnes) = \dfrac{L_{H2O}}{yr} * \dfrac{1000\ cm_{H2O}^3}{L_{H2O}} * \dfrac{6\ cm_{rock}^3}{4\ cm_{H2O}^3} * \dfrac{g_{rock}}{cm_{rock}^3} * \dfrac{ton_{rock}}{10^6\ g_{rock}} * \dfrac{ton_i}{ton_{rock}}$ |
| Activity of hydrogen | - | 3.09E-06 | 5.05E-08 | 1.24E-08 | 3.15E-06 | |
| Temperature | °C | 2.20 | 2.20 | 2.20 | 2.20 | set to average annual temperature at Tintina weather station |
| Aluminum | mg/L | 0.0766 | 0.0920 | 0.0030 | 0.1716 | |
| Alkalinity | mg/L as CaCO₃ | 21.313 | 35.449 | 3.562 | 60.324 | |
| Arsenic | mg/L | 0.0026 | 0.0047 | 0.0002 | 0.00751 | |
| Barium | mg/L | 0.0177 | 0.0358 | 0.0055 | 0.0589 | |
| Beryllium | mg/L | 0.0010 | 0.0010 | 0.0002 | 0.0022 | |
| Calcium | mg/L | 613.9869 | 34.4909 | 19.7245 | 668.202 | |
| Cadmium | mg/L | 0.0005 | 0.0001 | 0.0000 | 0.000615 | |
| Chloride | mg/L | 9.907 | 0.001 | 0.080 | 9.988 | |
| Chromium | mg/L | 0.01 | 0.01 | 0.00 | 0.0281 | |
| Copper | mg/L | 0.06 | 0.00 | 0.00 | 0.0641 | |
| Fluoride | mg/L | 0.34 | 2.36 | 0.14 | 2.853 | |
| Iron | mg/L | 14.15 | 0.03 | 0.00 | 14.179 | |
| Mercury | mg/L | 0.00 | 0.00 | 0.00 | 0.00202 | |
| Potassium | mg/L | 28 | 32 | 3 | 63.172 | |
| Magnesium | mg/L | 567 | 42 | 12 | 620.781 | |
| Manganese | mg/L | 6.70 | 0.01 | 0.02 | 6.725 | |
| Nitrate + Nitrite | mg/L as N | 0.00 | 0.00 | 0.00 | 0.290 | mmol N(5) for phreeq input, based on data from the underground of a mine in MT |
| Sodium | mg/L | 4 | 17 | 3 | 24.32 | |
| Nickel | mg/L | 0.14 | 0.00 | 0.00 | 0.143 | |
| Phosphorus | mg/L | 0.01 | 0.01 | 0.00 | 0.0163 | |
| Lead | mg/L | 0.00 | 0.00 | 0.00 | 0.0068 | |
| Sulfate | mg/L | 4026 | 336 | 99 | 46.44 | mmol S(6) for phreeq input |
| Antimony | mg/L | 0.0013 | 0.0028 | 0.0003 | 0.0044 | |
| Selenium | mg/L | 0.01 | 0.01 | 0.00 | 0.0172 | |
| Silicon | mg/L | 1.79 | 2 | 0.27 | 4.238 | |
| Strontium | mg/L | 39.7 | 1.88 | 0.21 | 41.824 | |
| Thallium | mg/L | 0.16 | 0.00 | 0.00 | 0.1655 | |
| Uranium | mg/L | 0.00 | 0.00 | 0.00 | 0.00249 | |
| Zinc | mg/L | 0.03 | 0.01 | 0.00 | 0.04272 | |

# APPENDIX J: Data Used for Wet Paste Seepage and 2% Paste in the Cement Tailings Facility

| Parameter | Units | 2% paste HCT | Dewatered cement paste | 4% paste HCT |
|---|---|---|---|---|
| | | Enviromin, 2015 | from metallurgy data | from Enviromin, 2015 |
| pH | s.u. | 4.09873 | 9.32 | 5.86000 |
| activity of hydrogen | - | 7.97E-05 | 4.79E-10 | 1.38E-06 |
| Temperature | °C | 23.80 | 21.0 | 23.85 |
| Alkalinity | mg/L as CaCO₃ | 2.40 | | 1.50000 |
| Aluminum | mg/L | 23.29400 | 0.2810 | 0.01000 |
| Antimony | mg/L | 0.00147 | 0.0523 | 0.00053 |
| Arsenic | mg/L | 0.02067 | 0.0452 | 0.00400 |
| Barium | mg/L | 0.03867 | 0.3020 | 0.02867 |
| Beryllium | mg/L | 0.00620 | 0.0000 | 0.00080 |
| Cadmium | mg/L | 0.00171 | 0.0000 | 0.00003 |
| Calcium | mg/L | 140.00000 | 47.5000 | 27.75000 |
| Chloride | mg/L | 4.66667 | 120.0000 | 1.33333 |
| Chromium | mg/L | 0.01333 | 0.0042 | 0.00500 |
| Copper | mg/L | 73.38237 | 2.7600 | 0.00200 |
| Fluoride | mg/L | 0.68333 | 0.2800 | 0.13333 |
| Iron | mg/L | 18.87500 | 0.0100 | 0.02000 |
| Lead | mg/L | 0.00327 | 0.0964 | 0.00020 |
| Magnesium | mg/L | 75.40000 | 0.6230 | 1.02500 |
| Manganese | mg/L | 3.20923 | 0.0008 | 0.00500 |
| Mercury | mg/L | 0.00014 | | 0.00003 |
| Nickel | mg/L | 10.35300 | 0.0160 | 0.00950 |
| Nitrate | mg/L as N | | 0.6000 | |
| Phosphorus | mg/L | 0.29933 | 0.0470 | 0.01067 |
| Potassium | mg/L | 3.16667 | 3.1000 | 2.09000 |
| Selenium | mg/L | 0.00267 | 0.0005 | 0.00100 |
| Silicon | mg/L | 5.65000 | 0.6600 | 0.18667 |
| Sodium | mg/L | 3.16667 | 40.7000 | 2.01667 |
| Strontium | mg/L | 2.50000 | 0.9880 | 0.32667 |
| Sulfate | mg/L | 890.00000 | 83.0000 | 45.00000 |
| Thallium | mg/L | 0.01710 | 0.0036 | 0.00113 |
| Uranium | mg/L | 0.01060 | 0.0000 | 0.00020 |
| Zinc | mg/L | 1.01200 | 0.0030 | 0.00800 |
| | | | | |
| | detection limits | | | |
| | not measured | | | |

# APPENDIX K: Mass-Load Inputs from the Base Case CTF at Year 6 of Mining

| Parameter | Units* | Surface exposure | | | | Wet paste dewatering | Ramp/drain term | | | | | Water to sump |
|---|---|---|---|---|---|---|---|---|---|---|---|---|
| | | From cemented surface | From exposed waste rock "lenses" | | | based on 55% of 2900 tons of paste per day going to the CTF, and 5% of that mass seeping out as water | Ynl | USZ | YnIB (ramp) | YnIB (liner), 3/8" (0.009525 m) | LZFW | FINAL MIX |
| | | | USZ | YnIB | LZFW | | | | | | | |
| | | HCT - 2% binder | HCT - 2012 USZ | HCT -2012 YnIB | HCT - 2015 LZFW | | HCT -2012 Ynl | HCT - 2012 USZ | HCT -2012 YnIB | HCT -2012 YnIB | HCT - 2015 LZFW | |
| Flow rate | m3/yr | 84000 | 84000 | 84000 | 84000 | 29029 | 11303 | 11303 | 11303 | 11303 | 11303 | 113029 |
| | L/week | 1615385 | 1615385 | 1615385 | 1615385 | 558250 | 217363 | 217363 | 217363 | 217363 | 217363 | 2173635 |
| Surface area | m2 | 132000 | 90000 | 61522 | 116068 | | 14878 | 1159 | 51304 | 12890 | 30782 | |
| specific gravity | g/cc | | 3.60 | 2.71 | 2.71 | | 2.71 | 3.60 | 2.71 | 2.71 | 2.71 | |
| surface area per mass | m2/kg | | 0.0559 | 0.0743 | 0.0743 | | 0.0743 | 0.0559 | 0.0743 | 0.2333 | 0.0743 | |
| Total mass (tonne = 1000 kg) | tonnes | | 1609 | 828 | 1562 | | 56550 | 5850 | 195000 | 15600 | 117000 | |
| Calculated Rm | tonnes | | 1609 | 828 | 1562 | | 200 | 21 | 691 | 55 | 414 | |
| Scaling factor w.r.t. HCT | - | 1.1023 | 0.0122 | 0.0054 | 0.0155 | | 0.0103 | 0.0012 | 0.0336 | 0.0084 | 0.0305 | |
| pH | s.u. | 4.06 | 7.54 | 9.67 | 9.10 | 9.32 | 9.277 | 8.555 | 8.877 | 9.477 | 8.807 | 4.185202 |
| Activity of hydrogen | - | 8.78E-05 | 2.91E-08 | 2.14E-10 | 7.92E-10 | 4.79E-10 | 5.28E-10 | 2.78E-09 | 1.33E-09 | 3.33E-10 | 1.56E-09 | 6.53E-05 |
| Temperature | °C | 2.2 | 2.2 | 2.2 | 2.2 | 2.2 | 2.2 | 2.2 | 2.2 | 2.2 | 2.2 | 2.2 |
| Aluminum | mg/L | 25.676 | 0.000722 | 0.000390 | 0.0009 | 0.28100 | 0.0001 | 0.0001 | 0.0024 | 0.0006 | 0.0018 | 19.155745 |
| Alkalinity | mg/L as CaCO₃ | 2.645405 | 0.200763 | 0.150353 | 0.355603 | 520.00000 | 0.2 | 0.0 | 0.9 | 0.2 | 0.7 | 136.245531 |
| Arsenic | mg/L | 0.022780 | 0.000024 | 0.000020 | 0.002067 | 0.04520 | 0.0000 | 0.0000 | 0.0001 | 0.0000 | 0.0041 | 0.030531 |
| Barium | mg/L | 0.042620 | 0.000166 | 0.000152 | 0.000012 | 0.30200 | 0.0002 | 0.0000 | 0.0009 | 0.0002 | 0.0000 | 0.109627 |
| Beryllium | mg/L | 0.006834 | 0.000010 | 0.000004 | 0.000012 | 0.00001 | 0.0000 | 0.0000 | 0.0000 | 0.0000 | 0.0000 | 0.005107 |
| Calcium | mg/L | 154.3153 | 5.783599 | 0.146289 | 0.499906 | 47.50000 | 0.8429 | 0.5533 | 0.9066 | 0.2278 | 0.9853 | 132.012186 |
| Cadmium | mg/L | 0.001885 | 0.000004 | 0.000001 | 0.000003 | 0.00004 | 0.0000 | 0.0000 | 0.0000 | 0.0000 | 0.0000 | 0.001418 |
| Chloride | mg/L | 5.143844 | 0.093324 | 0.000005 | 0.005102 | 120.00000 | 0.0034 | 0.0089 | 0.0000 | 0.0000 | 0.0101 | 34.717503 |
| Chromium | mg/L | 0.014697 | 0.000122 | 0.000054 | 0.000155 | 0.00421 | 0.0001 | 0.0000 | 0.0003 | 0.0001 | 0.0003 | 0.012333 |
| Copper | mg/L | 80.885875 | 0.000564 | 0.000014 | 0.000031 | 2.76000 | 0.0000 | 0.0001 | 0.0001 | 0.0000 | 0.0001 | 60.821450 |
| Fluoride | mg/L | 0.753206 | 0.003245 | 0.010024 | 0.014394 | 0.28000 | 0.0062 | 0.0003 | 0.0621 | 0.0156 | 0.0284 | 0.663491 |
| Iron | mg/L | 20.805010 | 0.133274 | 0.000108 | 0.000309 | 0.01000 | 0.0002 | 0.0128 | 0.0007 | 0.0002 | 0.0006 | 15.565068 |
| Mercury | mg/L | 0.00015156 | 0.00001890 | 0.00000004 | 0.00000008 | 0.00000 | 0.0000 | 0.0000 | 0.0000 | 0.0000 | 0.0000 | 0.000127 |
| Potassium | mg/L | 3.49047 | 0.26768 | 0.13545 | 0.40709 | 3.10000 | 0.1204 | 0.0256 | 0.8394 | 0.2109 | 0.8024 | 4.192195 |
| Magnesium | mg/L | 83.10982 | 5.34151 | 0.17699 | 0.74728 | 0.62300 | 0.5126 | 0.5110 | 1.0969 | 0.2756 | 1.4729 | 66.968354 |
| Manganese | mg/L | 3.53738 | 0.06311 | 0.00004 | 0.00021 | 0.00076 | 0.0007 | 0.0060 | 0.0003 | 0.0001 | 0.0004 | 2.676913 |
| Nitrate + Nitrite | mg/L as N | 0.00000 | 0.00000 | 0.00000 | 0.00000 | 0.60000 | 0.0000 | 0.0000 | 0.0000 | 0.0000 | 0.0000 | 0.290323 |
| Sodium | mg/L | 3.49047 | 0.03650 | 0.07407 | 0.15461 | 40.70000 | 0.1273 | 0.0035 | 0.4590 | 0.1153 | 0.3047 | 13.344965 |
| Nickel | mg/L | 11.41162 | 0.00131 | 0.00001 | 0.00020 | 0.01600 | 0.0000 | 0.0001 | 0.0001 | 0.0000 | 0.0004 | 8.486103 |
| Phosphorus | mg/L | 0.32994 | 0.00006 | 0.00003 | 0.00020 | 0.04700 | 0.0001 | 0.0000 | 0.0002 | 0.0001 | 0.0004 | 0.257565 |
| Lead | mg/L | 0.00360 | 0.00003 | 0.00002 | 0.00003 | 0.09640 | 0.0000 | 0.0000 | 0.0001 | 0.0000 | 0.0001 | 0.027505 |
| Sulfate | mg/L | 981.00446 | 37.92191 | 1.42496 | 4.57131 | 83.00000 | 4.2384 | 3.6281 | 8.8310 | 2.2187 | 9.0098 | 8.180338 |
| Antimony | mg/L | 0.00162 | 0.00001 | 0.00001 | 0.00013 | 0.05230 | 0.0000 | 0.0000 | 0.0001 | 0.0000 | 0.0003 | 0.014782 |
| Selenium | mg/L | 0.00294 | 0.00005 | 0.00005 | 0.00023 | 0.00050 | 0.0001 | 0.0000 | 0.0003 | 0.0001 | 0.0005 | 0.002642 |
| Silicon | mg/L | 6.22772 | 0.01683 | 0.00926 | 0.04278 | 0.66000 | 0.0114 | 0.0016 | 0.0574 | 0.0144 | 0.0843 | 4.865877 |
| Strontium | mg/L | 2.75563 | 0.37435 | 0.00796 | 0.00928 | 0.98800 | 0.0088 | 0.0358 | 0.0494 | 0.0124 | 0.0183 | 2.605138 |
| Thallium | mg/L | 0.01885 | 0.00155 | 0.00001 | 0.00001 | 0.00356 | 0.0000 | 0.0001 | 0.0000 | 0.0000 | 0.0000 | 0.016102 |
| Uranium | mg/L | 0.01168 | 0.00001 | 0.00001 | 0.00344 | 0.00000 | 0.0000 | 0.0000 | 0.0000 | 0.0000 | 0.0068 | 0.011937 |
| Zinc | mg/L | 1.11548 | 0.00029 | 0.00004 | 0.00012 | 0.00300 | 0.0001 | 0.0000 | 0.0003 | 0.0001 | 0.0002 | 0.830171 |

Notes (right margin):

- Flow rate: assumes that 10% of flow goes through the ramp/drain
- Surface area: 0.0456037 surface area of cylinder ((h = 15.24 cm, d = 7.62 cm)
- specific gravity: 2.72335 average rock density in ramp/drain
- surface area per mass: assumes that the surface area increases the same as in one week in the 2% humidity cell test
- Calculated Rm: Assumes 30% porosity, calculates the mass of waste rock in drain that can be saturated by the water flow in
- Alkalinity: not measured - estimated by Jeffrey Austin (metallurgist at Int'l MET), based on water data from other projects
- Calcium: 1595
- Nitrate + Nitrite: mmol N(5)/L for Phreeq Input - estimated by mine-affected water from an underground mine
- Sulfate: mmol S(6)/L for Phreeq input    785.8032282

$$R_{m,i}(tonnes) = \frac{L_{H2O}}{wk} * \frac{1000\ cm^3_{H2O}}{L_{H2O}} * \frac{7\ cm^3_{rock}}{3\ cm^3_{H2O}} * \frac{g_{rock}}{cm^3_{rock}} * \frac{ton_{rock}}{10^6 g_{rock}} * \frac{ton_i}{ton_{rock}}$$

# APPENDIX L: Mass-Load Inputs from the Base Case CTF at Closure

| Parameter | Units | Surface exposure | Ramp/drain term | | | | | Water to sump | |
|---|---|---|---|---|---|---|---|---|---|
| | | From cemented surface | YnI | USZ | YnIB (ramp) | YnIB (liner), 3/8" (0.009525 m) | LZFW | FINAL OUTPUT | |
| | | HCT - 4% binder | HCT - 2012 YnI | HCT - 2012 USZ | HCT -2012 YnIB | HCT -2012 YnIB | HCT - 2015 LZFW | | |
| Flow rate | m3/yr | 84000 | 8400 | 8400 | 8400 | 8400 | 8400 | 84000 | assumes that 10% of flow goes through the ramp/drain |
| | L/week | 1615385 | 161538 | 161538 | 161538 | 161538 | 161538 | 1615385 | |
| Surface area | m2 | 210000 | 11057 | 861 | 38127 | 9579 | 22876 | | |
| specific gravity | g/cc | | 2.71 | 3.60 | 2.71 | 2.71 | 2.71 | | 2.72335 average rock density in ramp/drain |
| surface area per mass | m2/kg | | 0.0743 | 0.0559 | 0.0743 | 0.2333 | 0.0743 | | 0.0456037 surface area of cylinder ((h = 15.24 cm, d = 7.62 cm) |
| Total mass (tonne = 1000 kg) | tonnes | | 56550 | 5850 | 195000 | 15600 | 117000 | | Assumes 30% porosity, calculates the mass of waste rock in drain that can be saturated by the water flow in 1 week |
| Calculated Rm | tonnes | | 149 | 15 | 513 | 41 | 308 | | assumes that the surface area increases the same as in one week in the 2% humidity cell test |
| Scaling factor w.r.t. HCT | - | 1.9415 | 0.0103 | 0.0012 | 0.0336 | 0.0084 | 0.0305 | | |
| pH | s.u. | 5.571870 | 9.28 | 8.56 | 8.88 | 9.48 | 8.81 | 5.57 | |
| Activity of hydrogen | - | 2.68E-06 | 5.28E-10 | 2.78E-09 | 1.33E-09 | 3.33E-10 | 1.56E-09 | 2.68E-06 | |
| Temperature | °C | 2.2 | 2.2 | 2.2 | 2.2 | 2.2 | 2.2 | 2.2 | |
| Aluminum | mg/L | 0.019415 | 0.0001 | 0.0001 | 0.0024 | 0.0006 | 0.0018 | 0.0199135 | |
| Alkalinity | mg/L as CaCO₃ | 2.912200 | 0.1522 | 0.0192 | 0.9318 | 0.2341 | 0.7009 | 3.1160209 | |
| Arsenic | mg/L | 0.007766 | 0.0000 | 0.0000 | 0.0001 | 0.0000 | 0.0041 | 0.0081899 | |
| Barium | mg/L | 0.055655 | 0.0002 | 0.0000 | 0.0009 | 0.0002 | 0.0000 | 0.0558004 | |
| Beryllium | mg/L | 0.001553 | 0.0000 | 0.0000 | 0.0000 | 0.0000 | 0.0000 | 0.0015599 | |
| Calcium | mg/L | 53.875708 | 0.8429 | 0.5533 | 0.9066 | 0.2278 | 0.9853 | 54.2272930 | |
| Cadmium | mg/L | 0.000058 | 0.0000 | 0.0000 | 0.0000 | 0.0000 | 0.0000 | 0.0000593 | |
| Chloride | mg/L | 2.588623 | 0.0034 | 0.0089 | 0.0000 | 0.0000 | 0.0101 | 2.5908658 | |
| Chromium | mg/L | 0.009707 | 0.0001 | 0.0000 | 0.0003 | 0.0001 | 0.0003 | 0.0097913 | |
| Copper | mg/L | 0.003883 | 0.0000 | 0.0001 | 0.0001 | 0.0000 | 0.0001 | 0.0039091 | |
| Fluoride | mg/L | 0.258862 | 0.0062 | 0.0003 | 0.0621 | 0.0156 | 0.0284 | 0.2701221 | |
| Iron | mg/L | 0.038829 | 0.0002 | 0.0128 | 0.0007 | 0.0002 | 0.0006 | 0.0402700 | |
| Mercury | mg/L | 0.000056 | 0.0000 | 0.0000 | 0.0000 | 0.0000 | 0.0000 | 0.0000563 | |
| Potassium | mg/L | 4.057666 | 0.1204 | 0.0256 | 0.8394 | 0.2109 | 0.8024 | 4.2575415 | |
| Magnesium | mg/L | 1.990004 | 0.5126 | 0.5110 | 1.0969 | 0.2756 | 1.4729 | 2.3768981 | |
| Manganese | mg/L | 0.009707 | 0.0007 | 0.0060 | 0.0003 | 0.0001 | 0.0004 | 0.0104514 | |
| Nitrate | mg/L as N | 0.000000 | 0.0000 | 0.0000 | 0.0000 | 0.0000 | 0.0000 | 0.0290323 | mmol N(5)/L for PhreeqC, estimated as 10% of of mine-affected value (18) during operations |
| Sodium | mg/L | 3.915292 | 0.1273 | 0.0035 | 0.4590 | 0.1153 | 0.3047 | 4.0162724 | |
| Nickel | mg/L | 0.018444 | 0.0000 | 0.0001 | 0.0001 | 0.0000 | 0.0004 | 0.0185083 | |
| Phosphorus | mg/L | 0.020709 | 0.0001 | 0.0000 | 0.0002 | 0.0001 | 0.0001 | 0.0207807 | |
| Lead | mg/L | 0.000388 | 0.0000 | 0.0000 | 0.0001 | 0.0000 | 0.0001 | 0.0004060 | |
| Sulfate | mg/L | 87.366012 | 4.2384 | 3.6281 | 8.8310 | 2.2187 | 9.0098 | 0.9385656 | mmol S(6)/L for Phreeq input          90.15860748 |
| Antimony | mg/L | 0.001035 | 0.0000 | 0.0000 | 0.0001 | 0.0000 | 0.0003 | 0.0010714 | |
| Selenium | mg/L | 0.001941 | 0.0001 | 0.0000 | 0.0003 | 0.0001 | 0.0005 | 0.0020285 | |
| Silicon | mg/L | 0.362407 | 0.0114 | 0.0016 | 0.0574 | 0.0144 | 0.0843 | 0.3793222 | |
| Strontium | mg/L | 0.634213 | 0.0088 | 0.0358 | 0.0494 | 0.0124 | 0.0183 | 0.6466757 | |
| Thallium | mg/L | 0.002200 | 0.0000 | 0.0001 | 0.0000 | 0.0000 | 0.0000 | 0.0022219 | |
| Uranium | mg/L | 0.000388 | 0.0000 | 0.0000 | 0.0000 | 0.0000 | 0.0068 | 0.0010732 | |
| Zinc | mg/L | 0.015532 | 0.0001 | 0.0000 | 0.0003 | 0.0001 | 0.0002 | 0.0156007 | |

## APPENDIX M: Mass-Load Inputs from Water Process Plant

| Parameter | Units* | Contributions into PWP | | | Mixed water, before PhreeqC | |
|---|---|---|---|---|---|---|
| | | Thickener overflow (from mill) | Water from UG | Water from CTF | FINAL FLOW PER YEAR | |
| Flow rate | m3/yr | 3807000 | 181000 | 113029 | 4111029 | includes 10000 m3/yr direct precipitation |
| Fraction of water input | | 0.926 | 0.044 | 0.027 | | =SUM(C4:E4)+10000 |
| pH | s.u. | 9.32 | 6.86 | 4.13 | 5.69 | |
| Activity of hydrogen | - | 4.79E-10 | 1.39E-07 | 7.40E-05 | 2.04E-06 | |
| Temperature | °C | 2.20 | 2.20 | 2.20 | 2.20 | |
| Aluminum | mg/L | 0.28100 | 0.01009 | 17.70390 | 0.74742 | |
| Alkalinity | mg/L as CaCO₃ | 500 | 183 | 97 | 474 | estimate |
| Arsenic | mg/L | 0.045 | 0.004 | 0.031 | 0.042863 | |
| Barium | mg/L | 0.302 | 0.00086 | 0.004 | 0.2798 | |
| Beryllium | mg/L | 0.00001 | 0.00048 | 0.00510 | 0.00017 | |
| Calcium | mg/L | 48 | 89 | 132 | 51.52 | |
| Cadmium | mg/L | 0.00004 | 0.00005 | 0.00141 | 0.000078 | |
| Chloride | mg/L | 120 | 1.4 | 34 | 112.128 | |
| Chromium | mg/L | 0.0042 | 0.0005 | 0.0123 | 0.00426 | |
| Copper | mg/L | 2.760 | 0.001 | 61.254 | 4.240 | |
| Fluoride | mg/L | 0.28 | 0.96 | 0.66 | 0.3200 | |
| Iron | mg/L | 0.010 | 0.002 | 0.636 | 0.0268 | |
| Mercury | mg/L | 0.00001 | 0.00001 | 0.00013 | 0.000010 | |
| Potassium | mg/L | 3.100 | 10.838 | 0.000 | 3.348 | |
| Magnesium | mg/L | 0.623 | 57.2 | 91.704 | 5.615 | |
| Manganese | mg/L | 0.00076 | 0.16539 | 2.68015 | 0.08167 | |
| Nitrate + Nitrite | mg/L as N | 0.60 | 18.00 | 0.00 | 0.022 | converted to mmol N(5) for phreeq |
| Sodium | mg/L | 40.7 | 14.7 | 13.4 | 38.703 | |
| Nickel | mg/L | 0.016 | 0.006 | 8.526 | 0.24950 | |
| Phosphorus | mg/L | 0.047 | 0.004 | 0.258 | 0.0508 | |
| Lead | mg/L | 0.09640 | 0.00002 | 0.02749 | 0.0900 | |
| Sulfate | mg/L | 83 | 304 | 765 | 1.158 | converted to mmol S(6) for phreeq |
| Antimony | mg/L | 0.0523 | 0.0032 | 0.0148 | 0.04898 | |
| Selenium | mg/L | 0.00050 | 0.00388 | 0.003 | 0.00071 | |
| Silicon | mg/L | 0.66000 | 1.54840 | 1.14212 | 0.7108 | |
| Strontium | mg/L | 0.988 | 10.534 | 2.616 | 1.451 | |
| Thallium | mg/L | 0.00356 | 0.00196 | 0.01607 | 0.00382 | |
| Uranium | mg/L | 0.00000 | 0.03710 | 0.01194 | 0.00197 | |
| Zinc | mg/L | 0.0030 | 0.0292 | 0.8255 | 0.02676 | |

*Red values are non-detect*